

Acquisitions and Bibliographic Services Branch

395 Wellington Street Ottawa, Ontario K1A 0N4 Bibliothèque nationale du Canada

Direction des acquisitions et des services bibliographiques

395, rue Wellington Ottawa (Ontario) K1A 0N4

Your He Votre returnse

Out the National Property

NOTICE

The quality of this microform is heavily dependent upon the quality of the original thesis submitted for microfilming. Every effort has been made to ensure the highest quality of reproduction possible.

La qualité de cette microforme dépend grandement de la qualité de la thèse soumise au microfilmage. Nous avons tout fait pour assurer une qualité supérieure de reproduction.

AVIS

If pages are missing, contact the university which granted the degree.

S'il manque des pages, veuillez communiquer avec l'université qui a conféré le grade.

Some pages may have indistinct print especially if the original pages were typed with a poor typewriter ribbon or if the university sent us an inferior photocopy. La qualité d'impression de certaines pages peut laisser à désirer, surtout si les pages originales ont été dactylographiées à l'aide d'un ruban usé ou si l'université nous a fait parvenir une photocopie de qualité inférieure.

Reproduction in full or in part of this microform is governed by the Canadian Copyright Act, R.S.C. 1970, c. C-30, and subsequent amendments. La reproduction, même partielle, de cette microforme est soumise à la Loi canadienne sur le droit d'auteur, SRC 1970, c. C-30, et ses amendements subséquents.

Canadä

STRUCTURE AND RESPONSE OF THE DIAPHRAGMATIC CIRCULATION

Alain Steve Comtois

Meakins Christie Laboratories and Department of Physiology,
McGill University, and Notre Dame Hospital, Université de
Montréal.

Doctoral Dissertation
Submitted August 1st, 1991.



Acquisitions and Bibliographic Services Branch

395 Wellington Street Ottawa, Ontano K1A 0N4 Bibliothèque nationale du Canada

Direction des acquisitions et des services bibliographiques

395, rue Wellington Ottawa (Ontario) K1A 0N4

Your file Votte référence

Our Me. Notice références

The author has granted an irrevocable non-exclusive licence allowing the National Library of Canada to reproduce, loan, distribute. or sell copies of his/her thesis by any means and in any form or format, making this thesis available to interested persons.

L'auteur a accordé une licence exclusive irrévocable et non à la Bibliothèque permettant nationale du Canada reproduire, prêter, distribuer ou vendre des copies de sa thèse de quelque manière et sous quelque forme que ce soit pour mettre des exemplaires de cette thèse disposition des à la personnes intéressées.

The author retains ownership of the copyright in his/her thesis. Neither the thesis nor substantial extracts from it may be printed or otherwise reproduced without his/her permission. L'auteur conserve la propriété du droit d'auteur qui protège sa thèse. Ni la thèse ni des extraits substantiels de celle-ci ne doivent être imprimés ou autrement reproduits sans son autorisation.

ISBN 0-315-94602-4



TABLE OF CONTENTS

			Page
Preface		•••••	i
CHAPTER	1:	INTRODUCTION	. 1
	REVIEW	OF LITERATURE	3
		Techniques of blood flow measurements	3
		Anatomy of diaphragmatic circulation	8
		Factors affecting skeletal muscle blood flow	. 10
		AL MUSCLE BLOOD FLOW SCLE FATIGUE	. 21
	RELEVA	NCE OF PRESENT WORK	. 23
CHAPTER	2:	ANATOMY OF DIAPHRAGMATIC	
		CIRCULATION	. 29
	SUMMARY 3		
	INTRODUCTION		
	MATERIALS AND METHODS		
	RESULTS		
	DISCUS	SION	. 48
CHAPTER	3:	RESTRICTION OF REGIONAL BLOOD FLOW	
		AND DIAPHRAGMATIC CONTRACTILITY	. 55
	SUMMAR	У	. 56
	INTROD	OUCTION	. 58

	MATERIALS AND METHODS				
	RESULTS 66				
	DISCUSSION 80				
CHAPTER	4: EFFECT OF SEPARATE HEMIDIAPHRAGM				
	CONTRACTION ON LEFT PHRENIC ARTERY				
	FLOW AND OXYGEN CONSUMPTION 91				
	SUMMARY 92				
	INTRODUCTION				
	MATERIALS AND METHODS				
	RESULTS 97				
	DISCUSSION 106				
CHAPTER	5: CONTRACTION DEPENDENT MODULATIONS IN				
	REGIONAL DIAPHRAGMATIC BLOOD FLOW 113				
	SUMMARY 114				
	INTRODUCTION 116				
	MATERIALS AND METHODS				
	RESULTS 125				
	DISCUSSION 137				
CAHPTER	6: OPTIMAL DIAPHRAGMATIC				
	BLOOD PERFUSION				
	SUMMARY				
	INTRODUCTION				
	MATERIALS AND METHODS				
	RESULTS				

CAHPTER	7: CONCLUSION	184
LIST OF	REFERENCES	190

ACKNOWLEDGEMENTS

I am grateful to Dr. J.L. Jankowski who introduced me to the physiological sciences and most particularly to the Meakins Christie Laboratories of McGill University. I am especially thankful to Dr. A. Grassino who kindly supervised and supported this work over a period of seven years, and to the Notre-Dame Hospital for providing excellent facilities. I would also like to thank all of those who participated directly and indirectly in the preparation of this thesis, especially Dr F. Hu for his tremendous collaboration and support, Dr J. Guerraty, Cardiac Thoracic Surgeon at the Notre-Dame Hospital, for teaching me surgical techniques, Dr. W. Gorczyca for sharing his knowledge on the preparation of anatomical specimens, the technical staff of the experimental surgery department of the Notre-Dame Hospital, M. Ouellet, F. Boisvert, and S. Boucher for their excellent support and technical skills, and G. Leger for her excellent assistance in the preparation of the thesis. Most of all I am indebted to Kathline Leger whose support never failed, and my son, Simon, with whom I couldn't spend all the time that I wished.

ABSTRACT

The anatomy of the diaphragmatic circulation was found to be composed of an internal arterial circle formed by the head to head anastomosis of the phrenic arteries and internal mammary arteries. Branches originating from the internal arterial circle anastomosed head to head with branches of the intercostal arteries (8th to 13th intercostal space) to form costophrenic arcades all along the muscular fibers of the crural and costal diaphragm. These anastomosis were found to be physiologically functional. Diaphragmatic circulation produced only by the intercostal arteries was able to sustain costal and crural contractility at the fatigue threshold (TTdi of 0.20). However, internal mammary artery perfusion was only able to maintain costal contractility. Left and hemidiaphragmatic arterial communications (shunting) were inexistant during electrophrenic unilateral and bilateral Diaphragmatic venous outflow was produced stimulation. mostly by the intercostal veins (60% of total diaphragmatic venous outflow) which drained into the azygos trunk. phrenic veins contributed 25% and the internal mammary veins contributed 15% of total diaphragmatic venous outflow. Diaphragmatic circulation was found to be proportional to the Pdi and was related to the duty cycle by a parabolic function with the highest flow rates being observed at a duty cycle of 0.50, regardless of the Pdi being generated.

RESUME

la circulation diaphragmatique L'anatomie de composée d'un cercle artériel interne formé de l'anastomose bout à bout des artères phréniques et des artères mammaires internes. Des ramifications provenant du cercle artérielle interne communiquent bout à bout avec des branches originant des artères intercostales (8ème au 13ème espace intercostal) pour former des arcades costo-phréniques qu'on retrouve dans le feuillet musculaire des régions diaphragmatiques crurales et costales. Ces anastomoses (arcades costo-phréniques) étant physiologiquement furent observées comme fonctionnelles. La circulation diaphragmatique maintenue uniquement par les artères intercostales (via les arcades costo-phréniques) permet de soutenir la contractilité costale et crurale au seuil de la fatigue (TTdi de 0.20). Par contre les artères mammaires internes permettent de maintenir la contractilité costale mais non la contractilité crurale au seuil de la fatigue. Une indépendance artérielle entre les hémidiaphragmes (droit et gauche) fut observée stimulation electrophrénique unilatérale lors de bilatérale. La circulation diaphragmatique veineuse est produite essentiellement par les veines intercostales (60% de l'effluent diaphragmatique total) qui se déversent dans la veine azygos. Les veines phréniques contribuent 25% et les veines mammaires internes 15% dе l'effluent diaphragmatique total. La circulation diaphragmatique est proportionelle à la pression transdiaphragmatique (Pdi) et est aussi reliée au cycle respiratoire par une fonction parabolique. La circulation diaphragmatique est à son point le plus élevé lorsque le cycle respiratoire se situe à 0.50 indépendamment de la Pdi générée.

Preface

This thesis is composed of seven chapters. The introduction (chapter 1) describes the relevance of this work applied to general problems in the field of respiratory physiology and reviews the literature which led to the development of the experiments performed in the subsequent chapters of this thesis. In the presentation of chapters 2, 3, 4, 5, and 6 the author availed himself of "the option, subject to the approval of the Department, of including as part of the thesis the text of an original paper, or papers, suitable for noisaimdua to learned journals for publication". Chapters 2, 3, 4, and 5 have been published in the Journal of Applied Physiology and the appropriate full references are mentioned in the introduction. Chapter 6 has been accepted for publication in the Journal of Applied Physiology and will be printed in the fall of 1991. Chapter 7 composes the conclusion and presents the elements of this work considered as original contributions to the present knowledge in the field of respiratory physiology.

Assistance was obtained at various moments throughout the evolution of this thesis. Drs. W. Gorczyca and J. Guerraty provided surgical assistance and M. Ouellet provided technical assistance in the preparation of the anatomical specimens presented in chapter 2. The animal experiments performed in chapters 3, 4, 5, and 6 have been done in collaboration with Dr F. Hu and with the technical

assistance of F. Boisvert and S. Boucher. Dr F. Hu has kindly authorized me to include the original manuscripts where he his first author to form chapters 4, 5, and 6 as part of this thesis. Mr. Boudreau, of the Notre-Dame Hospital Illustration Department as prepared drawings which were reproduced in part by R. Derval, L. Lapierre, and the late P. Casgrain. G. Leger prepared the format and typescript of this thesis.

CHAPTER 1

INTRODUCTION

INTRODUCTION

The respiratory muscles are mainly responsible for the act of breathing and they are functionally classified as inspiratory and expiratory muscles. In addition, all of them are active in other non-respiratory acts such as speech, cough, posture, etc. The inspiratory muscles include the diaphragm, the external intercostal muscles, the scalene parasternal muscles, the muscles, and sternocleidomastoid muscles (72). The expiratory muscles regroup the abdominal muscles (postural muscles), the internal intercostal muscles (72), and to some extent in humans, the triangularis sterni muscles (27). Nonetheless, like other skeletal muscles the respiratory muscles are dependent on adequate energy supplies to maintain their rate of contractility against a given load (11, 12). fatiguability, where fatiguability endurance against (fatigue) is defined as the loss in the capacity for developing force which is reversible by rest (74), is a function of continuous regeneration of high energy phosphate bonds (e.g. local supplies of ATP) by aerobic and anaerobic pathways (92), as well as exchanges of catabolites with the extracellular milieu (4). Blood circulation through muscle tissue is thought to be the main vector by which these pathways can fulfill their role of replenishing ATP supplies and catabolite wash-out (4, 92).

Skeletal muscle blood flow responds to local neural. humoral, and mechanical factors affecting the intramuscular vasculature (7). As well, blood perfusion through the muscle can be dependant on hemodynamic factors such as arterial pressure, blood volume, and cardiac output (7). Thus, the energy reconstitution of exercising skeletal muscles is dependent on an adequate blood supply to the muscles themselves. If the rate of energy utilization becomes greater than the rate of energy reconstitution. fatigue will develop. The purpose of this introduction is to review the factors known to influence skeletal muscle blood flow and most particularly respiratory muscle blood flow, the relationship of blood flow and skeletal muscle fatigue, and the relevance of the present work to the current understanding of respiratory muscle function. Most of the introduction will be devoted to studies of diaphragmatic circulation since most of the research carried in the field of respiratory muscle blood flow has examined circulation through this most important muscle inspiration.

I REVIEW OF LITERATURE

TECHNIQUES OF BLOOD FLOW MEASUREMENTS

Numerous methods exist to measure blood flow in organs and in vessels (1-13, 15-23, 28, 39-41, 43-53, 55, 57-60, 62-68, 71, 75-76, 80-89, 94-97, 99-100). They vary from

timed collection of venous blood to radioactive tracers. All have advantages and disadvantages, and though they all measure blood flow, great care must be taken when interpreting the results obtained by these various methods. Some methods may represent whole organ blood flow while others may represent nutritive blood flow, some may represent average flow at a particular instant in time, while others may represent instantaneous changes in flow rates (48).

Methods of flow rate measurements

Methods that monitor instantaneous changes in flow rate measure whole tissue blood flow, i.e. shunting and nutritive blood flow through an area of tissue (48). Early studies of blood flow in skeletal muscles consisted of cannulating veins and measuring timed collection of venous affluent (72). Hot wire anemometry, a technique used by Anrep (1, 2), consisted of cannulating an artery that supplied an organ or a muscle and measuring the rate of decay of the volume of blood in a reservoir (connected to the cannula perfusing the artery) which was proportional to the change in electrical resistance caused by the air flowing passed (cooling) the hot wires placed over the reservoir. The rate of change in resistance represented the blood flow through that artery. A simpler method that has been used with success, by Bellemare et al (12) recently, was a drop counting technique to measure diaphragmatic blood

These authors measured blood drop count rate flow rate. from the cannulated phrenic vein in open-chest dogs. Lately electromagnetic flowmeters and pulsed Doppler flowmetry (4, 8-9, 19, 22-23, 37-40, 43-47, 52-53, 76, 80, 89, 96) have been used to measure blood flow of arteries supplying organs muscles. These techniques have the advantage of measuring immediate changes in blood flow in the arteries on which they are placed. The electromagnetic flow probes create a magnetic field around the vessel, and electrodes placed on the surface of the vessel (normal to the electric field vector) record an electric current proportional to the blood flow (99). Pulsed Doppler flow probes (not to be confused with continuous Doppler) operate on the basis of a radar system (37, 38, 99). The single piezo-electric crystal contained in those types of flow probes functions alternately as an emitter and receiver at a frequency of 69.2 KHz (37). The ultrasounds (20 MHz) are emitted by the crystal and are bounced back by moving erythrocytes in the vessel. In so doing, a Doppler shift is recorded by the crystal and it is proportional to the blood flow in the vessel. Pulsed Doppler flow probes have the advantage of being smaller and lighter than electromagnetic flow probes, thus very little disturbance of the vessel being studied (38). In addition, they have a stable zero baseline value which is not the case for the electromagnetic flow probes because they depend on good electrode contact on the vessel to maintain a stable zero baseline (37, 38, 99).

Methods for measuring capillary blood perfusion

Radioactive methods have the advantage of measuring blood flow distribution of the whole organ (48). However, this type of method measures mean rather than instantaneous flow rates (48). Two types of radioactive methods have currently been used in the literature (48). The inert radioactive labelled tracer gaz method and the trapping in the microcirculation of radioactive labelled micropheres.

The tracer gaz method, like the instantaneous methods (electromagnetic and Doppler flow probes), measure total organ blood flow, i.e. shunting and nutritive flow through an organ (48). Basically it consists of measuring the rate of disappearance of a radioactive labelled inert gaz injected into an organ. Two approaches can be used with this method. First, the radioactive sample can be injected directly into the tissue and the rate of its disappearance measured with external gamma probes placed over the site of injection (88), or second (Adapted from the Kety-Schmidt (55) nitrous oxide wash-out technique), a venous vessel of an organ of interest is cannulated and the rate of disappearance of the radioactive tracer measured (86, 87). A constant continuous injection of a tracer into the systemic circulation is performed over a relatively long period of time (20 min). During this period of time simultaneous withdrawals of samples from the arterial and cannulated venous vessel are taken. This permits the construction of the wash-in phase. The wash-out phase (without a constant continuous injection of tracer) requires an additional 20 minutes of sampling and this constructs the rate of disappearance of the tracer which is proportional to the blood flow rate.

The advantage of the inert radioactive gaz methods is that multiple runs (up to 8) of blood flow measurements can be performed in the same subject. The limitation however with these tracer methods, is the fact that, the first technique requires exposure of the organ being investigated in order to permit injection of the radioactive tracer into its tissues, and in the case of the second technique (washout method), is the amount of time taken to measure flow rate (approximately 40 minutes per run) and the amount of blood drawn.

Radioactive micropheres measure nutritive blood flow The micropheres (15 to 25 um) are injected into the left ventricle directly and travel in the systemic The micropheres become trapped into the circulation. microcirculation (capillary bed) of the organs and the level of radioactivity measured in the various organs proportional to the blood flow rate. This technique requires the timed collection of a sample from a peripheral permits conversion of artery, which radioactivity measurements into blood flow rates. The advantage of this method is that organ blood flow rate can be expressed as a percentage of the cardiac output which is interesting when blood flow distribution is a considered factor. However, the limiting aspects of micropheres is that the number of runs are limited by the amount of different isotopes that can be used, and that they measure blood flow at a particular instant in time.

ANATOMY OF DIAPHRAGMATIC CIRCULATION

The diaphragm is a thin muscle that separates the abdominal compartment from the thoracic compartment. anatomy textbooks (14, 30, 33-34, 70, 98) mention that the diaphragm is perfused by various arterial supplies. These include the phrenic arteries, which are thought to be the major vessels perfusing the diaphragm, the intercostal arteries, and the internal mammary arteries. The phrenic arteries are thought to perfuse mainly the posterior (crural) diaphragm, the sternal, and most of the costal portions of the diaphragm (14). Small branches of the intercostal arteries are thought to perfuse the peripheral portions of the diaphragm adjacent to the ribs, and small branches from the internal mammary arteries are thought to perfuse the anterior segment of the diaphragm adjacent to sternum (33). In humans the inferior phrenic arteries originate from the celiac trunk and in dogs and other species originate from the superior phrenico-abdominal artery (30, 34). The venous drainage in humans and dogs seems to be performed mostly by the inferior phrenic veins

which empty directly into the inferior vena-cava just distal to the site of the hepatic veins on the inferior vena-cava (12, 30, 34, 86-87). As with the arterial system the intercostal veins and the internal mammary veins could contribute to local venous drainage in the periphery of the diaphragm (30, 33). Locally the arteries seem to anastomose extensively between themselves, and the venous system seems to anastomose with other diaphragmatic veins as well (98). Recently, Lockhat and co-workers (60) addressed this issue by studying the collateral sources of the costal and crural diaphragm in the dog. They produced acute occlusions of the internal mammary arteries and of the intercostal arteries. They observed that occlusion of the internal mammary arteries did not affect diaphragmatic circulation (measured by radioactive micropheres), and only when the intercostal arteries were occluded did they observe a decrease in blood flow in the crural segment of the diaphragm with very little change in blood flow in the costal segment. These results suggest that extensive communications between the arteries supplying the diaphragm seem to exist.

The microcirculation of the diaphragm, as reported by Shraufnagel and co-workers (90), seems to resemble the microcirculation of other skeletal muscles. However, according to their observations the anatomical arrangement of the microvasculature seems to prevent kinking of the vessels during diaphragmatic contractions. Thus the

diaphragm seems to be perfused by numerous vessels that apparently anastomose extensively between themselves, however the vascular architecture within the muscular leaflet remains unknown as well as the extent to which diaphragmatic arteries can become occluded before showing clinical signs of muscle failure (such as paradoxical breathing).

FACTORS AFFECTING SKELETAL MUSCLE BLOOD FLOW

Perfusion pressure (arterial pressure)

Skeletal muscle blood flow, as with any other organ, is a function of the arterial perfusion pressure (42, 72). Factors that affect the arterial perfusion pressure are cardiac output and peripheral vascular resistance, which if expressed mathematically can be represented by the following equation:

$$P = Q \times R \tag{1}$$

where P is the arterial perfusion pressure, Q is the cardiac output, and R is the peripheral vascular resistance. As well, cardiac output and peripheral vascular resistance are affected by several factors which are mediated via neural and/or humoural vectors. Cardiac output and peripheral vascular resistance, under normal conditions, are influenced by the level of activity or force of contraction of exercising skeletal muscles (72). They can also be

influenced by pathological conditions such as hemorrhagic, cardiogenic or septic shock (50, 89, 100).

The blood circulation of respiratory muscles, being skeletal muscles themselves, is influenced by the same factors, i.e. perfusion pressure gradient and vascular resistance (52). Respiratory muscle blood flow can be expressed by rearranging equation 1 as follows:

$$Qdi = ^P/R$$
 (2)

where Qd: represents respiratory muscle blood flow, ^ P is the perfusion pressure gradient (arterial pressure minus venous pressure), and R is the vascular resistance of the respiratory muscles. Under normal resting conditions the perfusion pressure gradient remains relatively constant and vascular resistance can be modified by several factors which include the following: 1) the level of respiratory muscle activity, 2) mechanical factors such as respiratory muscle length and intramuscular pressure, and 3) respiratory muscle contraction pattern.

Muscle activity

Respiratory muscle activity is the most important determinant of respiratory muscle blood flow (1, 8-10, 12, 16-17, 19, 20-23, 28, 31, 43-47, 50-53, 59-60, 62-68, 75-76, 80-81, 83-89, 96-97, 100). Numerous studies have demonstrated that respiratory muscle blood flow is a function of minute ventilation. Hyperventilation caused by

CO2 breathing or physical exertion (e.g. running on a treadmill) increases diaphragmatic blood flow 35 ml/min/100g and approximately approximately ml/min/100g, respectively (33, 87). Recently Manohar and co-workers (66-67) have measured in maximally exercising ponies diaphragmatic blood flow values of 265 ml/min/100g. Nevertheless, the greatest increases in diaphragmatic circulation have been observed either during loaded breathing or phrenic nerve pacing (16, 81). High inspiratory resistances and phrenic nerve pacing have been shown to produce levels of diaphragmatic circulation in the range of 200-400 ml/min/100g (16, 81). Flow values, which normalized to weight are much greater than those observed in most skeletal muscles (7, 48). In fact, the heart seems to be the only organ with higher blood flow values, approximately 500 ml/min/100g, under near maximal activation Reid and Johnson (81) in a series of elegant (65).experiments were able to calculate the upper limit of diaphragmatic circulation by producing a vasodilated diaphragmatic vascular bed via infusions of adenosine and nitroprusside while the animals (dogs) breathed 6 % CO2 against added inspiratory resistances. Under those conditions diaphragmatic circulation was a parabolic function of the arterial perfusion pressure (Part) and during normotensive conditions yielded a maximal blood flow value of approximately 200 ml/min/100g. A value comparable to the one observed by Buchler et al (16) during electrical phrenic nerve pacing in dogs. These authors (16), under normotensive conditions, reported values that were in the range of 200-400 ml/min/100g. Thus all of the above experiments seem to demonstrate that during high inspiratory resistive breathing diaphragmatic circulation attains its highest possible flow rate, a value surpassed only by the myocardial circulation.

Mechanical factors

As mentioned earlier, an adequate energy supply (blood flow) is necessary to maintain a certain level of contraction indefinitely. If the energy supply becomes interrupted, muscle failure eventually occurs. Energy supply or reconstitution has been shown to be interrupted during forceful contractions (7). Investigations of limb skeletal muscles have shown that perfusion of the soleus (5) and of the elbow flexor muscles (15) was found to be occluded during sustained contractions of 15% and 50% of the muscle's maximal tension, respectively. Humphreys and Lind (49), using the hand grip muscles, found increases in blood flow up to tensions of about 40% of the muscle's maximal tension, and it decreased thereafter until 70% of the maximal tension was reached. However, the flow at 70% of maximal tension was still greater than observed at rest. Similar observations were reported by Bonde-Petersen et al (15) where blood flow in the elbow flexors was greatest at 22% of maximal tension and decreased thereafter as the force developed increased. At levels of 50% of maximal force, blood flow through the elbow flexors was found to be zero.

Even though absolute blood flow was greater with increasing metabolic demands the endurance time to contractile failure decreased, supporting the evidence that the relative increases in absolute blood flow were inadequate to support the energy requirements, and that the blood flow through the contracting muscle was probably impeded, and thus, leading to muscular fatigue (7, 15, 49). In support to this argument, Lind and McNichol (58) studied the post-exercise hyperemia of the hand grip muscles, which if present, would indicate an inadequate blood supply during the time of contractile activity. They observed that measurements of absolute blood flow values during contraction of the hand grip muscles, (up to levels of 30% of maximal tension) was larger than blood flow values seen at rest. However, at tensions of 15% of the maximal tension a post-exercise hyperemia became apparent which increased with greater levels of tension They also reported that the calculated blood developed. flow debt increased exponentially with increasing levels of tension, concluding that blood flow limitation occurred, at low levels of tension, despite the relative increase in absolute blood flow during the contraction (58). observation suggests that the absolute increase in blood supply was inadequate to meet the metabolic demands during increased contractile activity. Similar increases of

absolute blood flow in the dog diaphragm have been reported by several authors (81, 83-88). Numerous investigators, using radioactive labelled micropheres, observed in the canine diaphragm a progressive increase in blood flow by stimulating breathing with various levels of inspiratory resistances and unobstructed hyperventilation ру breathing. These authors (83-88) concluded that there was no limit to the increase in blood flow in the dog diaphragm. However, Donovan and colleagues (28) demonstrated by using the same method of blood flow measurement, radioactive labelled micropheres, that blood flow to the dog diaphragm could become limited. This group of investigators produced sustained isometric contractions at various levels of force by using electrophrenic stimulation of the dog diaphragm. They found absolute blood flow up to increases in transdiaphragmatic pressures (Pdi = Gastric pressure -Pleural pressure) of 85% of the maximal Pdi which progressively decreased thereafter, but nevertheless were still greater than control values.

Similarly, but in one of the earlier studies on diaphragmatic circulation, Anrep (1) observed in the diaphragm of dogs (spontaneously breathing at rest) that the blood flow, measured by a hot wire anemometer, through the left phrenic artery was decreased during inspiration (contraction phase) and that during the expiratory pause blood flow resumed to the level of the previous pause. This

decrease during inspiration in phrenic artery blood flow, as reported by Anrep et al (1), is similar to the decrease observed in coronary circulation during systole. In the heart it has been well demonstrated that coronary blood flow decreases during systole and that the majority of myocardial perfusion occurs during diastole (57). In the heart it has been shown that left coronary circulation is inversely proportional to left ventricular pressure. The mechanism thought to be at work is the transmission of left ventricular pressure to the left ventricular wall which causes intramyocardial pressure to increase. An increase in intramyocardial pressure increase the resistance to blood flow in the vessels perfusing the left ventricle thereby decreasing left coronary circulation during systole. This same mechanism affects skeletal muscle blood flow and was proposed for diaphragmatic blood flow by Anrep and associates in a subsequent study on phrenic artery blood flow (2). They demonstrated that blood flow through skeletal muscle was diminished in proportion to the strength of contraction. concluded from their observations that the muscular contraction caused a mechanical compression of the blood vessels between the muscle fibers, thus impeding blood flow through These early observations by Anrep and cothe muscle. workers (1-2) on the inhibitory effects of muscle tension on blood flow are consistent with the more recent observations made by other investigators (5-6, 15, 49, 58). early observations made by Anrep et al (1-2) and the more

recent one by Donovan et al (28) is at variance with the conclusion that there is no inhibitory effect to the increase of blood flow in the diaphragm but otherwise consistent with the observations made in other skeletal muscles and coronary circulation. In fact, a recent study conducted by Bellemare et al (12) observed the breath by breath variation of blood flow in the dog diaphragm. These authors (12), using a blood drop count rate (BDCR) from the catheterized left inferior phrenic vein and bilateral electrophrenic stimulation, reported that the blood flow through the dog diaphragm was dependent on the intensity of contraction and the duration of contraction. The intensity of contraction was expressed as the ratio of Pdi over maximal Pdi; Pdi/Pdimax, and the duration of contraction, normally called duty cycle, was the ratio of inspiratory time (ti) over the total time taken for one respiratory cycle (ttot); ti/ttot. The product of these two ratios was called the tension time index of the diaphragm or TTdi. From their results it was observed that large combinations of Pdi's and ti/ttot's could be used which would limit blood flow and produce postexercise hyperemia. Thus no single Pdi critical or ti/ttot critical would produce a limitation in blood flow, but the product of these two parameters yielded a single TTdi critical which would impede blood flow and cause post-exercise hyperemia. The TTdi critical for the dog diaphragm was approximately 0.20. Thus under isometric contractions (ti/ttot = 1) the dog diaphragm performs like other skeletal

muscles, i.e. blood flow limitation occurs at 20% of maximal tension. This concept of dynamic occlusion has lately been supported by another group of investigators. Bark et al (10) using a diaphragmatic strip preparation found results that were similar to those of Bellemare et al (12). They reported that development of moderate to high levels of diaphragm tension compresses the intradiaphragmatic vasculature and impedes blood flow through the diaphragm.

Several factors may explain the differences in diaphragmatic circulation observed by various investigators. The techniques used by certain investigators to evaluate blood flow with radioactive labelled micropheres determines the mean or average blood flow to an organ (48), in this case the diaphragm. The breath by breath variations that can occur are not apparent with such techniques. can observe increases in absolute blood flow relative to resting conditions but it does not necessarily mean that the blood supply is sufficient to maintain the metabolic Robertson (83-85) and Rochester (86-88) might not demands. have achieved contraction patterns susceptible to produce blood flow limitation. TTdi calculations from Rochester's and Robertson's data seemed to be well below the TTdi, found by Bellemare et al (12), necessary to produce fatigue in the dog diaphragm. Furthermore Robertson et al (83) did not find an increase in diaphragmatic venous lactate, suggesting that the blood supply was probably adequate. These authors

(83-88) did not measure post-exercise hyperemia which is an indication of inadequate blood flow during the contraction.

The diaphragm, up to now, seems to behave as another skeletal muscle susceptible to numerous factors that can affect its circulation. However, the diaphragm has a particular arrangement compared to the other skeletal muscles of It is a partition between two compartments, thoracic and abdominal. The thoracic surface of the diaphragm during inspiration is exposed to increasing negative pleural pressures (Ppl) while simultaneously the abdominal surface is subjected to positive abdominal pressures (Pab). there exists a transmural pressure in the muscular leaflet of the diaphragm tending to expand its cross-sectional area. Recent investigators (17) have shown that changes in abdominal pressure or pleural pressure have direct effects on diaphragmatic circulation. These authors (17) reported that during sustained diaphragmatic contractions high Pab decreased diaphragmatic circulation, whereas a sustained contraction that developed a high Ppl had the opposite effect, it increased diaphragmatic circulation. They concluded from these observations that a high Pab reduced the arterial perfusion driving pressure and that a high Ppl increased the cross-sectional area thus reducing impedance to diaphragmatic circulation.

Local neural and humoral factors

A number of intrinsic factors modulate the diaphragmatic vascular tone, they are neural and humoral. studies (8, 44) have shown that certain humoral factors such as hypoxia have a direct effect on diaphragm blood flow. One study in particular (8) measured diaphragm blood flow during constant activation and hypoxia. The results indicated that diaphragmatic blood flow was greater by 20% when compared to normoxic conditions. This suggested that hypoxia had a direct vasodilating effect on the vascular bed which compensated to maintain oxygen delivery at a rate susceptible to maintain oxygen consumption at a comparable level to the one observed during normoxia. Another characteristic of the diaphragmatic blood flow similar to other skeletal muscles (7) and the coronary circulation (57) is the ability for autoregulation of its circulation. et al (52) has shown that the diaphragmatic circulation was autoregulated in the range of 70 - 120 mmHg of arterial perfusion pressure. Below this range diaphragmatic circulation became linearly related to the arterial perfusion pressure. This characteristic of autoregulation was observed at three levels of inspiratory work. This is an important finding indicating that the diaphragm can compensate effectively sudden drops in arterial perfusion pressure or cardiac output (hemorrhagic or cardiogenic shock).

Another role that can be attributed to skeletal muscle blood flow is the washout of catabolites during or following muscle activity. The amount of blood volume delivered to a skeletal muscle per unit of time and muscle mass has been shown to be related to its endurance to exercise, both because blood delivers O2 and nutrients, and because of its ability to wash-out catabolites generated during contractile activity (4). This maintains an adequate extracellular environment susceptible to the maintenance of continuous muscle activity. A recent study conducted by Supinski et al (96) supported this argument. They demonstrated that diaphragmatic fatigue could be reversed by increasing diaphragm blood flow. In their study diaphragmatic blood flow was increased by elevating the perfusion pressure of the phrenic artery in a diaphragmatic strip preparation. They concluded that greater flow rates produced an increase in the Wash-out of the catabolites and helped to maintain the extracellular environment optimal for continuous muscle activity.

II SKELETAL MUSCLE BLOOD FLOW AND MUSCLE FATIGUE

Barcroft and associates (6) has demonstrated that calf muscle blood flow in the calf muscle of the leg in humans increased during strong rhythmic contraction. They also observed that blood flow during the contraction phase was lower than between contractions. This suggests that blood flow could become limited during forceful sustained contractions.

tions and could eventually lead to fatigue. In support to this concept numerous investigators have shown that the rate of fatiguability of respiratory muscles increases in the face of decreased blood perfusion. Hussain et al (50-51) has shown that septic shock reduces tremendously the endurance time of the diaphragm to an added respiratory load, and this correlates with a decreased diaphragmatic circulation. Cardiogenic shock and hemorrhagic shock produce similar results (89-100). Thus a large amount of evidence supports the concept of increased fatiguability when the contracting muscle is faced with a reduced blood perfusion.

It is thought that an adequate blood flow is necessary to maintain constant levels of high energy phosphate coumpounds (ATP). Several studies (24, 92), however, have demonstrated that ATP stores are not depleted during forceful contractions suggesting that the contractile proteins do not fail due to a lack of energy stores but probably due to the build up of metabolic byproducts in the intracellular or This is possibly because extracellular environment (92). inadequate blood perfusion (lack of O2) may lead the contracting muscle to revert to anaerobic pathways thus leading to increased intracellular hydrogen ions concentrations (61, It has been shown that activation of glycolitic pathways cause an increase in intracellular hydrogen and phosphate ions which lead to the disruption of membrane events at the sarcoplasmic reticular level. On the other hand muscle blood flow is involved in the wash-out of catabolites during muscle activity. It has been demonstrated by Barclay and co-workers (4) that in limb muscles the rate of wash-out is an important determinant of muscle endurance.

III RELEVANCE OF PRESENT WORK

The anatomy and functional interrelationship of the arteries supplying the diaphragm remains to be answered. we have seen in the previous section it is known that numerous arteries perfuse the diaphragm. However, it is unknown if the arteries are end vessels like those supplying the heart and brain or if they communicate extensively among themselves. Recent evidence (21-23, 60) seems to favor the latter, and in addition it is suspected that the diaphragmatic arteries anastomose extensively since diaphragmatic infarct is not a clinical entity reported in the medical literature, and nor is diaphragmatic dysfunction reported following internal mammary or phrenic artery ligation and graft following myocardial coronary angioplasty. Knowledge of the relationship of the diaphragmatic arteries within it's muscular leaflet would help to understand how arterial perfusion is produced and maintained in the face of different forms (mostly thoracic vs mostly abdominal breathing) and tension of contractile activity. The anatomy of the diaphragmatic circulation is described in Chapter 2. The issue that is addressed is the anastomoses among arteries that perfuse the diaphragm and the anastomoses of the venous vessels that drain the diaphragm.

Anatomically if anastomoses of arteries are found it does not necessarily prove that these communications are physiologically competent. Anatomical studies are usually conducted postmortem and the tissues investigated are not necessarily fresh which may lead to distorted conclusions. In studying the vascular organization in organs one must inject a coumpound or coloring agent that will make the vessels of interest visible. In so doing the organs are artificially perfused by the investigator and if the perfusion pressure is not kept constant or becomes too large, collateral communications may open which otherwise under physiological conditions would remain closed or inexistant. well, blood clots may form in an anatomical specimen which would prevent the injection of colorings in some of the vessels that perfuse an organ. Physiological confirmation of an anatomical description is a valued complement in order to validate a proposed anatomical model. The end to end anastomosis of the inter-arterial communications within the muscular leaflet of the diaphragm are investigated in Chapter 3 and Chapter 4 under physiological conditions. Chapter 3 describes the functionality of each vessel supplying the diaphragm (phrenic arteries, internal mammary arteries and intercostal arteries) in maintaining contractility of the diaphragm at the fatigue threshold as proposed by Bellemare et al (11, 12). Chapter 4 addresses the issue of left and right hemidiaphragmatic arterial communications.

In the first section of the introduction it was mentioned that numerous factors can affect the diaphragmatic circulation. These include mechanical, neural, and humoural factors. However mechanical factors, such as the level of tension, seem to be the most important in modulating diaphragmatic circulation. The mechanical factors relevant to the muscles of respiration are the pattern of breathing (frequency of breathing and the duty cycle) and the tension of the respiratory muscles developed with every breath. These two parameters, as described earlier, affect diaphragmatic circulation directly. Bellemare et al (12) showed that blood flow to the diaphragm became limited when the TTdi developed (regardless of the Pdi and the duty cycle) was greater than 0.20. On the other hand, Buchler et al (16) demonstrated that a high frequency of breathing (101 -160 breaths/min) increased diaphragmatic blood flow. Nonetheless, Buchler et al (16) observed that a high frequency of breathing combined with an elevated duty cycle (0.75) resulted in a decreased diaphragmatic circulation when compared to values obtained at low breathing frequencies (10 - 49 breaths/min) with the same duty cycle. results obtained by these two investigators indicate that the pattern of contraction and the frequency of breathing have direct effects on the diaphragmatic circulation.

However, diaphragmatic vascular response to these parameters and especially venous drainage remain unknown. Chapter 5 describes the response of the various vessels draining the diaphragm to a number of different breathing patterns at two levels of different breathing frequencies. The object of this investigation is to measure the contribution of the various vessels draining the diaphragm.

Reid and Johnson (81) have shown that maximal diaphragmatic blood flow rate was related to the perfusion pressure by a quadratic equation when the diaphragmatic vasculature was made completely flaccid. Thus under normotensive conditions maximal diaphragmatic circulation ranged in the area of 210 ml/min/100g. This maximal blood flow value can be defined as the optimal (highest) blood flow rate obtained for a given duty cycle under conditions of iso-tension and iso-perfusion pressure. However, in their study the duty cycle at which maximal blood flow occurred was not men-A close examination of the data obtained by tioned. Bellemare et al (12) and other investigators (9, 10, 89) shows that the blood flow rate was optimal at a duty cycle of 0.5. In addition, Buchler et al (16) has shown that a high duty cycle impedes diaphragmatic blood flow. Thus, the available data in the literature seems to indicate that the duty cycle is an important modulator of diaphragmatic circu-Chapter 6 describes the role of the duty cycle in lation. modulating diaphragmatic circulation. The issue being explored is the role of the duty cycle in producing an optimal blood flow rate regardless of the tension being developed by the diaphragm.

Therefore in summary definite conclusions on diaphragmatic blood flow to understand its role on fatigue cannot be made. Our intent was to develop a dog preparation suitable to study the effects of tension and timing of contraction on the blood flow of the diaphragm. Our objectives were:

- I) to describe the functional anatomy of the three major arterial supplies to the diaphragm. This description is found in chapter 2 which is published in the Journal of Applied Physiology. Reference: Comtois, A., W. Gorczyca and A. Grassino. Anatomy of diaphragmatic circulation. J. Appl. Physiol. 62 (1): 238-244, 1987.
- II) to explore how the "functional regions" (costal and crural) of the diaphragm are affected by blood flow restriction. This description is found in chapter 3 which is published in the Journal of Applied Physiology. Reference: Comtois, A., F. Hu and A. Grassino. Restriction of regional blood flow and diaphragmatic contractility. J. Appl. Physiol. 70 (6): 2439-2447, 1991.

- III) to determine the existence, if any, of arterial anastomosis between both hemidiaphragms. This description is found in chapter 4 which is published in the Journal of Applied Physiology. Reference: Hu, F., A. Comtois and A. Grassino. Effect of separate hemidiaphragm contraction on left phrenic artery flow and O2 consumption.

 J. Appl. Physiol. 69 (1): 86-90, 1990.
- IV) to determine the effects of various contraction the venous outflow of patterns on the diaphragm. This description is found chapter 5 which is published in the Journal of Applied Physiology. Reference: Hu, F., Comtois, A., and A. Grassino. Contractiondependent modulations in regional diaphragmatic blood flow. J. Appl. Physiol. 68 (5): 2019-2028, 1990.
- V) to determine the role of the duty cycle in modulating the blood perfusion to the diaphragm. This description is found in chapter 6 which has been accepted the Journal publication in of Applied Physiology. Reference: Hu, F., A. Comtois, and A. Grassino. Optimal diaphragmatic blood perfusion. Accepted for publication in the J. Appl. Physiol.

CHAPTER 2

ANATOMY OF THE DIAPHRAGMATIC CIRCULATION

SUMMARY

The diaphragmatic circulation was studied in 48 mongrel dogs weighing 10-35 Kg by injecting acrylic coloring into the arteries and veins of the diaphragm. The phrenic arteries and internal mammary arteries were found to anastomose head to head, forming an internal arterial circle around the medial leaflet of the diaphragm tendon. arterial circle emitted vascular branches that travelled between muscle fibers towards the periphery of diaphragm. These ramifications anastomosed with vessels of the intercostal arteries to form costo-phrenic arcades all along the fibers of the crural and costal diaphragms. intercostal arteries were related to one another by small vessels within the muscular diaphragm, thus forming an arterial ring around the insertions of the diaphragm on the The venous drainage has an anatomical distribution similar to that observed on the arterial side, but with the additional presence of valves that could play a role in directing blood flow.

Keywords: Dog, diaphragm, diaphragm circulation, respiratory muscles, anatomy of the diaphragm, arterial circulation of the diaphragm.

INTRODUCTION

Bellemare et al (12) did retrograde injections of methylene green dye in the left phrenic vein, and reported numerous important anastomosis between the intercostal and phrenic veins, as well as with the ipsilateral internal Such anastomosis had not been seen in mammary vein. previous studies (83-88). However, these investigators (12, 83-88) did not focus on macroscopic circulation of the diaphragm, since they were interested in breath by breath modulation of blood flow within the diaphragm. Additionally the coloring injections made in some of these studies were localized to specific regions (12, 86). Even though most general anatomy textbooks (30, 33, 70, 98) mention the various arterial supplies to the diaphragm (superior and inferior phrenic arteries, intercostal arteries, internal mammary arteries) the anastomosis that exist between these tributaries remain poorly described. anastomosis exist among the three major blood supplies to the diaphragm, this raises the possibility of a blood flow pool reaching and leaving the diaphragm, which could make sampling and analyses of blood from one region significant of the region's metabolism and function than The work described in this paper is a presently thought. detailed description of the canine diaphragmatic macroscopic circulation, demonstrated by multiple injections of acrylic coloring into its arteries and veins.

MATERIALS AND METHODS

The study was carried out on a total of 48 mongrel dogs weighing 10-35 kg. The diaphragmatic vessels were injected with acrylic colorings (Liquitex, Binney and Smith Inc., Easton, PA.), via the phrenic, internal mammary, and intercostal vessels as indicated in Table 1. From Table 1 we can see that 33 dogs were injected for the study of the arterial circulation, 12 dogs for the study of the venous circulation, 1 dog had both circulatory systems injected, and 2 dogs were studied for venous valves. Before being injected into the diaphragmatic vasculature, the acrylic was with water and acrylic coloring (1:2). After dilution the coloring was able to reach vessels with external diameters of approximately 50-75 microns (uM). Usually, the acrylic would settle in about two hours in the smallest vessels. order to prevent leaking of acrylic from the largest vessels, two to three cc of acrylic mixed with liquified gelatine was injected into the largest arteries. Afterwards the solidified gelatine would prevent reflux of coloring from the vessels. The colors red and green (green provides better visual contrast against the reddish background of the muscle tissues) were used to highlight the arterial circulation, while blue and yellow were used in the venous circulation. After preliminary studies to develop the injection techniques, we were able to set criteria for reproducibility of the various vascular configurations.

TABLE 1
Vessels cannulated for injection of coloring

Systems studied	И	Injected via	Ŋ	Bad
				preparations
Arterial	·			
circulation	33	PA	16	3
		AMI	5	
		ICA	4	
		PA,IMA	2	
		PA,ICA	1	
		PA, IMA, ICA	5	1
Venous				
circulation	12	PV	10	3
		ICV	1	1
		IMV,ICV	1	1
Both systems	1	PA, ICA, PV		
Venous valves	2			
TOTAL	48			9

PA, phrenic arteries; IMA, internal mammary arteries; ICA, intercostal arteries; PV, phrenic veins; IMV, internal mammary veins; ICV, intercostal veins.

These configurations were; 1) anastomosis between phrenic and intercostal arteries; 2) anastomosis between phrenic arteries and internal mammary arteries; and 3) anastomosis between internal mammary and intercostal arteries.

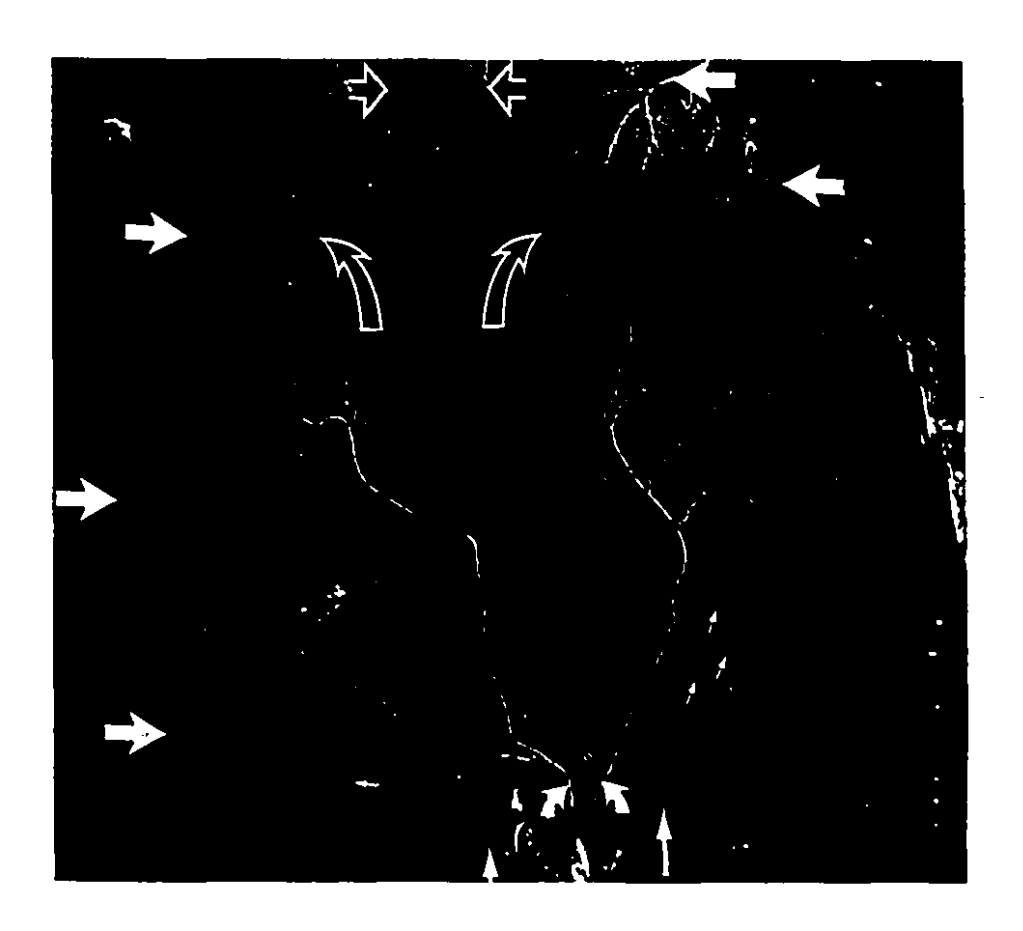
Before the injection of acrylic colorings, the dogs were given 10,000 units of heparin to prevent the formation of thrombi in the vessels. They were subsequently exsanguinated by a venous vent (femoral vein) and the systemic circulation rinsed by injecting, via the thoracic aorta, normal saline solution until there was virtually no more blood flowing out of the femoral vein. All the injections of coloring were done in situ by hand operated syringes. The perfusion pressure was kept below the arterial pressure, and did not induce extravasation of the coloring material into the surrounding tissues. The amount of acrylic coloring injected was relative to the amount of filling of the vessels upon visual examination.

Upon completion of the injections the dog's trunk was skinned, and the animal transected at a high thoracic and low lumbar level. This maintained the insertions of the diaphragm to the sternum, ribs, and vertebral column intact. This transected portion was placed upside down in a container so that the visceral mass could push on the diaphragm and give it a convexity towards the thoracic cavity. The container was then filled with 10% formaldehyde and the tissues allowed to fix for approximately 10 days.

Thus the geometrical configuration of the diaphragm resembled that seen in situ. After the period of tissue fixation, the thoracic and abdominal viscera were removed. so that the diaphragmatic vessels could be exposed for examination under a dissecting microscope. In a further process, the diaphragmatic tissue was cleared to reduce the tissue optical density. The clearing procedure was as follows: the tissues were placed in 25% ethanol, and moved to 50%, 75%, 95%, and 100% ethanol at intervals of 24 hours. After the absolute ethanol step, the tissues were placed in 100% methyl salicylate for 24 hours. This last step was the process of clearing. The clearing of the tissues permitted visualization of the vessels previously hidden between the muscle fibers, thus allowing us to gain a three dimensional perspective of the vascular architecture via dissecting microscopy observation.

RESULTS

Figure 1 is a panoramic abdominal view of a cleared diaphragm. It shows a head to head anastomosis of the right phrenic artery with the right internal mammary artery, as well as anastomosis of the left phrenic artery with intercostal arteries. The internal mammary and phrenic arteries form an internal arterial circle around the medial leaflet of the diaphragm tendon. A close examination of the colored preparations does not show the apparent gap indicated with the curved empty arrow in Fig. 1. Inspection



Abdominal view of diaphragm injected with acrylic coloring and cleared in methyl salicylate. Bottom: Curved white arrows point out phrenic arteries, and medium-size white arrows indicate the accessory phrenic arteries. Thin white arrows show supply to crural diaphragm. In periphery of diaphragm large white arrows show intercostal arteries. Top: internal mammary arteries are shown by empty white arrows, and head to head anastomosis of internal circle are indicated by empty curved white arrows.

under dissecting microscope shows there is no gap in the vasculature either. The origin of the phrenic arteries varied from dog to dog, but the most common origin was from the superior abdominal arteries. In some dogs the phrenic arteries originated directly from the abdominal aorta, and in about three dogs the left phrenic artery originated from the coeliac trunk. The curved full arrows in the bottom of Fig. 1 point to the phrenic arteries originating from the abdominal aorta. Although the origin of the phrenic arteries varied among different dogs, it was always present, except in one dog were no left phrenic artery was seen. its place several small arterial vessels originated from the left superior abdominal artery and irrigated the crural portion of the diaphragm. The diameter of the smallest vessels observed with this method was approximately 50-75 microns.

Costal arterial circulation: The phrenic arteries and internal mammary arteries anastomose head to head to form an internal arterial circle along the central tendino-muscular junction of the diaphragm muscular leaflet. This arterial ring gives off centrifuge branches travelling between the muscle fibers towards the periphery of the diaphragm as shown in Fig. 2, where the costal diaphragm is seen illuminated from underneath and photographed via a dissecting microscope magnified at x 20. These branches anastomose with ramifications of the intercostal arteries

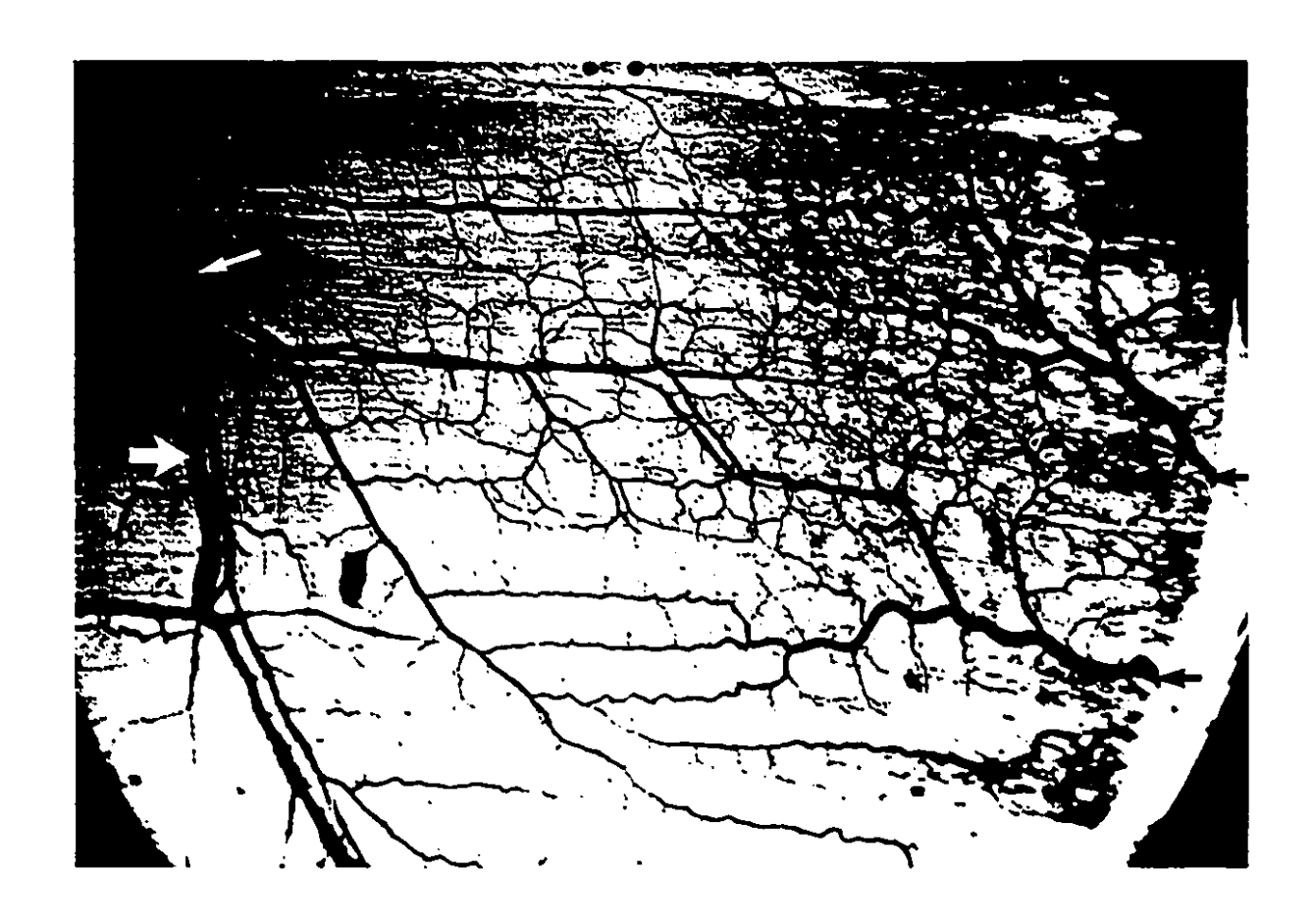


Figure 2. Magnified view (x 20) of a costo-phrenic arcade. Small white arrow, left, indicates a branch of internal circle. Small dark arrows, right, show branches of intercostal arteries. Large white arrow points to a branch of venous drainage.

(right arrows in Fig. 2) to form costo-phrenic arcades. The small white arrow shows a collateral ramification of the internal circle giving off branches that anastomose head to head with branches of intercostal arteries (indicated by the small dark arrows on the right side of the lateral-costal diaphragm). The vessels follow the muscle fibers in a parallel fashion. By communicating among themselves, via small branches within the muscular diaphragm, the intercostal arteries forms a ring in the neighborhood of the area of the diaphragm on the ribs, as seen between the arrows on the right side.

Fig. 3 is a diagram illustrating the results we have obtained. The costal diaphragm is irrigated by three main sources (dark arrows): the phrenic arteries and internal mammary arteries forming the internal circle, and the intercostal arteries which anastomose head to head with ramifications of the internal circle to yield costo-phrenic arcades all along the fibers of the costal diaphragm.

Crural arterial circulation: The head to head anastomosis of the phrenic arteries and internal mammary arteries (forming the internal circle), are shown in Fig 1, by the empty curved white arrows. The small white arrows in the same figure indicate the collateral vessels of the internal circle which supplies blood to the crural portion of the diaphragm. The segments of the diaphragmatic crura, most proximal to their origins at the level of the lumbar

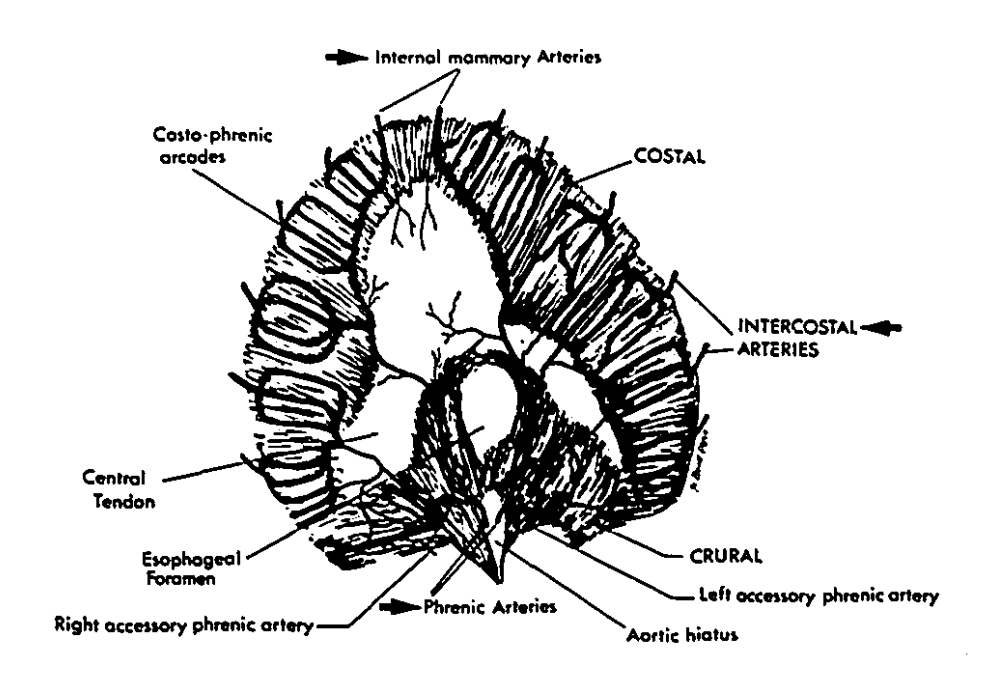


Figure 3. Abdominal view of diaphragm illustrating the internal circle formed by the phrenic and internal mammary arteries. In addition branches of intercostal arteries communicating via costo-phrenic arcades with the internal circle.

Dark arrows show the three main arterial supplies to the diaphragm

vertebras (L3 and L4), are supplied by branches of the vertebral arterial plexus. In about 80% of the dogs studied, a small arterial vessel, that we named "accessory phrenic artery" (medium sized white arrows in bottom of Fig. 1), would originate from the right and left superior abdominal arteries distal to the origin of the phrenic arteries. This accessory phrenic artery would rise towards the crura of the diaphragm in a fashion similar to the phrenic arteries (some dogs had two to three accessory phrenic arteries) and then anastomose with branches of the internal circle and some branches of the twelfth and thirteenth intercostal arteries to form costo-phrenic arcades in the crural portion of the diaphragm. The aortic hiatus of the diaphragm is supplied by small collateral vessels of the phrenic arteries. The ramifications of the internal circle bringing blood to the eosophageal foramen anastomose head end to head on the ventral side of the foramen, thus permitting the right and left phrenic artery to communicate with each other.

Sternal arterial circulation: The sternal area, on either side of the median line of the diaphragm, is supplied by branches of the right and left internal mammary arteries. The right and left ventro-costal portions of the diaphragm (immediately adjacent to the sternal area on either side) receives its blood supply from the musculophrenic arteries. These latter arteries originate from their respective right

and left internal mammary arteries. The musculophrenic arteries anastomose with branches of the internal circle, in a manner similar to the intercostal arteries with the internal circle, to form costo-phrenic arcades in the ventro-costal portions of the diaphragm. As mentioned earlier, these costo-phrenic arcades are found in the costal and crural portions of the diaphragm. We did not observe any significant head to head anastomosis between arteries of both hemidiaphragms.

Reproducibility of arterial configurations: The various arterial configurations of the diaphragm are given in Table 2. The internal arterial circle was not completely visualized in 24% of cases. In 21% of cases no anastomosis between the internal mammary arteries and intercostal arteries was seen. One of the reasons why these relations were not observed may be due to insufficient filling of the vessels.

Intercostal arteries: The intercostal arteries, which are found immediately below the ribs, can be separated in two groups: 1) CEPHALAD (T1-T8) intercostal arteries, and 2) CAUDAL (T9-T13) intercostal arteries. The posterior CEPHALAD intercostal arteries originating from the thoracic aorta anastomose directly with the anterior CEPHALAD intercostal arteries that originate from the internal mammary arteries. The posterior CAUDAL intercostal arteries, while still communicating with the anterior CAUDAL

TABLE 2
Configuration of diaphragmatic blood supply

Vascular	Found in	Number of	
Features	(%animals)	animals studied	
Arcades (Crural portion)	100%	29	
Arcades (Costal portion)	100%	29	
PA-ICA anastomosis	100%	29	
PA-IMA anastomosis	76%	29	
(Internal circle)			
IMA-ICA anastomosis	79%	29	

PA, phrenic arteries; ICA, intercostal arteries, IMA, internal mammary arteries.

intercostal arteries, give off branches that insert into the costal periphery of the diaphragm. The relationship of these vessels with the diaphragm can be observed best in the schematic representation of Figure 4. This view shows the diaphragm in a median plane as seen from the left, where the dorsal side is on the right. The tributaries of the caudal intercostal arteries can be seen to reach the costal periphery of the diaphragm, while small branches of the internal mammary arteries and the musculophrenic arteries reach the sternal area and ventro-costal portions of the diaphragm, respectively. As described previously these vessels join the internal circle via the costo-phrenic arcades. These vessels (internal mammary, musculophrenic, and intercostal arteries) approach the diaphragm via the thoracic side, are exposed to the negative pleural pressure swings of the thoracic compartment.

Venous circulation: The venous circulation was injected in 12 dogs via the vessels shown in Table 1, with seven dogs offering satisfactory visualization. The venous circulation shows a similar anatomic distribution in comparison with the arterial circulation. The ipsilateral internal mammary vein joined head to head with branches of the inferior phrenic vein. This head to head anastomosis formed an internal venous circle similar to the internal arterial circle in its course along the tendino muscular region. The intercostal veins joined head to head with branches of the inferior

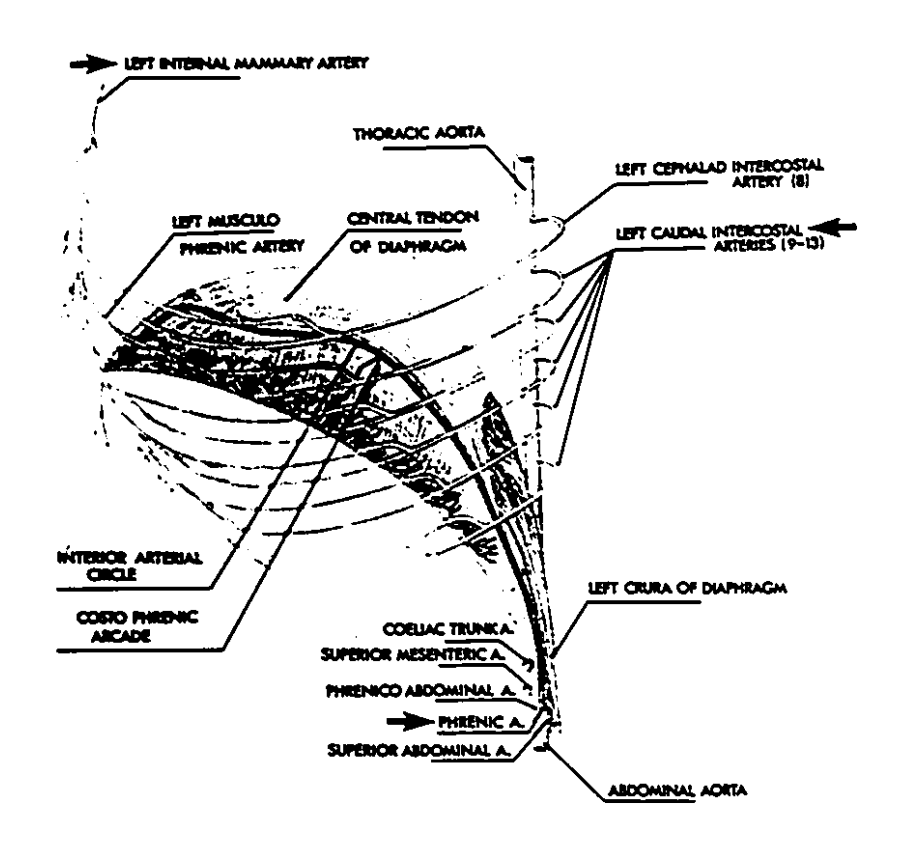
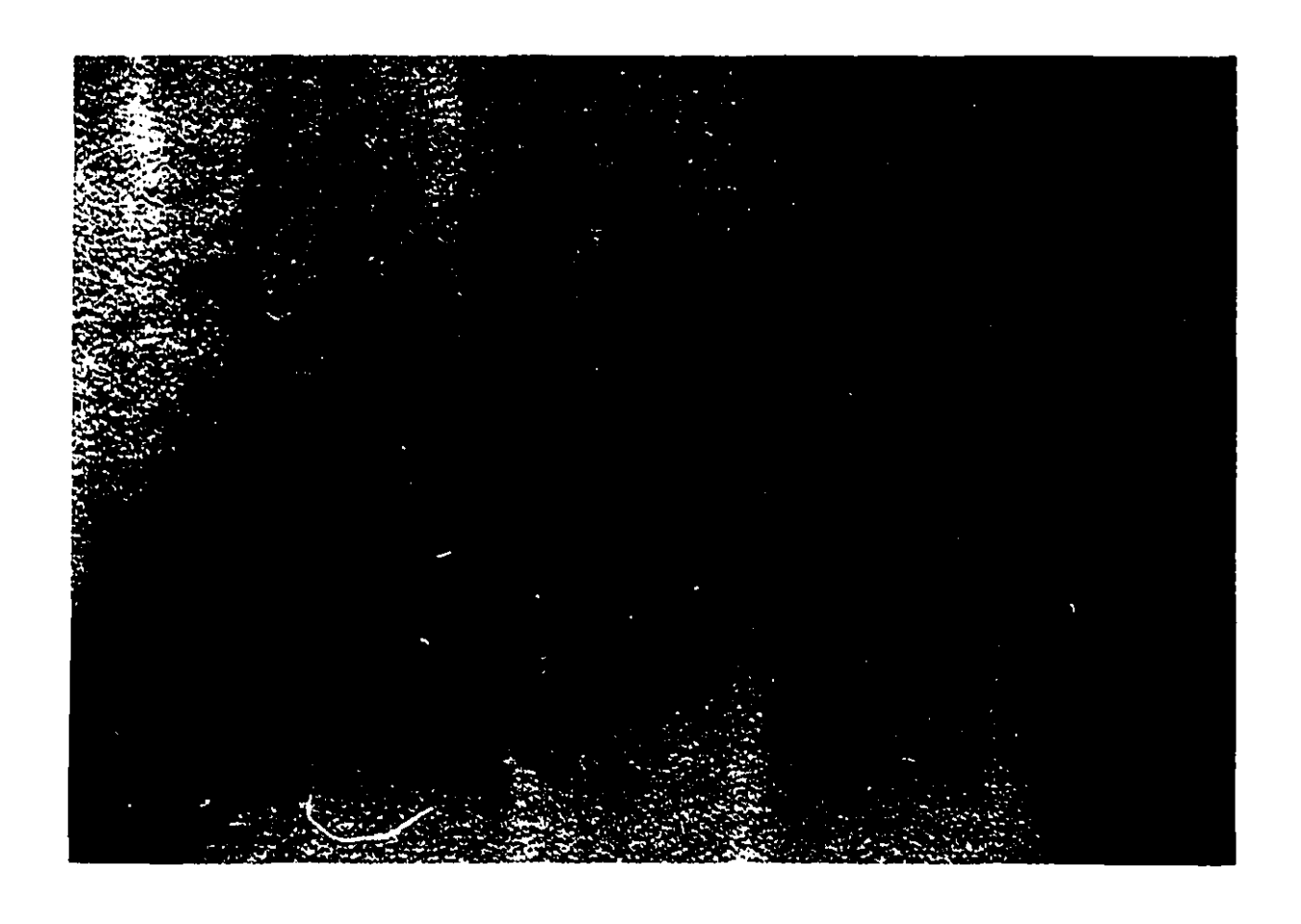


Figure 4. Schematic representation of the relation of the intercostal arteries with the diaphragm. Dark arrows point out the major arterial supplies to the diaphragm.

phrenic veins. Figure 5 is a magnified view (x45) of intercostal vein ramifications (shown on the top) joining head to head with a branch of the phrenic vein on the Numerous anastomosis, similar to the one shown in Fig. 5, formed arcades in the muscular leaflet of the diaphragm. The pattern of distribution of the venous arcades was alongside those of the arterial circulation, as shown by the large white arrow in Fig. 2. However, as seen in Fig. 5 the retrograde injection of material in the veins was stopped abruptly by valves preventing the filling of smaller veins. Histological longitudinal sections of the veins, shown in Fig. 5, showed valves in the areas indicated by the arrows. Nevertheless we were able to see arcades which were similar in configuration to the ones observed on the arterial side.

The intercostal veins draining the diaphragm belonged to the caudal group T8-T13. The posterior portions of the intercostal veins joined into the azygous vein, which brings its venous affluent to the superior vena-cava. The anterior portions of the intercostal veins reached the internal mammary veins, which then drained into the superior vena-cava as well. Thus the pattern of the venous drainage is very similar to the arterial supply.



Close-up view of a venous arcade at x45. Top is toward intercostal veins; bottom is toward left phrenic vein. Arrows indicate valves. Additional valves can be seen in vessels not indicated by arrows.

DISCUSSION

We found that the, the diaphragm is irrigated by three main arterial supplies, indicated by the large arrows in Fig. 4: 1) the phrenic arteries; 2) internal mammary arteries, which form the internal arterial circle in 76% of cases; and 3) the intercostal arteries which anastomose head to head with branches of the internal circle to form costophrenic arcades all along the muscular leaflet of the diaphragm seen in all animals. These vessels can also be observed in Fig. 1 by the curved white arrows pointing at the internal mammary arteries and the large white arrows showing the intercostal arteries.

Most of the anatomic descriptions of diaphragmatic circulation available in the literature are at best incomplete. This work is an attempt to provide a detailed description of the anastomosis between the three main arterial and venous supplies of the diaphragm. Until now the phrenic arteries were thought to be the most important in maintaining a blood supply to the diaphragm, and in effect they have the biggest diameter. However, we now suspect that the blood supply to the diaphragm has the potential to be maintained by the other two major arterial supplies. Although the individual intercostal arteries are smaller in diameter, there are at least 5 pairs contributing to the blood supply, and together with the internal mammary

arteries, they could reach all regions of the diaphragm via the head to head anastomosis system.

Previous work in other species provided partial description of some of the features we point out here. Biscoe and Bucknell (14) described the arterial supply of the cat diaphragm by injecting barium sulfate (Micropaque) into the ascending aorta until the surface vessels of the diaphragm seemed satisfactorily filled by visual inspection. Then the diaphragm was dissected and X-ray pictures taken, from which the arterial supply of the diaphragm was derived. They noticed that the intercostal arteries, T8-T13, internal mammary arteries, and the phrenic arteries linked directly with an anastomotic artery in the periphery of the central tendon of the diaphragm. Another group of investigators (54) studied the diaphragmatic circulation of camel fetuses by injecting an 8% vinylite solution into the ascending aorta. The injection was assumed to be completed when the coloring material was present in the limb's arteries. study shows a similar arterial supply to the one we described (internal mammary, intercostal T8-T13, and phrenic arteries), but no anastomosis were shown between these various tributaries (54).

Our results are in general agreement with those of Biscoe and Bucknell (14). Their anastomotic artery could be what we observe as the head to head anastomosis of the internal mammary and phrenic arteries. However it is

surprising that they did not observe the formation of any costo-phrenic arcades, as we observed. It appears that the degree of filling of the vessels could have been incomplete, since it was evaluated by visually inspecting the vessels adequate filling with Micropaque, an uncolored radiopaque material. This as well is probably the reason why Kanan (54) did not detect any anastomosis between the arteries perfusing the diaphragm of the camel's fetus in situ, where complete filling was judged by appearance of colored material in the limb's arteries without any direct inspection of the diaphragm. We insured the presence of even filling by direct observation and perfusion until the coloring was seen in each of the other two arterial systems. Further examination of the diaphragm via a dissecting microscope, after fixation in formaldehyde and clearing in methyl salicylate, allowed us to observe more details of the circulation than what was previously reported. Figure 3 is an example of the material available for our description. Although we can not rule out species differences diaphragmatic arterial circulation between cats, camels, and dogs, it is possible that a more precise control of coloring injection would reveal them. Comparing the diaphragmatic circulation of Biscoe and Bucknell (14) and Kanan (54) with ours, one gets the impression that the extra information we show is the produce of a better definition in the vessel's network caused by a more complete filling of the vessels. In the preliminary studies that we have done on the human diaphragm (cadaver), using a radio-opaque material as Biscoe and Bucknell (14) did, we observed a similar organization of anastomosis and arcades as we have seen in the dog diaphragm. Furthermore, a similar arrangement of anastomosis and arcades can be observed in the rat diaphragm (91).

The venous circulation, as shown in Fig. 2 and Fig. 5, was composed of branches running parallel with ramifications of the internal arterial circle to join intercostal veins. Other branches of the phrenic veins joined with the ipsilateral internal mammary vein. The phrenic veins inserted directly on either side of the portion of the inferior venae-cavae, which passes through the central tendon (inferior venae-cavae foramen) These anastomosis of phrenic vein ramifications with branches of intercostal veins and ipsilateral internal mammary veins were observed Bellemare et al (12). Spaltehoz, which was the first to put out a schematic picture of blood vessel distribution in the muscle, noticed that venules and larger veins usually accompany the arteries (101). This was observed in our studies as well, were veins accompanied in a parallel fashion the vessels of the arterial circulation as shown by the large white arrow of Fig. 2. Furthermore we detected the presence of valves in the venous system which could play a role in directing blood flow. These observations were similar to those reported by Biscoe and Bucknell (14) but do not support the data of Martin et al (69) which suggest that the right dome of the sheep diaphragm would be drained 90% by the corresponding phrenic vein. Our observations indicate that the drainage of the intercostal and internal mammary veins could be more important than suggested by Martin et al (69). In some instances we observed branches of phrenic veins that communicated directly with intercostal However retrograde injections of coloring were veins. difficult to obtain (due to the valves), so that these were not easily reproducible to the same extent from animal to animal. The orientation of some of the valves indicated that flow was directed toward the intercostal veins. Therefore the draining contributions of the tributaries other than the phrenic veins might be quite significant and just as important.

The technique that we used consisted of injecting acrylic colors into the vessels of the diaphragm. This is an emulsion composed of minute solid particles of plastic resin suspended in water. These particles were sufficiently large that the material was prevented from going through the capillaries. We never observed acrylic colors in the phrenic veins, thus ruling out the possibility of precapillary arterio-venous shunts. This observation agrees with what has been reported in other skeletal muscles (35, 101). But we do not know whether there are any arterio-venous shunts beyond the precapillary level. Since the

injections were usually done 5-10 minutes postmortem, the thrombi that could have developed did not seem to affect the injection of colorings. The level of pressure used to inject the colorings was similar or below arterial pressure and prevented any major extravasation into the surrounding tissues.

With the above results of the diaphragmatic circulation in mind, we can now start exploring the regional functional contribution of the three main arterial supplies. suspect that the entire diaphragm could ultimately be perfused by any single one of these three arteries. If we suppose that the phrenic arteries are the main blood supply to the crural portions of the diaphragm, on occlusion the blood supply to that area would probably still be maintained by the other major arterial supplies (internal mammary and intercostal arteries) due to head to head anastomosis between the three main arterial supplies (costo-phrenic arcades). This is probably the reason why diaphragmatic infarct and muscle necrosis have not been described. negative pleural pressure swings should increase transmural pressure gradient in two of the arterial supplies of the diaphragm, the internal mammary and intercostal arteries. On the other side, increases in abdominal pressure would lead to a decrease in diameter of the phrenic arteries. Therefore, when high and transdiaphragmatic pressures (Pdi) are generated, there could exist a Pendulluft effect in blood flow between the arteries exposed to the pleural pressures and those exposed to abdominal pressures.

In conclusion, the diaphragmatic circulation is a complex vascular system designed to supply the diaphragm from three separate sources made possible via a head to head arterial anastomotic system somehow similar to the polygram of Willis in the brain. The need for a such a design is not clear; however we speculate that it may be related to the fact that the diaphragm is often subjected to high and variable transdiaphragmatic pressures, i.e., negative thoracic and positive abdominal pressures. This may subject the abdominal or chest wall vessels to higher transmural pressure, creating a variable resistance affecting alternatively one or the other of the blood supply or drainage sources.

CHAPTER 3 RESTRICTION OF REGIONAL BLOOD FLOW AND DIAPHRAGMATIC CONTRACTILITY.

SUMMARY

We have tested the hypothesis that the diaphragmatic head to head arterial anastomosis system should maintain adequate diaphragmatic function even during occlusion of some of its arteries. In 6 anesthetized, open chest dogs, left phrenic vein blood flow (Qphv) was measured by pulsed Doppler. Contractility was measured by sonomicrometry in the left costal and crural diaphragm. The diaphragm was paced for 15 minutes by continuous bilateral supramaximal phrenic nerve stimulation. In 5 separate runs the following arteries were occluded at min 5: 1, left phrenic artery (PA), or 2, internal mammary artery (IMA), or 3, PA and IMA, or 4, descending aorta (DA), or 5, DA and IMA. Occlusion was then released at min 10 of the run. In runs 1, 2 and 3 there were no changes in contractility in costal or crural diaphragm, and no changes in Qphv. However, in runs 4 and 5, Qphv decreased to 55.2% ± 7.4% and 24.0% ± 6.5% of control values, respectively. In run 4, % max. shortening from FRC (%LFRC) of the crural diaphragm decreased by 39.1%, while %LFRC of the costal diaphragm increased by 41.4%, and Pab decreased by 47.0%. In run 5, Pab decreased by 53.5% and %LFRC of the crural and costal diaphragm decreased by 45.5% and 5.8%, respectively. Also relative post-occlusion hyperaemia was greater in 5 (64.8%) than in 4 (40.2%). conclude: the blood supply by intercostal arteries is maintain normal costal and sufficient to crural contractility in a diaphragm developing mild level of work (TTdi < 0.20), and IMA perfusion alone can sustain normal contractility of the costal but not of the crural diaphragm.

Keywords: Diaphragm blood flow, ischemia, fatigue, diaphragmatic circulation, canine diaphragm, respiratory muscle.

INTRODUCTION

In the heart it is well demonstrated that acute occlusions of coronary arteries, lasting from 5-15 min, cause severe loss of myocardial function in the zone supplied by the occluded artery (39, 40). However unlike the heart the diaphragmatic arteries communicate extensively between themselves (20). Morgan and Johnson (71) observed that occlusion of the left inferior phrenic artery did not affect diaphragmatic circulation during resting breathing, but did so during inspiratory resistive breathing where blood flow was decreased by 32% in the crural and 20% in the costal segments. However diaphragmatic work, measured by lower body plethysmography, remained unchanged, both during resting conditions and inspiratory resistive breathing, suggesting contractility was not affected. A study done by Bellemare et al (12) revealed numerous anastomoses between left inferior phrenic vein and the ipsilateral intercostal and internal mammary veins in the canine diaphragm. In a subsequent study (20) the pattern of interarterial and intervenous anastomoses was described within the muscular leaflet of the diaphragm. It was found that the three major arterial supplies communicate extensively among themselves and that the venous vessels had a similar anastomosis without arterio-venous pattern of eny However these studies were conducted anastomoses. postmortem, thus with inert vessels, and the physiological functionality of these arterial anastomoses still remained unclear. Therefore we hypothesized that acute occlusion of some of the diaphragmatic arteries, in vivo, may not cause loss of diaphragm function in its costal and crural segments. The purpose of this study was to quantify the extent of regional blood flow limitation required to induce failure of diaphragmatic contractility. We chose to test this hypothesis while the diaphragm was paced submaximally and generated a tension time index (TTd:) of 0.20, which is at the fatigue threshold (11).

MATERIALS AND METHODS

Surgical and instrumentation procedure

The study was conducted on 6 anesthetized open chest mongrel dogs. The initial anaesthetic dose was 35 mg/Kg of sodium pentobarbital administered intravenously. Supplemental doses were given thereafter to maintain a level of anaesthesia that abolished the corneal reflex. weight of the animals ranged from 14-38 Kg. mental set-up is illustrated in Fig. 1. Arterial pressure was recorded from the left common carotid artery via a liquid filled catheter connected to a pressure transducer (Sanborn, B-670B). The common jugular vein, of the same side, was cannulated to administer saline and anaesthetic. The left femoral artery was cannulated to obtain arterial blood samples for blood gas analysis.

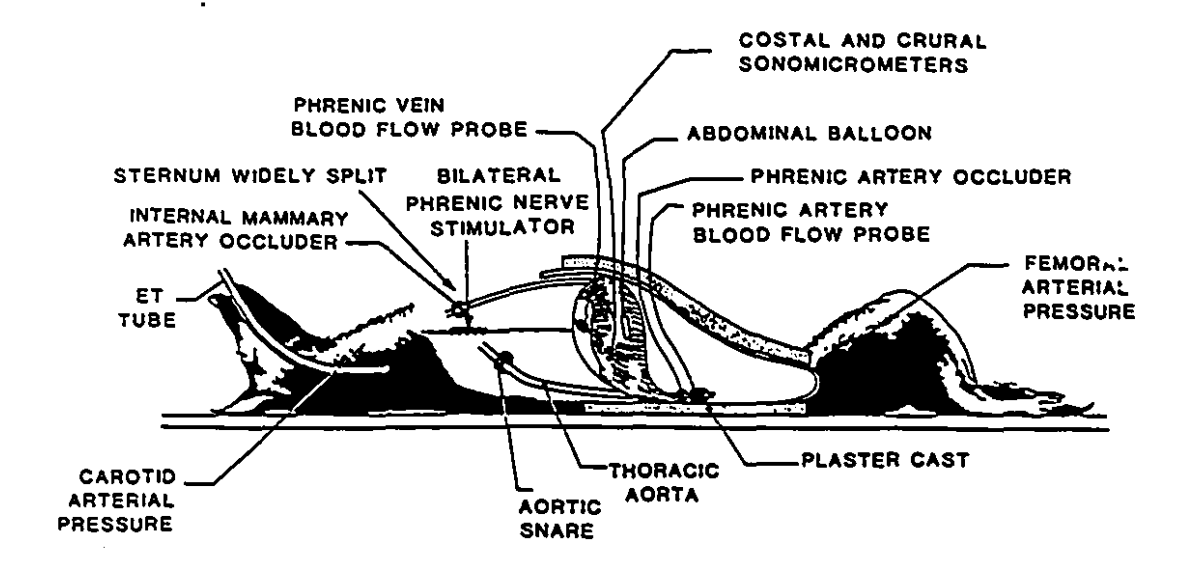


Figure 1. Experimental set-up. ET, endotracheal tube. See text for explanation.

A midline laparotomy from the xiphoid process to the lower third of the abdomen permitted access to the left abdominal surface of the diaphragm. The left phrenic vein was dissected free from the central tendon so that a 2.5 mm diameter blood flow probe (Valpey-Fisher, model HDP-25-20S), designed to operate with a 20 MHz ultrasonic pulsed Doppler module (Valpey-Fisher, model PD-20), could be fitted around it.

The left phrenic artery was dissected free from the retro-peritoneum proximal to its point of origin on the left superior abdominal artery and was fitted with a hydraulic vessel occluder (2 cm in diameter) (In Vivo Metric Systems, model OC2). This occluder was used to perform reversible occlusions of the left phrenic artery.

Piezoelectric crystals were placed in the crural and costal left hemidiaphgragm. These crystals measured length changes, via sonomicrometry as described by Newman et al (73), using 5 MHz ultrasound length gauge modules (Valpey-Fisher, model LG-1). Abdominal pressure (Pab) was recorded by the conventional method (11, 12, 56, 73) using a thin walled latex balloon catheter and pressure transducer (Validyne, model MP-45.4). The abdominal balloon was placed between the liver and the stomach. Afterwards the abdomen was closed in three layers in order to obtain a good seal of the abdominal compartment.

A midline sternotomy was performed to expose the descending aorta proximal to the origin of the left subclavian artery, the left internal mammary artery, and both phrenic nerves alongside the superior vena cava. A snare made of umbilical tape placed through a plastic tubing was passed around the descending aorta at the level of dissection mentioned above. A hydraulic vessel occluder, 3 cm in diameter (In Vivo Metric Systems, model OC3), was placed around the left internal mammary artery. The occluder was positioned 10-15 cm from its point of origin on the left subclavian artery. The snare and hydraulic occluder were used to occlude reversibly the descending aorta and left internal mammary artery, respectively. Silver wire stimulating electrodes were placed on each exposed phrenic nerve and isolated from the surrounding tissues. were electrodes were connected to an electrical square wave stimulator (Grass, model S-48). The stimulator was used to The chest was left opened impose diaphragmatic pacing. (thus pleural pressure was equal to atmospheric pressure) but nevertheless covered with a piece of cellophane to prevent drying of the pericardium, lungs, and especially both phrenic nerves.

A cast was then placed around the abdomen, which covered the abdominal trunk from the 11th rib to the iliac crests. This cast was used to determine Pab max and maintain a constant level of Pab/Pab max generation during di-

aphragmatic pacing. In applying the cast great care was taken to remove as much air as possible from the abdominal compartment.

Left costal and crural segment length changes (Lcos and Lcru, respectively), Pab, left inferior phrenic vein blood flow (Qphv), and left common carotid arterial pressure (Part) were recorded simultaneously on an eight channel strip chart recorder (Hewlett Packard, model 7758A) and an eight channel magnetic tape recorder (Hewlett Packard, model 3968A). The recorded signals from the magnetic tape were then digitized at a sampling frequency of 100 Hz for computer analysis.

The Loos, Loru, and Qphv signals were obtained from the length gauge modules and pulsed Doppler, mentioned previously, which were all mounted in a six channel mainframe Pulsed Doppler blood flow/Dimension System (Valpey-Fisher, model VF-1), thus offering the possibility of measuring simultaneously and with the same unit, blood flow and length changes. The signals of these modules were sent to medium gain amplifiers (HP, model 8802A) to be recorded on paper and magnetic tape, as previously mentioned. Part and Pab signals were obtained from pressure transducers which were connected to pressure amplifiers (HP, model 8805C).

Left inferior phrenic vein flow probe calibration

Flow volume calibrations for Qphv probes, were done on an additional group of 6 anesthetized mongrel dogs following the procedure described by Hu et al (47). The following is a brief description of the procedure. Anaesthesia was performed and maintained as above. The phrenic nerves were mounted with stimulating electrodes as described above. Flow probes, the same used during the studies, were implanted around the left inferior phrenic vein as explained above. Upon completion of surgical procedures, the animals were heparinized (1000 units/Kg).

The left inferior phrenic vein was cannulated (inside diameter, 1.8 mm; outside diameter, 2.0 mm), via the left femoral vein, in order to permit collection of blood volume according to time. Blood volume was collected in a graduated cylinder while simultaneously recording the Doppler shift 'f. Left inferior phrenic vein blood volumes were collected at various flow rates. These were obtained by pacing the diaphragm at various levels of phrenic nerve stimulation. Diaphragmatic pacing would be initiated and maintained for three to four minutes in order to permit stabilization of blood flow and systemic arterial blood pressure. Following stabilization, blood would be collected in a graduated cylinder for a period ranging from one to two minutes. The collected blood volumes would be standardized according to time as ml/min and plotted against their

respective Δf . The equation of this relation would then be the calibration factor used to convert Δf signals (provided by the left inferior phrenic vein flow probe during the actual experiments) into flow volume values.

Experimental protocol

At the beginning of each experiment the Pab max would be determined by supramaximally stimulating the diaphragm via both phrenic nerves. This was done by fixing the frequency at 100 Hz and adjusting the voltage so as to obtain the highest Pab generated by the diaphragm. Then the voltage would be increased by 20% and set at this position for the remainder of the experiment. This voltage was found to range from 8-10 volts. Afterwards the frequency was adjusted so as to obtain a Pab/Pab max equal to 50%. Usually a stimulating frequency of 20-30 Hz would yield the desired level.

Diaphragmatic pacing was done at a rate of 15 contractions per minute (Ttot = 4 sec; Ti = 1.6 sec; Ti/Ttot = 0.4). TTdi, being the product of Pab/Pab max * Ti/Ttot, was thus set at 0.20, which is the threshold for development of diaphragmatic fatigue (11). Fatigue in this study being defined as the inability to maintain the target Pab. At this level of TTdi (0.20), if pacing is maintained continuously, diaphragmatic fatigue eventually occurs in approximately 45 minutes (11).

As indicated in Table 1, each experiment consisted of 5 runs. Each run was composed of 15 minutes of continuous diaphragmatic pacing, according to the parameters mentioned above, followed by a rest period of 20 minutes, minimum. Run 1 was left phrenic artery occlusion; Run 2 was left internal mammary artery occlusion; Run 3 was left phrenic and left internal mammary artery occlusion; Run 4 was descending aorta occlusion; and Run 5 was descending aorta and left internal mammary artery occlusion. Blood gas analyses were done at the onset of anaesthesia and afterwards, every hour on the hour, so that pH and PCO2 could be maintained constant.

Statistical analysis

All values are reported as mean ± SE. Statistical analysis was performed by using two way analysis of variance. Significant difference level was established at P < 0.05. Relationship between two variables was determined by using linear regression analysis.

RESULTS

Arterial blood pressure (115 \pm 12 mmHg) and blood gases (PO2 150 \pm 8 mmHg, PCO2 30 \pm 3 mmHg, and pH 7.38 \pm 0.03) remained constant throughout most of the experiment while the diaphragm was paced to generate a TTa; of 0.20. During the arterial occlusion period of Runs 4 and 5 Part increased to 141 \pm 29 mmHg, while blood gases and pH were not

TABLE 1
EXPERIMENTAL PROTOCOL

NON	PRE-OCCLUSION	OCCLUSION	POST-OCCLUSION
	Time (min)	Time (min)	Time (min)
	5 (0-5)	5 (5-10)	
1		LEFT PHRENIC ARTERY	
2		LEFT INTERNAL MAMMARY	
		ARTERY	
3		LEFT PHRENIC AND INTERNAL	
		MAMMARY ARTERY	
4		DESCENDING AORTA	
		PROXIMAL TO LEFT	
		SUBCLAVIAN ARTERY	
		DESCENDING AORTA	
		AND LEFT INTERNAL	
		MAMMARY ARTERY	

NB 15 MINUTE PACING PERIOD

15 CONTRACTIONS/MINUTE

Pab/Pab max = 0.50, Ti/Ttot = 0.40, thus TTdi = 0.20

significantly different from those mentioned above. Table 2 is a summary of some parameters measured in this study. values shown in this table are the means ± SE of the values obtained during each 5 minute interval (pre-occlusion control, occlusion, post-occlusion control) of the total 15 minute pacing period. It can be observed that occlusion of left phrenic artery (Run 1), or left internal mammary artery (Run 2), or combination of both (Run 3) had no significant effect on left inferior phrenic vein blood flow (Qphv), on shortening of costal (\Delta Lcos), or crural (\Delta Lcru) segments of the diaphragm or on abdominal pressure (Pab) swings. the other hand, occlusion of the descending aorta (Run 4) resulted in a significant decrease in Qphv, A Lcru, and Pab during the occlusion period, while & Lcos, during the same period, was observed to significantly increase, i.e. fatigue developed in the crural segment. When all the major arterial supplies to the diaphragm were occluded (Run 5), Qphv, △ Lcos, △ Lcru, and Pab all significantly decreased during the time of occlusion, i.e. fatigue developed in both crural and costal segments. However, during Run 5, a residual Qphv of 10 ml/min/100g was always present.

Diaphragmatic circulation (Qphv): Fig. 2 illustrates left inferior phrenic vein blood flow (Qphv) according to the time duration of the run expressed in minutes. It can be noticed that Qphv from Fig. 2 was not affected significantly during occlusions of PA (Run 1), IMA (Run 2), and PA-IMA

TABLE 2

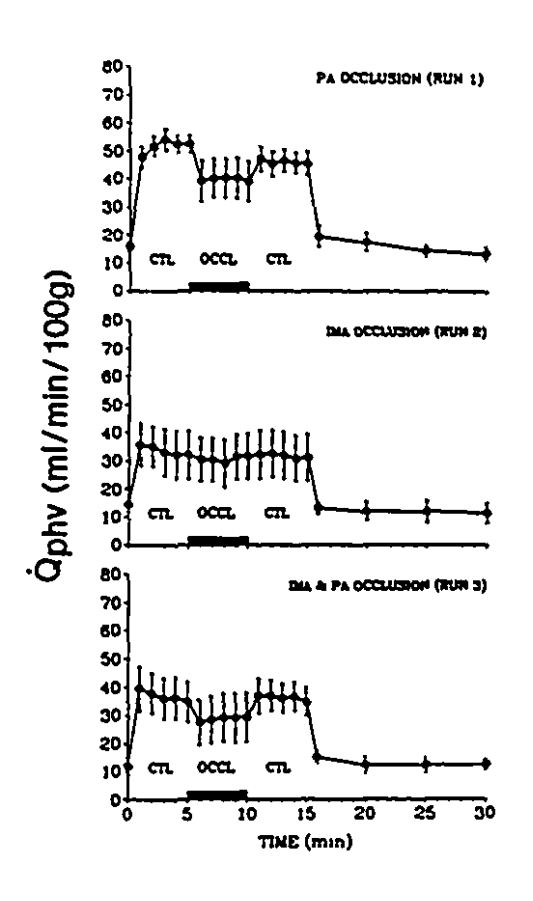
Average Qphv, Lcos, Lcru, and Pab values for all 5 runs.

(Average ± SE of 6 dogs)

RUN		Qph	7		Lcos			Leru	ı		Pab	
	(ml,	/min/	100g)	(D	ELTA :	mm)	(D	ELTA	mm)	((cmH2O)
	PRE	occ	POST	PRE	occ	POST	PRE	occ	POST	PRE	occ_	POST
1	51.7	40.1	46.2	2.9	2.9	2.6	4.5	4.1	4.3	40.9	36.9	35.1
	3.9	7.9	4.6	0.5	0.5	0.5	0.5	0.7	0.5	5.7	5.8	4.4
2	33.8	30.8	31.8	2.1	2.0	2.1	3.7	3.3	3.3	31.7	28.9	28.1
	8.2	8.1	8.4	0.4	0.4	0.3	0.9	0.8	1.0	9.4	8.2	7.9
3	37.0	28.8	36.2	2.8	2.3	2.2	3.8	3.3	3.6	37.0	33.0	32.2
Fut	7.5	8.5	5.4	0.4	0.6	0.6	0.6	0.7	0.5	8.2	6.5	5.9
4	43.4	23.9	51.1	3.2	4.5	3.1	4.1	2.3	3.5	36.7	22.8	31.9
	5.5	3.2	11.8	0.3	0.5	0.6	0.6	0.5	0.6	7.0	4.8	6.2
5	36.1	8.7	51.5	2.9	2.6	2.6	3.5	1.8	3.0	31.7	17.8	27.8
	6.3	2.4	13.3	0.3	0.5	0.7	0.8	0.4	0.7	7.0	4.1	5.4

NB. For every RUN top numbers are MEANS and bottom numbers are SE.

Numbers represent means and SE for every 5 minute interval of experimental protocol.



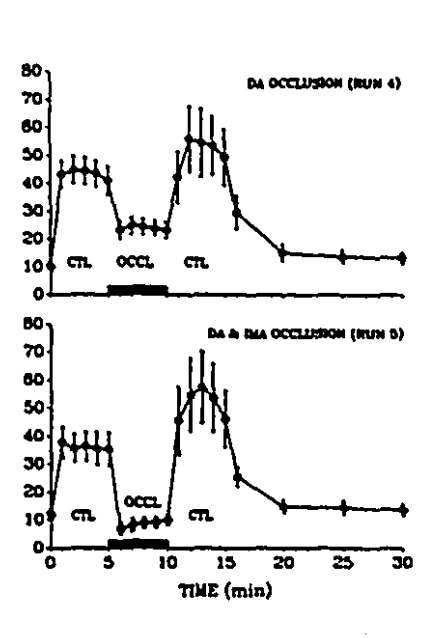


Figure 2. Phrenic vein blood flow (Qphv) for all 5 runs during each intervals (Pre-occlusion, Occlusion, and Post-occlusion). PA, phrenic artery; IMA, internal mammary artery; DA, descending aorta Values shown are mean ± SE.

(Run 3). However, when DA (Run 4) and DA-IMA (Run 5) occlusions were performed Qphv significantly decreased to 55.2% ± 7.4% and 24.0% ± 6.5% (mean Qphv occ/mean Qphv pre, from Table 2) of their pre-occlusion control period values, respectively. By examining closely Runs 4 and 5 of Fig. 2, one can notice large hyperaemias during the post-occlusion periods. These post-occlusion hyperaemias were consistently observed in every animal that we studied during Runs 4 and 5, but not during Runs 1 to 3.

Post-occlusion hyperaemia: The post-occlusion hyperaemia was estimated by measuring the areas under the curves of Fig. 2 (Runs 1-5) for each 5 minute period; i.e. the volume of blood draining from the diaphragm during pre-occlusion, occlusion and post-occlusion. The post-occlusion hyperaemia for all the Runs is illustrated in Fig. 3 as the % increase from pre-occlusion. It can be noticed that no significant post-occlusion hyperaemia was observed for Runs 1, 2, and 3. However, significant increases were observed during Run 4 (40.2%) and Run 5 (64.8%). In addition Fig. 3 illustrates the percent decrease from pre-occlusion observed during the occlusion periods. Runs 1-3 showed no significant changes in diaphragm blood volume during the occlusion period, while during Run 4 and Run 5 blood volume decreased by 35.8% and 65.7%, respectively. Notice that the magnitude of the changes observed in post-occlusion hyperaemia were similar to those produced during the occlusion.

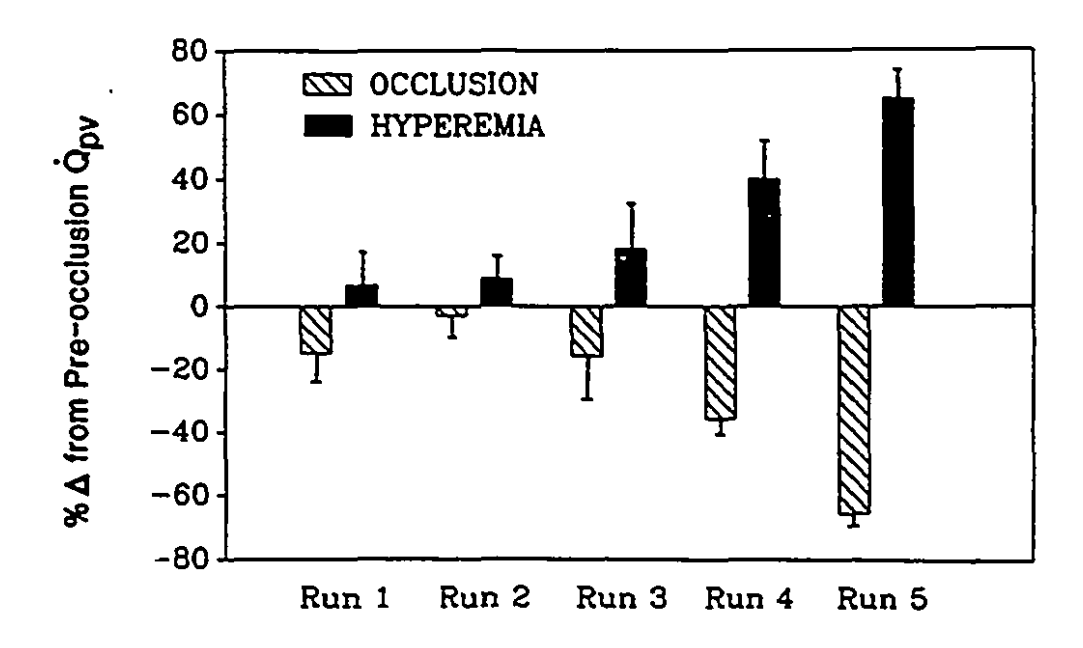


Figure 3. Post-occlusion reactive hyperaemia. Percent change, relative to Pre-occlusion interval, in phrenic vein blood flow (Qphv) during Occlusion and Post-occlusion intervals. Values for all 5 runs are shown (mean ± SE). RUN 1, PA occlusion; RUN 2, IMA occlusion; RUN 3, IMA & PA occlusion; RUN 4, DA occlusion; RUN 5, DA & IMA occlusion.

Diaphragmatic force: Fig. 4 shows the abdominal pressure (Pab), developed before, during, and after diaphragmatic pacing, as a function of time for every run. figure the rate of Pab decay during Pre-occlusion, Occlusion, and Post-occlusion was determined for all 5 runs, and are indicated in Table 3. It can be seen that the average rates of decay (illustrated in Fig. 4 and shown in Table 3) during the pre-occlusion, occlusion, and postocclusion periods for Runs 1-3 were constant and similar between themselves during the whole 15 min pacing period. However, when DA (Run 4) and DA-IMA (Run 5) were occluded the rate of decay (-2.9 and -3.2 cmH2O/min, respectively) was significantly more negative and returned to control values after reestablishing blood flow; i.e. during the post-occlusion pacing period. In Run 4 and 5 Pab decreased by 47.0 % and 53.5%, respectively, during the occlusion period.

Costal vs crural contractility: Figures 5 and 6 show the effect of arterial occlusion on diaphragmatic shortening in the costal and crural portions of the diaphragm, respectively. Diaphragmatic shortening was expressed as shortening measured in the costal and crural portions of the diaphragm. Shortening for the costal and crural portions was calculated by subtracting the length measured during the contraction of either the costal or the crural portion, from

TABLE 3

Abdominal pressure (Pab) rate of decay for every 5 minute interval of the pacing period (Average 6 dogs).

Pab

		Pab		
RUN	Pre-occl.	Occl.	Post-occl.	
1	-0.3	-0.9	-0.4	
2	-0.1	-0.2	-0.1	
3	-0.3	-0.5	-0.3	
4	-0.3	-2.9	-0.3	
5	-0.2	-3.2	-0.2	

NB All numbers are expressed in cmH2O/min. Negative sign indicates a decreasing rate.

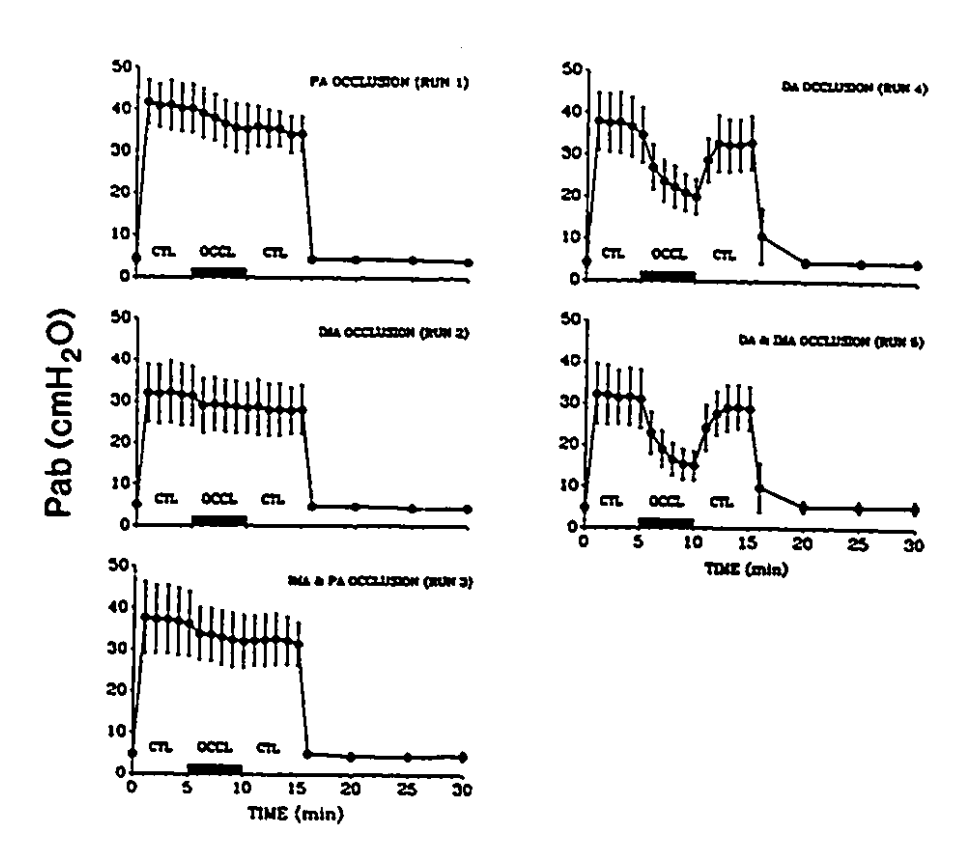
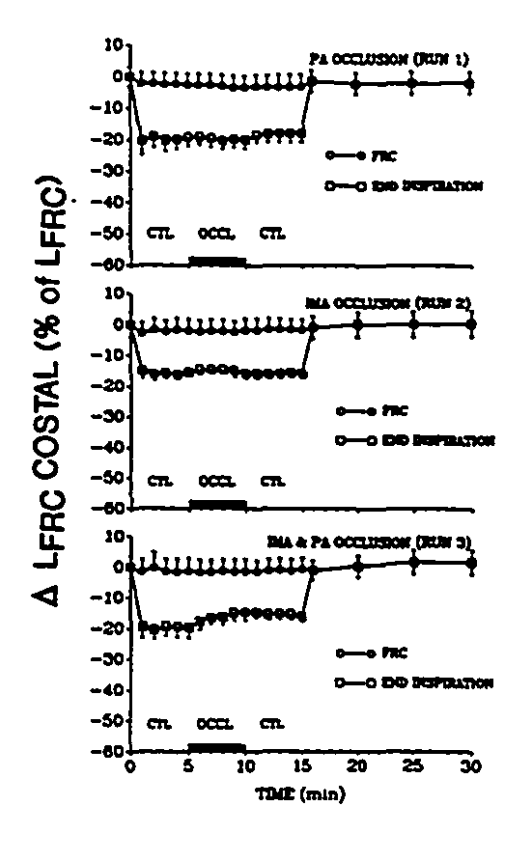


Figure 4. Abdominal pressure (Pab) developed for all 5 runs during the various intervals (Preocclusion, Occlusion, and Post-occlusion). PA, phrenic artery; IMA, internal mammary artery; DA, descending aorta Values shown are mean ± SE.



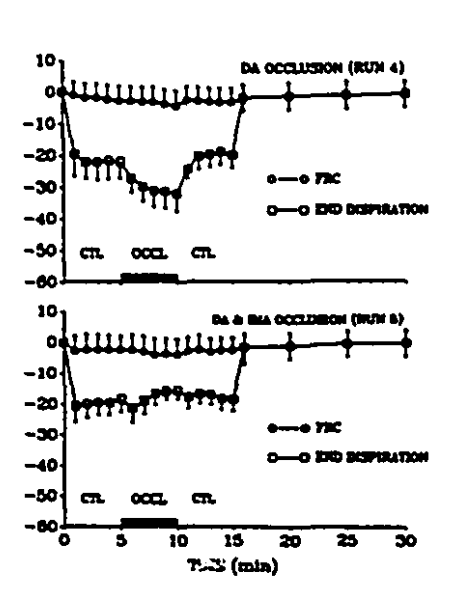
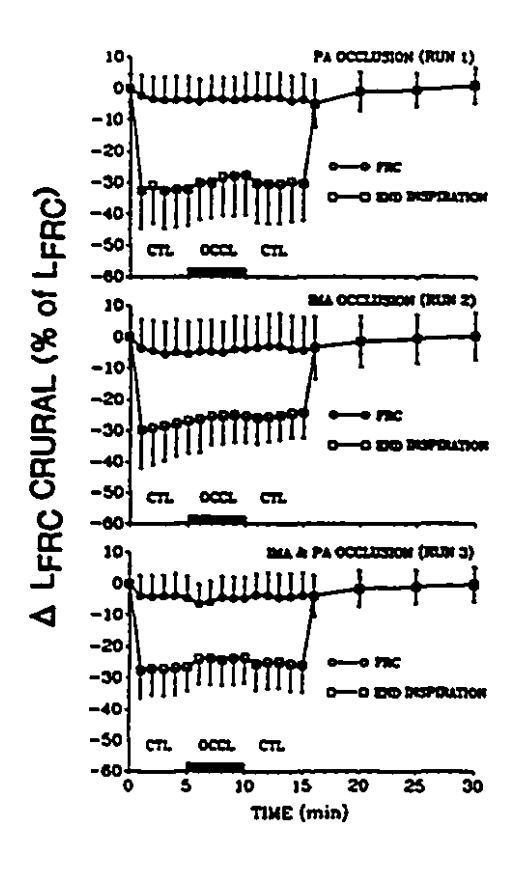


Figure 5. Costal shortening (Lcos) for all 5 runs during the various intervals (Pre-occlusion, Occlusion, and Post-occlusion). PA, phrenic artery; IMA, internal mammary artery; DA, descending aorta Values shown are mean ± SE.

=



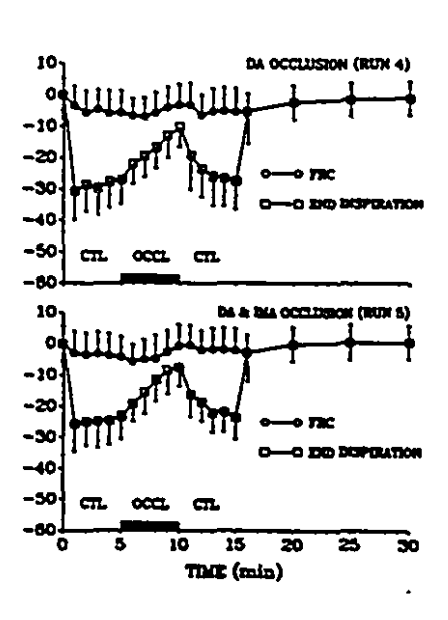


Figure 6. Crural shortening (Lcru) for all 5 runs during the various intervals (Pre-occlusion, Occlusion, and Post-occlusion). PA, phrenic artery; IMA, internal mammary artery; DA, descending aorta Values shown are mean ± SE.

the length measured at FRC. Fig. 5 indicates that Runs 1-3 had no effect on costal contractility as demonstrated by the constant amount of shortening during the whole 15 minute pacing period. On the other hand, costal shortening during the occlusion period in Run 4 increased significantly by 41.4% ((Lcos Occlusion - Lcos Pre-occlusion) / Lcos Preocclusion * 100, from Table 2), while during the occlusion period of Run 5 no increase in costal shortening was observed, but instead a non-significant 5.8% decrease (calculated as above from Table 2) in shortening noticed. Crural shortening in Runs 1-3 (Fig. 6) also showed no significant changes from pre-occlusion during the occlusion period. Whereas, Run 4 and Run 5 showed significant decreases in crural shortening during the arterial occlusion periods. The order of the decrease was 39.1% in Run 4 and 45.5% in Run 5 (calculated as above from Table 2).

Fig 7. illustrates costal and crural shortening in relation to one another. This plot indicates that under control conditions and during Runs 1-3 crural shortening was greater than costal shortening. On the other hand, when Runs 4 and 5 were produced costal shortening became larger than crural shortening. However, costal shortening during Run 5 decreased in comparison to Run 4, but was similar to the values observed in Runs 1-3. This suggests that the costal diaphragm is resistant to ischemia or receives blood not drained via the phrenic veins, and can continue to

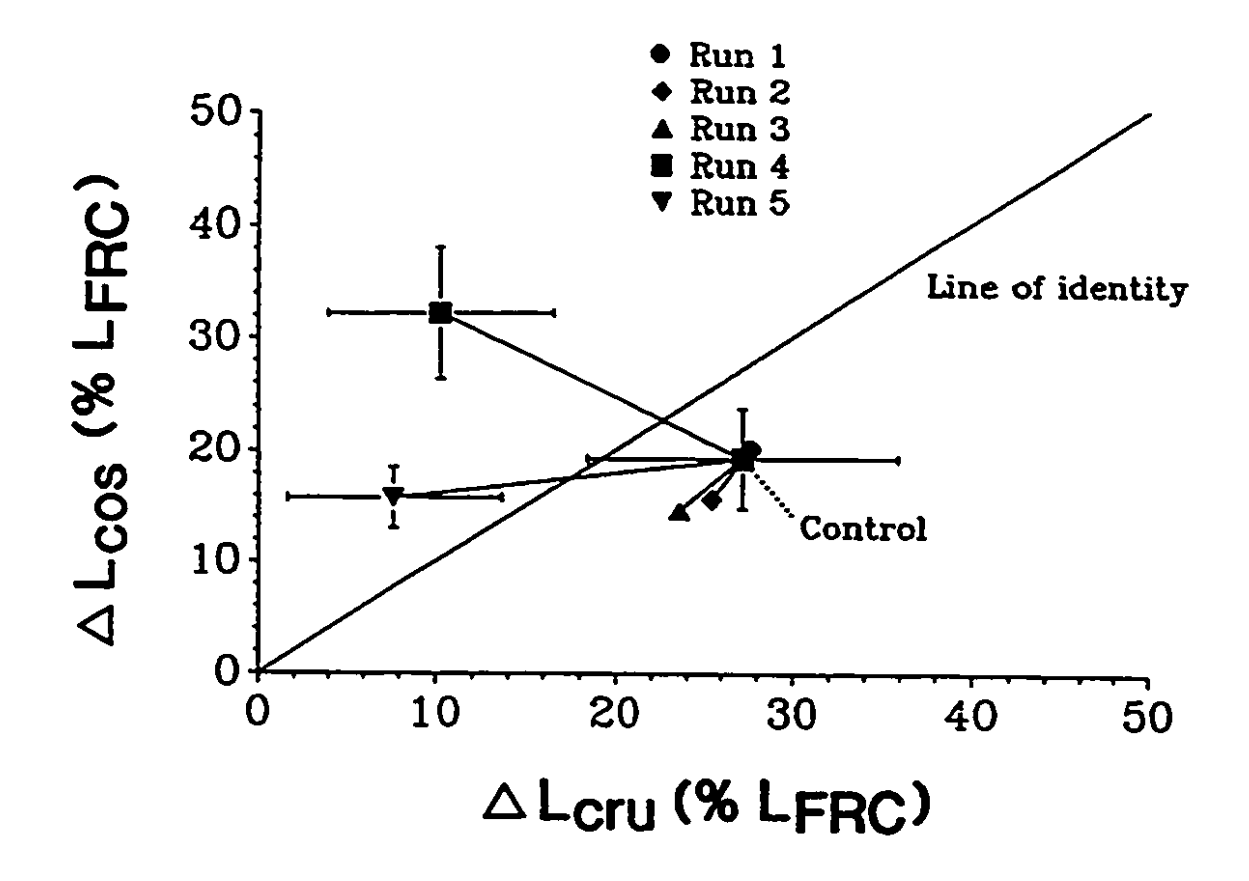


Figure 7. Costal shortening (Lcos) in relation to Crural shortening (Lcru) during the occlusion interval of the various runs. SE bars for RUNS 1-3 were omitted for sake of clarity. RUN 1, PA occlusion; RUN 2, IMA occlusion; RUN 3, IMA & PA occlusion; RUN 4, DA occlusion; RUN 5, DA & IMA occlusion.

function quite normally in the presence of occluded arteries.

DISCUSSION

Our experiments were designed to test the functionality of intradiaphragmatic anastomoses (costo-phrenic arcades) and extradiaphragmatic anastomoses in maintaining adequate diaphragmatic circulation at the fatigue threshold. The level at which the arterial occlusions were performed permitted this discrimination. Circulation through the costo-phrenic arcades was evaluated in Run 3 when the diaphragm was perfused by the posterior intercostal arteries (IMA & PA occlusion). Circulation through the extradiaphragmatic anastomoses, i.e. the shunts between the anterior and posterior intercostal arteries, in addition to the costo-phrenic arcades, was evaluated in Run 4 when perfusion of the diaphragm was maintained by the IMA (Descending aorta occlusion).

Experimental set-up: Shortening of the costal and crural diaphragm via sonomicrometry (73) has been well demonstrated in numerous investigations. The same can be said for abdominal pressure measurements obtained by latex balloon-catheter systems (11, 12, 56, 73). In our experiments a cast was placed around the abdomen. As stated in the methods, great care was taken to remove as much air as possible from the abdominal compartment. However, we cannot

rule out the possibility of some air remaining. This air combined to trapped gas in the GI tract would allow some degree of freedom for abdominal compression. The abdominal cast in our preparation extended from the 11th rib on either side to the pelvis. The compliance of the abdominal cast was very small (6-8 layers of 6 inch wide Paris rolls) and the thighteness was controlled by monitoring the Pab as to obtain a baseline pressure of approximately 15 cmH20. Another possible degree of freedom, was a cephalad displacement of the thorax during pacing. Since the abdominal compartment is stiffened by the cast it can act as a fulcrum point for the diaphragm during a contraction and displace the thorax in a cephalad direction, thus allowing some amount of diaphragmatic shortening. We believed that our shortening occurred mainly by this latter mechanism. Under those conditions Pab was strongly related to shortening.

Few studies have utilized instantaneous methods of blood flow evaluation in the diaphragm and this remains a novel approach to the study of diaphragmatic circulation. Qdi was estimated by measuring left inferior phrenic vein blood flow with a pulsed ultrasonic Doppler blood flowmeter. This method has the advantage of allowing continuous and instantaneous measurements of blood flow within the vessels, and disruption of the organ being studied is minimal. Vatner and co-workers (99) compared simultaneously

electromagnetic and Doppler flowmeters in chronically prepared animals. They reported no significant differences between the outputs of both flowmeters. Thus the Doppler was as reliable as the electromagnetic flowmeter in evaluating blood flow rates. The major advantage of the Doppler was the stability of zero baseline values and these were obtainable without occluding the vessels which can produce a reactive hyperemia lasting up to 5 minutes.

In comparison to Supinski et al (97)where a diaphragmatic strip preparation is used and perfusion maintained only by one vessel (phrenic artery) our model leaves total diaphragmatic circulation intact. For hemodynamic studies this model has the advantage of studying an intact vasculature. It does not allow measurement of total diaphragmatic blood flow as radioactive microspheres do (51, 62, 71, 81-86). On the other side, it provided us with an evaluation of regional circulation during various arterial occlusions. In addition, the number of runs one can do is not limited by the number of radio-isotopes available, thus making repetition possible and easy.

We opted to normalize Qphv to the diaphragmatic muscle mass served by this vessel since we wanted a mean of comparing our blood flow values to those already reported in the current literature. By doing this we expected our values to be lower since the inferior left phrenic vein represented only part of the vessels draining the diaphragm.

We found Qphv at rest to be similar to values reported by Bellemare (12) and other investigators (84-86). However, the blood flow rates during diaphragmatic pacing were lower than those reported by other investigators (17, 51, 52, 60) for the same level of diaphragmatic work. This can be explained by the fact that the area of muscle mass drained by the phrenic vein was overestimated in our study. It has been suggested that intercostal and internal mammary veins could have an important contribution to diaphragmatic venous blood drainage (12, 20).

Arterial network of diaphragmatic circulation: The arterial network of diaphragmatic circulation is illustrated in Fig. It indicates the major arteries supplying the diaphragm and their relationship to one another. The anterior (originating from the internal mammary arteries) posterior (originating from the thoracic aorta) intercostal arteries communicate end to end to form an arterial network that can supply the diaphragm either from the internal mammary arteries or the posterior intercostal arteries. Morgan et al (71) demonstrated that occlusion of the left inferior phrenic artery caused no significants changes in diaphragmatic circulation in dogs spontaneously breathing at rest. However when inspiratory work was increased diaphragmatic blood flow was lower when compared to control, while diaphragmatic work was unchanged. We observed similar

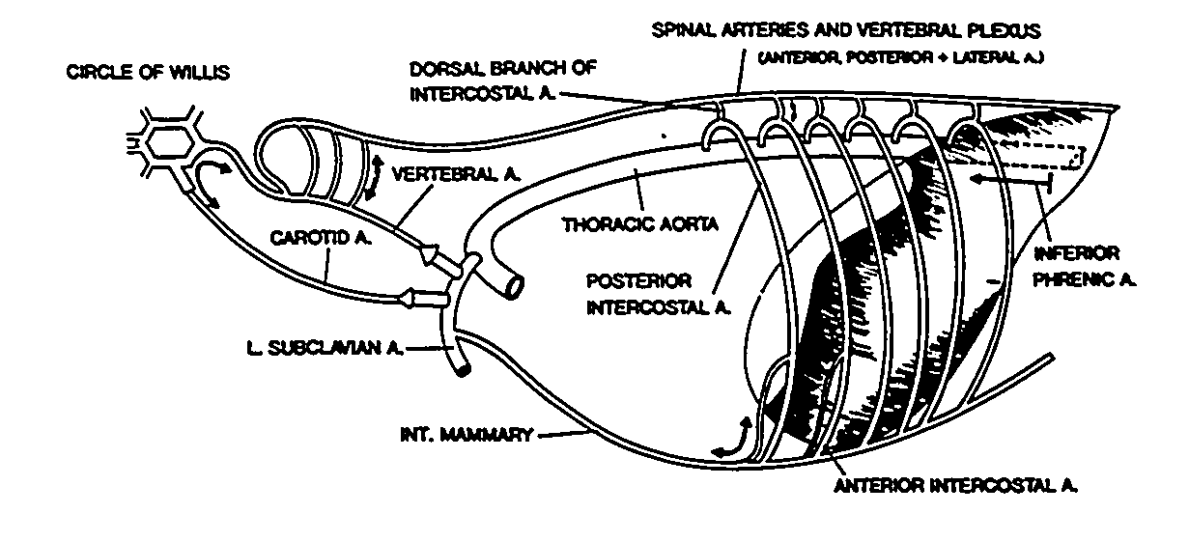


Figure 8. Extra-diaphragmatic anastomosis of the major arteries (phrenic arteries, posterior intercostal arteries, and anterior intercostal arteries via the internal mammary arteries) supplying the diaphragm.

results where occlusion of the inferior phrenic artery produced a small decrease in phrenic vein blood flow without affecting diaphragmatic contractility. Thus the amount of circulatory channels available to the diaphragm seem to make the inferior phrenic arteries almost redundant. It is interesting to notice that this artery is the only one exposed to abdominal pressure swings while the other two major supplies (intercostal and internal mammary arteries) are exposed to intrathoracic pressure swings.

Data obtained by Lockhat (60) showed that costal perfusion was unchanged while crural perfusion was decreased by more than 50% during diaphragmatic perfusion maintained by In our Run 4, perfusion was maintained by IMA IMA only. only, and shows that contractility of the costal is kept intact while contractility of the crural fails. results are compatible with Lockhat's (60) finding which indicate that IMA is the limiting point of the homogeneity of diaphragmatic circulation. Conversely when diaphragmatic circulation was maintained by the posterior intercostal arteries (Run 3; occlusion of phrenic and internal mammary arteries) no regions of the diaphragm seemed to be affected up to a TTdi of 0.20. Thus posterior intercostal artery circulation seems to support total diaphragmatic perfusion better than anterior intercostal artery circulation. interesting observation was that diaphragmatic circulation persisted when all major arteries supplying the diaphragm

were occluded. The most probable communication was via the vertebral plexus of the spinal cord and vertebral column. In another group of dogs (unpublished results) a cast of the vertebral plexus, made by injecting methyl-acrylate (Batson coumpound), showed extensive communications with posterior intercostal arteries via the dorsal branch. anatomical evidence explains Lockhat's (60) results showing that the upper cord (C1-T9) perfusion increased 200% of control value when all arterial supplies to the diaphragm were occluded. Such an increase in flow can leak into the extradiaphragmatic channels and still maintain a level of diaphragmatic perfusion similar to the one observed during spontaneous breathing at rest. Therefore, extradiaphragmatic channels coupled to rich intradiaphragmatic network of arteries makes the diaphragm an extremely resistant muscle to ischemia. This is an important asset since this muscle is subjected to sudden and often prolonged demands as in exercise. Our results are consistent with those reported by other investigators that studied the effects of hypotension and shock in limb skeletal muscles and in respiratory muscles (42, 51, 89). Hobbs and McCloskey (42) reported that force output and blood flow in hindlimb skeletal muscles (soleus and medial gastrocnemius) of cats decreased 57% and 53%, respectively, when arterial pressure was reduced from 125 to 75 mmHg. Similarly, Hussain et al (51) reported that blood flow and force output of the respiratory muscles, and more

specifically the diaphragm, were reduced during septic shock. Our experiments produced compatible results. individual arteries supplying the diaphragm were occluded the arterial pressure distal to the site of occlusion would fall towards zero. For example, during the occlusion period in Runs 4 and 5 (descending aorta occlusion) the femoral arterial pressure was 20 mmHg while the common carotid arterial pressure was 140 mmHg. The diaphragm has been shown to be autoregulated in the range of 75-120 mmHg (52) but because of experimental limitations these investigators did not go beyond 120 mmHg. In our case the increase in common carotid arterial pressure could have opened more of the intercostal diaphragmatic anastomotic channels. The most susceptible ones being the head to head anastomoses of the anterior and posterior intercostal arteries. this possibility is unlikely since resting and contracting skeletal muscles have been shown to be autoregulated in the range of 70 to 150 mmHg (94, 95).

Recently Lockhat and co-workers (59) reported that an ischemic period of 2 hours in the diaphragm working against an increased inspiratory elastic load resulted in a decrease in metabolites (glycogen, ATP, and phosphocreatine) which, with the exception of ATP, returned to control values 1 hour after recovery. In this study the arterial occlusions to the diaphragm were done in the same manner as in our Run 5. Studies on membrane excitation during ischemia (92),

suggests that the critical energy requirement may be at the site of the membrane. During muscle contraction K is lost from the muscle fibers. The Na/K pump reestablishes the equilibrium, but it is a process that requires energy. Therefore depletion of energy substrates reduces K uptake which in turn decreases intracellular [K] (93). This reduces membrane excitability, thereby enhancing fatigue at the level of excitation-contraction coupling. Thus the loss of force and contractility observed in some of our Runs (4 and 5) could have been due to an immediate drop in nutritional flow or electrolyte imbalance at the muscle membrane site.

Costal vs crural contractility: Heyndrickx et al (37, 38) have shown that occlusion of the left anterior descending coronary artery results in loss of contractility in the ischemic region while the non-ischemic region continues to contract normally. They observed that while the perfused portion continues to shorten normally the ischemic region is in fact lengthening. They attributed this to a bulging effect that occurs when the heart muscle is contracting and developing left ventricular pressure. This causes the ischemic portion to be stretched to its limit, thus lengthened, without seeing any fall in left ventricular pressure.

In our study we observed a similar phenomenon. However, the ischemic diaphragmatic segment did not lengthen

1.1

but permitted the unaffected portion to shorten more. synopsis was observed in Run 4 (descending aorta occlusion) where the costal portion was able to shorten more to the detriment of lost crural contraction. In our model, diaphragm shortening is directly proportional to Pab. our studies the maximal diaphragm shortening was 40% of Even though we had a cast, it was loose enough to Lfrc. permit considerable shortening. The cast was used to decrease the compliance of the abdominal compartment, which in this case increased the maximal Pab that can be generated by diaphragm shortening. Thus when both segments were able to contract normally the Pab would be generated by both segments. But when one segment would become deficient then the other segment would be allowed to shorten to its maximum capacity, while the deficient shortening in the other segment would be unable to add to the Pab. incapacity to shorten would be reflected as a loss in Pab. This explains why the increase in costal shortening during the occlusion period in Fig 5, Run 4, reached a plateau. By min 2 of the occlusion period (min 7 into the run) costal shortening was maximal, and crural being deficient could no longer offer resistance to costal shortening and contribute, by the same token, to Pab.

Phrenic nerve ischemia: The loss of contractility during Run 5 could be due to phrenic nerve ischemia since the arterial source for these nerves is from the internal

mammary arteries (20). Parry et al (78) have shown that occlusion of the vasa nervorum of the tibial nerve, produced by injection of arachidonic acid into the femoral artery, caused transient effects on nerve conduction. However the conduction block was observed 5-15 minutes after the injection, reaching a madir at 30 minutes and persisting up to 2 hours. The occlusions of arteries in our studies were very acute, lasting only 5 minutes, way before any signs of conduction blocks might be observed if we refer ourselves to changes Parry (78). Therefore the in contractility were likely due to ischemic muscles per se, and not ischemic nerves stimulating an ischemic muscle.

In conclusion, the diaphragm contracting at a level fatigue threshold, is quite resistant deprivation of most of its arterial blood supply. The costo-phrenic arcades seem to offer a communication that can be recruited quite easily in the event of arterial occlusions of phrenic or/and internal mammary arteries. The contractility in both regions (costal and crural) is preserved adequately by the posterior intercostal arteries (Run 3). On the other hand only the costal diaphragm resisted fatigue when the diaphragm was perfused only by the internal mammary arteries (Run 4), and both segments fatigued when IMA and DA (Run 5) were occluded.

CHAPTER 4

EFFECT OF SEPARATE HEMIDIAPHRAGM CONTRACTION ON LEFT PHRENIC ARTERY FLOW AND OXYGEN CONSUMPTION

SUMMARY

Phrenic artery blood flow has been shown to increase during bilateral phrenic nerve stimulation (BPNS). However, the role of unilateral phrenic nerve stimulation [left (LPNS) or right (RPNS)] on the blood flow and oxygen consumption of the contra-lateral hemidiaphragm is not known and is explored here. In 6 anesthetized, mechanically hyperventilated dogs, left phrenic artery blood flow (QLpha) was measured (Doppler technique). Supramaximal (10 volts, 30 Hz, 0.25 ms duration) LPNS, RPNS and BPNS at a pacing frequency 15/min and duty cycle of 0.50 was delivered in separate runs. Left hemidiaphragmatic blood samples for gas analysis were obtained by left phrenic vein cannulation. During RPNS, Qlpha and left hemidiaphragmatic oxygen consumption (VOzLdi) did not change significantly when compared to control. During LPNS and BPNS, there was a significant increase in QLpha and VO2Ldi (P < 0.01). was no significant difference in Qlpha and VO2Ldi between LPNS and BPNS (P>0.05). We conclude: 1) there is a complete independence of left-right hemidiaphragmatic circulation on both at rest and during diaphragm pacing; 2) during unilateral stimulation transdiaphragmatic pressure (Pdi) is not related to diaphragmatic blood flow.

Keywords: Phrenic artery blood flow, diaphragmatic oxygen consumption, hemidiaphragmatic contraction, dog.

INTRODUCTION

Increments in diaphragmatic contraction induced by bilateral phrenic nerve stimulation, exercise, breathing or chemical stimulation such as hypercapnia and hypoxia, have been shown to increase diaphragmatic blood flow (Qdi) (9-10, 12, 16-17, 31, 45, 47, 53, 63, 75-76, 80-89) and oxygen consumption (VO2di) (68, 75, 80-81, 83-84, The increase in Qdi has been shown to be proportional to tension time index (TTdi) (12) or to Pdi (9. 47). On the other side, it has been shown that there is no substantial vascular communication between the hemidiaphragms (20), and little cross flow would be This has been qualitatively confirmed in one expected. animal studied by Nichols et al (76). If TTdi or Pdi has a major influence on Qdi, as proposed, unilateral phrenic nerve stimulation (resulting in lower Pdi than bilateral phrenic nerve stimulation) should then result in lower Qdi and VO2di. To test this hypothesis, and to quantify the role of cross hemidiaphragm perfusion, we studied the left phrenic blood flow (QLpha) and left hemidiaphragmatic oxygen consumption (VO2Ldi) during steady state (the 4th minute) by pacing left, right or both hemidiaphragms.

MATERIALS AND METHODS

Six mongrel dogs, weighing 17.8 to 23 kg, were anesthetized with pentobarbital sodium (25mg/kg, iv).

Maintenance doses were supplemented during the experiment as to keep the corneal reflex abolished. The animals were placed in supine position and were mechanically ventilated through an endotracheal tube with a Harvard respiratory pump. Tidal volume (20-25ml/kg) and rate (16-18 breath/min) were adjusted to maintain arterial oxygen tension (PaO2) above 120 mmHg.

An intravenous catheter was placed in the anterior forelimb through which 5% dextrose solution in saline was delivered to replace fluid loss. A catheter was introduced into the right femoral artery to the level of the abdominal aorta and connected to a water-filled differential pressure transducer (Sanborn B-670 B) for recording left phrenic artery blood pressure (Ppha) and for withdrawing arterial blood sample. A No.7F catheter filled with heparinized saline was advanced from the right femoral vein into the left inferior phrenic vein and sutured on the diaphragm. The 7F catheter with two T ports was connected to a waterfilled differential pressure transducer (Sanborn B-670 B) for recording of left phrenic vein pressure (PLphv) and for sampling left phrenic vein blood. The difference between Ppha and PLphv was calculated as the driving pressure. other end of the 7F catheter was introduced into the left femoral vein through which blood drainages by left phrenic vein returned to systemic circulation. During resting (control) and diaphragm pacing (4th minute), blood samples were simultaneously withdrawn from the abdominal aorta and the left phrenic vein, and were analyzed with a Radiometer ABL-3 blood gas analyzer.

The left phrenic artery blood flow was measured with the Doppler technique as described before (47). through a midline abdominal incision a Doppler ultrasonic flow probe (diameter 2 mm) was placed around the left phrenic artery. QLpha (expressed in ml/100g/min) was calculated as the product of average Doppler shifts (\triangle KHz) obtained at the fourth minute of diaphragm pacing and by using a converting coefficient of 6.27 (ml/min/KHz). blood flow was then normalized to 100g of the weight of the left hemidiaphragm. One pair of piezoelectric transducers measure diaphragmatic shortening Was used to sonomicrometry. These were mounted 1.5-2.0 cm apart and sutured along the same muscle fibers on the left costal Two thin-walled latex balloons (5 cm long) connected to differential pressure transducer (Validyne MP-45.4), were filled with 1.0 ml air and positioned in the abdominal peritoneal cavity and in the lower oesophagus. These balloons recorded abdominal pressure (Pab) and pleural pressure (Ppl) swings relative to atmospheric pressure. The transdiaphragmatic pressure (Pdi) was the difference of Pab and Ppl. The abdomen was closed in two layers with suture.

A pair of electrodes connected to a Grass S-48 stimulator, were introduced into the right jugular vein and

the left carotid artery respectively. The tip of the stimulating electrodes were positioned in the proximity of the right and left phrenic nerve. The diaphragm was paced by supramaximal stimulation (approximately 10 volts, 30 Hz and 0.25 ms duration) of either the left phrenic nerve, the right phrenic nerve or bilaterally at a pacing frequency of 15 cycles/min, and at a duty cycle 0.50 for 5 minutes. The supramaximal voltage was determined as being 50% greater than the voltage necessary to produce the maximal twitch. The order of stimulation was randomized. After each pacing there was a recovery time of at least 20 minutes.

After the end of the experiments, the animals were given an overdose of anesthesia. Then, the diaphragm was dissected and weighed.

Data Recording

Ppha, PLphv, Pab, Ppl, left costal diaphragm length (Lcos) and QLpha (Doppler shifts) were recorded on an eight-channel strip-chart recorded (Hewlett-Packard 7758 A). Phrenic arterial oxygen tension (PaO2ph), left phrenic venous oxygen tension (PvO2ph), phrenic arterial carbon dioxide tension (PaCO2ph), left phrenic venous carbon dioxide tension (PvCO2ph), phrenic arterial pH value (pHaph), left phrenic venous pH value (pHvph), phrenic artery oxygen content (CaO2ph) and left phrenic vein oxygen content (CvO2ph) were printed on paper by the Radiometer ABL-3 blood gas analyzer.

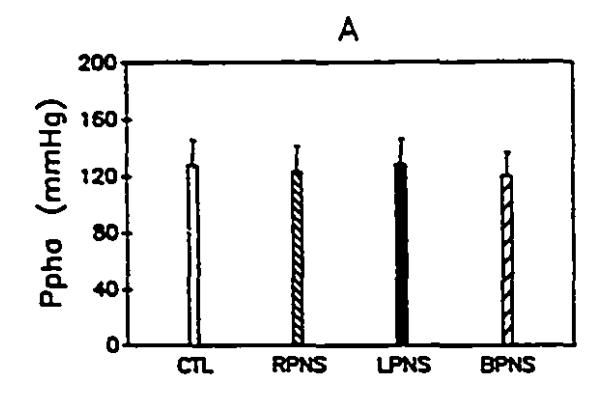
Statistical analysis

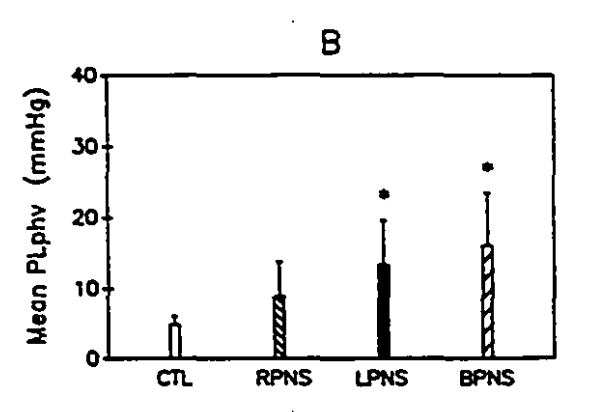
The values reported in this paper are the stable mean value (five contraction cycles) obtained during control and during the fourth minute of diaphragm pacing. All measurements were expressed as mean ± SD. A two-way analysis of variance was used to determine significant differences. A statistical level of significance of P < 0.05 was selected.

RESULTS

Phrenic artery and left phrenic vein blood pressure (Ppha and PLphy) during left. right and bilateral phrenic nerve stimulation (LPNS, RPNS and BPNS): The phrenic artery perfusion pressures obtained by cannulating the abdominal aorta were 123.0 ± 18.2, 128.3 ± 18.1 and 120.0 ± 16.7 mmHg during LPNS, RPNS and BPNS respectively. They were not significantly different from the control value of 127.5 ± 18.1 mmHg (passive diaphragm, mechanical ventilation). Neither was the difference significant among LPNS, RPNS and BPNS (Fig. 1A).

Figure 1B shows the mean left phrenic vein blood pressure (PLphv) when the diaphragm was paced by RPNS, LPNS and BPNS. Mean PLphv increased significantly from control value (P < 0.05) during LPNS and BPNS.





A) Mean phrenic artery blood pressure during control (CTL, passive diaphragm, mechanical Figure 1. LPNS,, left ventilation); phrenic stimulation; RPNS, right phrenic stimulation; and RPNS, bilateral phrenic nerve There stimulation. are no significant differences among them. B) Mean left phrenic vein blood pressure during CTL, LPNS, RPNS and BPNS. * significant

changes from CTL, P < 0.05

Left costal diaphragm shortening, transdiaphragmatic pressure and diaphragmatic work index (Wdi-index) during LPNS, RPNS and BPNS: During LPNS and BPNS the left costal diaphragm shortened by 56.7 ± 11.6% and 47.5 ± 14.7% LFRC, respectively (LFRC was defined as the length of the diaphragm at the end of passive expiration in the supine position). Conversely, the left costal diaphragm lengthened by 7.7 ± 3.3% LFRC during RPNS (Fig. 2A). There was a significant difference (P < 0.01) between RPNS and LPNS as well as between RPNS and BPNS. As well, a significant difference (P < 0.05) was observed between RPNS and control (passive diaphragm, mechanical ventilation).

Figure 2B shows the transdiaphragmatic pressure (Pdi, the difference of abdominal pressure and oesophageal pressure) generated by LPNS, RPNS and BPNS. The highest Pdi generated during BPNS was approximately the sum of the Pdi generated by LPNS and RPNS. There was a significant difference (P < 0.01) between BPNS and LPNS as well as between BPNS and RPNS. There was also a significant difference (P < 0.01) between control and diaphragm pacing (LPNS, RPNS and BPNS). However, there was no significant difference between RPNS and LPNS.

Figure 2C shows the diaphragmatic work index (Wdi-index) as the product of left costal diaphragm shortening

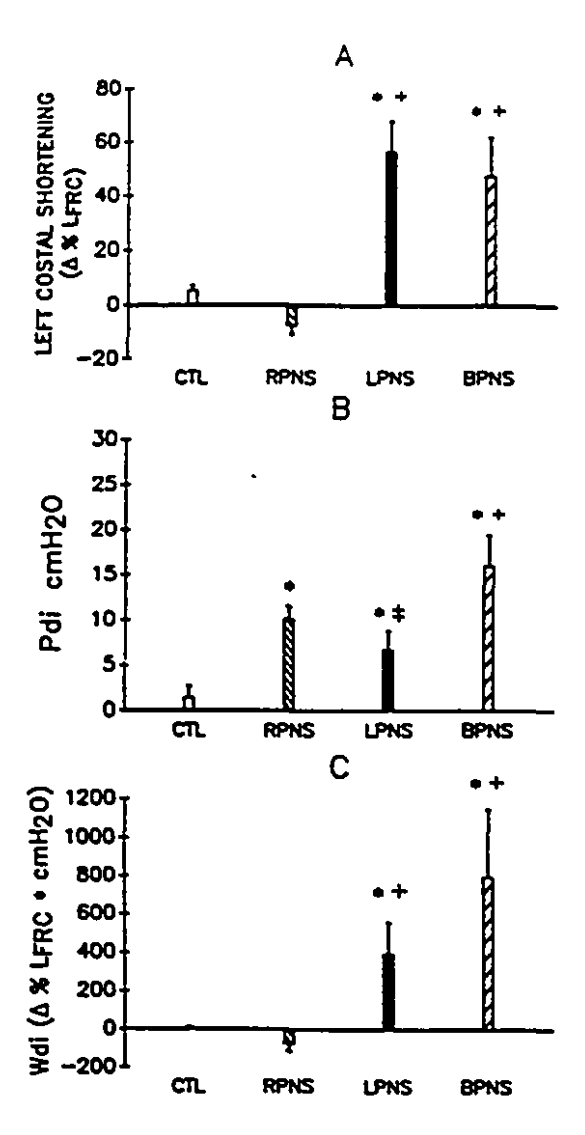
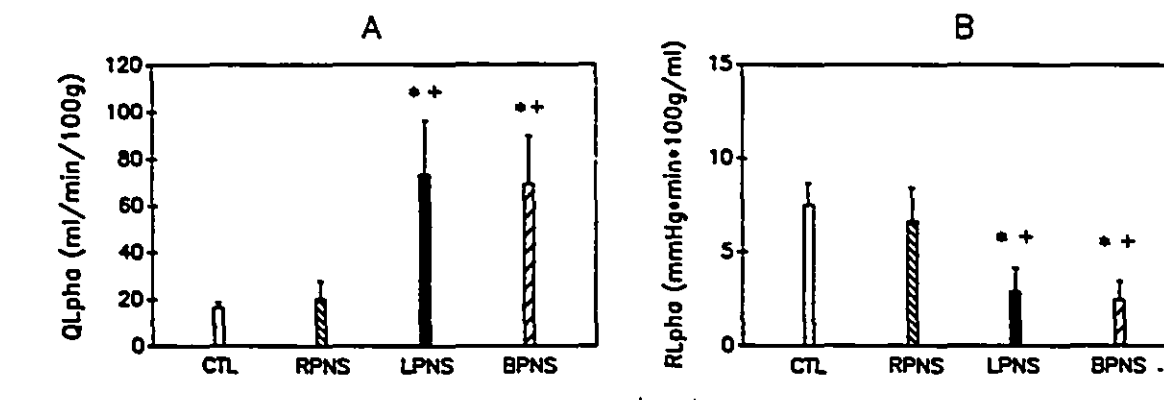


Figure 2. A) Length change of left costal diaphragm. There is a marginally passive shortening during CTL (effect of respirator) and significant lengthening during RPNS. There are significant shortenings during LPNS and BPNS. *P < 0.05-0.01, compared with CTL; + P<0.01, compared with RPNS. Tansdiaphragmatic pressure B) generated during CTL, LPNS, RPNS and BPNS. There is a marginally passive Pdi generated during CTL (effect of respirator) approximately equal Pdi generated during either RPNS or LPNS. There is a doubling in Pdi value during BPNS. * P < 0.01, compared with CTL; P < 0.01, compared with RPNS; = P < 0.01, compared with BPNS. C) Diaphragmatic work index (the product of left costal diaphragm shortening and Pdi) during CTL, LPNS, RPNS and The Wdi-index is negative because of left diaphragm lengthening during RPNS. * P < 0.01, compared with CTL; + P < 0.01, compared with RPNS.

(^ % LFRc) and Pdi (cmH2O) during LPNS, RPNS and BPNS. The Wdi-index was negative during RPNS because of left diaphragm lengthening. The Wdi-index during BPNS was approximately double the Wdi-index during LPNS because the Pdi was double.

Left phrenic artery blood flow (QLpha) and resistance (RLpha) during LPNS, RPNS and BPNS: Figure 3A shows that QLpha did not change significantly from control (16.4 ± 2.2 ml/min/100g) during RPNS (20.2 ± 7.7 ml/min/100g). However, there was a significant increase (P < 0.01) during LPNS (73.2 ± 23.2 ml/min/100g) and BPNS (69.1 ± 20.5 ml/min/100g). There was no significant difference between LPNS and BPNS. But there was a significant difference (P < 0.01) between RPNS and LPNS as well as between RPNS and BPNS.

Figure 3B shows that left phrenic artery resistance (RLpha, the quotient of left diaphragmatic driving pressure divided by QLpha) did not change significantly from control during RPNS. However, there was a significant decrease (P < 0.01) during LPNS and BPNS. There was no significant difference between LPNS and BPNS. But there was a significant difference (P < 0.01) between RPNS and LPNS as well as between RPNS and BPNS.



A) Left phrenic artery blood flow during CTL, LPNS, RPNS and BPNS. There is no significant changes during RPNS. * P < 0.01, compared with CTL; + P < 0.01, compared with RPNS. B) Left phrenic artery resistance is the quotient of left diaphragmatic driving pressure (Ppha-PLphv) divided by QLpha. There are significant decreases during LPNS and BPNS. * P < 0.01, compared with RPNS.

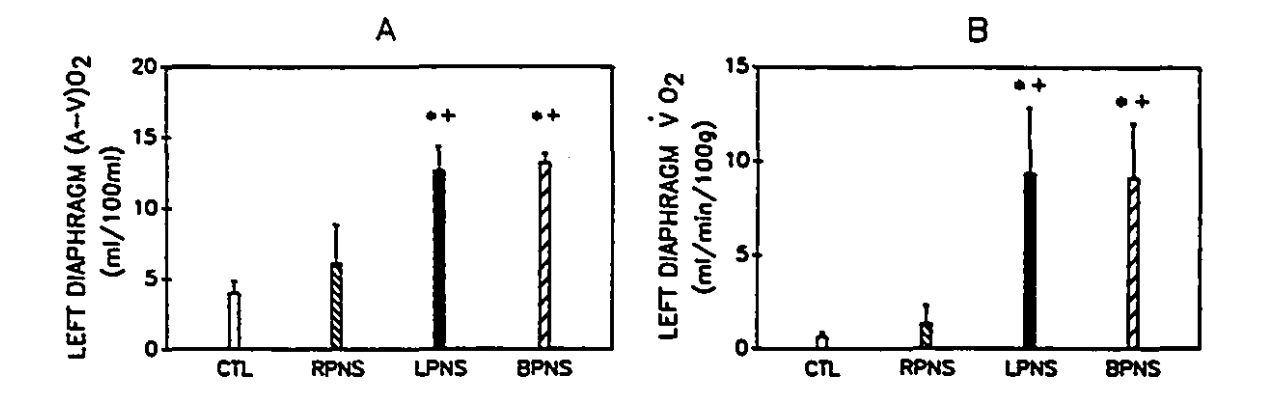
Phrenic arterial and left phrenic venous blood gases. oxygen extraction and left hemidiaphragmatic oxygen consumption (VOzLdi) during LPNS. RPNS and BPNS: Phrenic arterial and left phrenic venous oxygen and carbon dioxide tension, pH value and oxygen content are shown in table 1. Note that there was a significant decrease (P < 0.01) in left phrenic venous oxygen tension and content during LPNS and BPNS in comparison to RPNS and control. These results indicated that more oxygen was extracted during LPNS and BPNS.

Figure 4A shows that left hemidiaphragmatic oxygen extraction, i.e. arterial and venous oxygen difference (CavO2Lph) did not change significantly from control during RPNS. However, there was a significant increase (P < 0.01) during LPNS and BPNS. There was no significant difference between LPNS and BPNS. But there was a significant difference (P < 0.01) between RPNS and LPNS as well as between RPNS and BPNS. Figure 4B shows that left hemidiaphragmatic oxygen consumption contributed by the left phrenic artery (VO2Ldi = the product of Ca-VO2ph and QLpha) did not change significantly from control during RPNS. However, there was a significant increase (P < 0.01) during LPNS and BPNS. There was however a significant difference (P < 0.01) between RPNS and LPNS as well as between RPNS and BPNS.

TABLE 1 Left phrenic arterial and venous blood gases, and oxygen content during LPNS, RPNS and BPNS (Mean \pm SD)

		CTL			RPNS			LPNS			BPNS		
Pa02ph	(mmHg)	176.6	±	80.8	198.6	±	116.5	199.6	±	122.2	185.5	±	74.4
Pv02ph	(mmHg)	58.3	±	9.2	48.6	±	13.2	*+28.3	±	2.9	*+24.9	±	1.2
PaCO2ph	(mmHg)	30.5	±	11.2	26.1	±	7.6	26.0	±	6.4	20.2	±	3.6
PvCO2ph	(mmHg)	42.3	±	0.8	33.9	±	5.2	49.4	±	7.7	41.0	±	5.7
pH pha		7.40	±	0.06	7.41	±	0.06	7.40	±	0.04	7.47	±	0.05
pH phv		7.27	±	0.07	7.33	±	0.06	7.27	±	0.0	7.33	±	0.05
CaOzph	(ml/dl)	21.9	±	1.7	21.9	±	2.1	22.0	±	2.1	21.8	±	1.3
Cvo2ph	(ml/dl)	18.0	±	1.6	16.0	±	2.6	*+9.4	±	1.2	*+8.7	±	1.5

CTL: control (passive diaphragm); RPNS: right phrenic nerve stimulation; LPNS: left phrenic nerve stimulation; BPNS: bilateral phrenic nerve stimulation; PaO2ph (mmHg): phrenic arterial oxygen tension; PvO2ph (mmHg): left phrenic venous oxygen tension; PaCO2ph (mmHg): phrenic arterial carbon dioxide tension; PvCO2ph (mmHg): left phrenic venous carbon dioxide tension; ph pha: phrenic arterial ph value; ph phv: left phrenic venous ph value; CaO2ph (ml/dl): phrenic arterial oxygen content; CvO2ph (ml/dl): left phrenic venous oxyten content; * P < 0.01 compared with CTL; + P < 0.01 compared with RPNS.



Left hemidiaphragmatic oxygen extraction Figure 4. A) (arterial and venous difference) during CTL, LPNS, RPNS and BPNS. There are no significant changes during RPNS. * P < 0.01, compared with CTL; + P < 0.01, compared with RPNS. B) Left hemidiaphragmatic oxygen consumption contributed by the left phrenic artery (the product of phrenic arterial and venous oxygen content difference, and QLpha). There are significant increases during LPNS and BPNS. The phrenic artery contributes about 20% of the total diaphragmatic blood flow (76). 0.01, compared with CTL; + P < 0.01, compared with RPNS.

DISCUSSION

The major findings of this study are: 1) QLpha and VO2Ldi do not change significantly during right hemidiaphragmatic contraction, both increase during left hemidiaphragmatic contraction, and no further increase is evident following bilateral hemidiaphragmatic contraction.

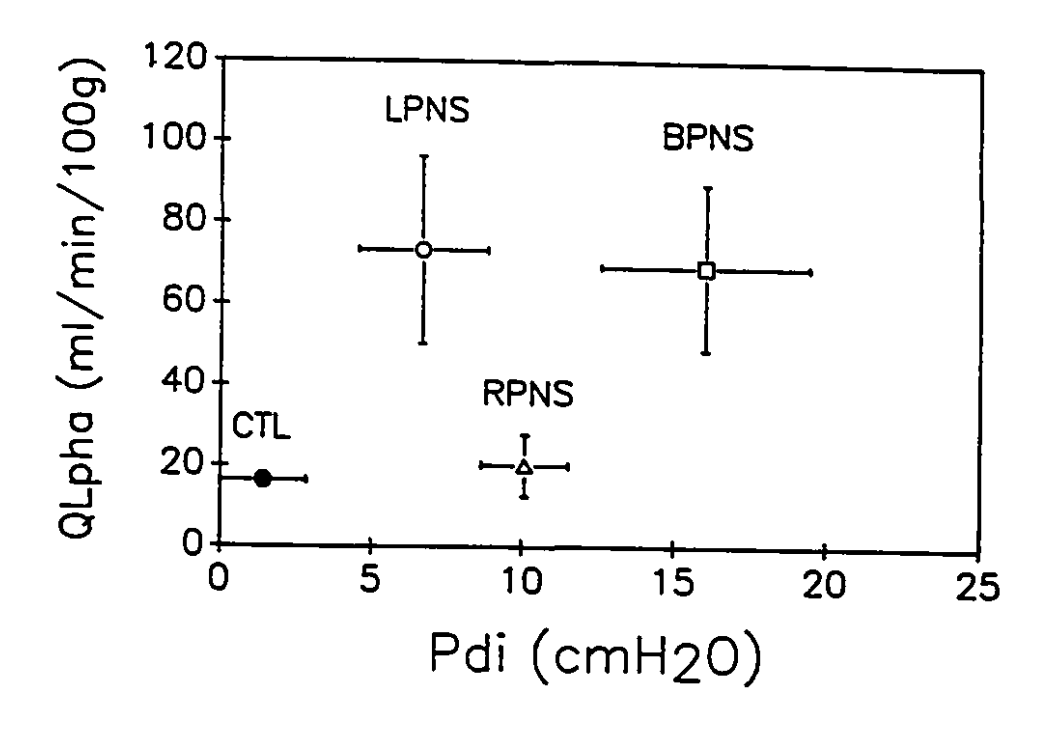
2) The concurrent activity of right hemidiaphragmatic contraction has no influence on QLpha and VO2Ldi.

One of the purposes of these experiments was to test the hypothesis that the right and left hemidiaphragms are hemodynamically independent as suggested by previous anatomical studies (20). We used supramaximal left, right and bilateral phrenic nerve stimulations (10 volts, 30 Hz and 0.25 ms duration) at a pacing frequency of 15 cycles per minute and duty cycle of 0.50 for 5 minutes because left inferior phrenic arterial blood flow was optimal under these conditions (45) and no diaphragmatic fatigue appears within 15 minutes (19). The lack of significant changes in mean phrenic arterial perfusion pressure (Fig. 1A), arterial oxygen and carbon dioxide tensions, arterial oxygen content and pH values (Table 1) among LPNS, RPNS and BPNS suggests that increases in QLpha and VOzLdi during LPNS and BPNS should be strongly related to left hemidiaphragmatic contractile activities and be independent of right hemidiaphragmatic contraction. Furthermore, the lack of difference in QLpha and VO2Ldi between LPNS and BPNS

suggests that the supplemental contribution of right hemidiaphragamatic contraction should have no influence on QLpha and VO2Ldi, i.e. hemidiaphragms seem to behave as having independent blood flow control. This is expected, given their embryological formation from separate halves. However, this independence between halves contrasts with the rich anastomosis between several arterial systems within each half (20).

Our values of QLpha during resting (passive diaphragm) and supramaximal diaphragm pacing by bilateral phrenic nerve stimulation, are similar to those reported in previous studies (1, 19, 45, 47, 53,76) even though in the present experiments, no abdominal cast was used and shortening of the diaphragm was considerably larger during stimulation. In this work, we find that the increase in QLpha during LPNS and BPNS is due to a decrease in left hemidiaphragmatic vasculature resistance rather than an increase in driving pressure (the difference of Ppha and PLphv). hemidiaphragm was paced, the phrenic venous pressure rose during the contraction phase. This would result in a decrease in the driving pressure and consequently decrease arterial inflow. However, other events may attenuate such effect. Increases in work and metabolic requirements would tend to increase the arterial inflow owing to a decrease in vasculature resistances. During the relaxation phase the phrenic venous pressure did not change much, neither did the driving pressure. Even though the mean venous pressure increased (see Fig. 1B) when the left hemidiaphragm was paced (LPNS and BPNS), the left phrenic arterial resistance decreased (see Fig. 3B). Therefore, the effect of venous pressure on arterial inflow is difficult to quantify.

oxygen consumption of the left hemidiaphragm The portion supplied by the left inferior phrenic artery is calculated as the product of QLpha and left phrenic arterial-venous oxygen content difference. Previous studies (75, 80-81, 83-84, 86-87) have suggested that diaphragmatic oxygen requirements can be met by increasing blood flow or oxygen extraction or both. We find that increases in VOzLdi during LPNS and BPNS is achieved by increasing both QLpha and oxygen extraction. The fact that there is no significant difference in QLpha and VO2Ldi between LPNS and BPNS even though the Pdi (Fig. 2B) and work index of the diaphragm (Fig. 2C) are doubled during BPNS, suggests that abdominal pressure should not be a major obstacle to diaphragmatic circulation, at least within the pressure range developed in this experiment (2 to 20 cmH2O) (see Fig. 5). A strong relationship between Pdi or TTdi and Qdi was observed during bilateral hemidiaphragm pacing (9, 10, 12, 16, 45, 47, 52, 75-76, 80). During unilateral left phrenic nerve stimulation, the left phrenic artery delivers a similar amount of blood as during bilateral stimulation,



Eigure 5. Left phrenic artery blood flow is plotted against transdiaphragmatic pressure during CTL, LPNS, RPNS and BPNS. There is no significant difference in QLpha between LPNS and BPNS, even though the Pdi is double during BPNS.

however, the Pdi is only half. Hence, Pdi in itself is not a determinant of blood flow. The intramuscular tension may on the other side be the determinant factor in limiting blood flow. The relation between Pdi and tension may change with the mechanical coupling as in unilateral stimulation. It is possible that a dissociation between Pdi and intradiaphragmatic tension may happen during bilateral activation as well, for example, when Pdi increases by the action of intercostals, and the diaphragm remains relatively less active or even contracts pliometrically. We do not know of any information available to test such a possibility.

Another interesting finding is that the left costal diaphragm lengthened about 7.7% Lfrc (Fig. 2A and Fig. 6) when the right hemidiaphragm contracted and shortened. The abdominal contents would Ъe displaced ру right hemidiaphragmatic contraction and the resting left hemidiaphragm is cephalically pushed and its lengthened. Supinski et al. (97) reported that there was an inverse relationship between muscle fibre length diaphragmatic blood flow. Our results, however, indicate that QLpha does not change significantly from control when the left costal diaphragm is significantly lengthened during RPNS. The range of change is about 7.7% LFRC, as shown in Fig. 6. At the same time, there is a slight decrease in left phrenic arterial resistance during RPNS (fig. 3B).

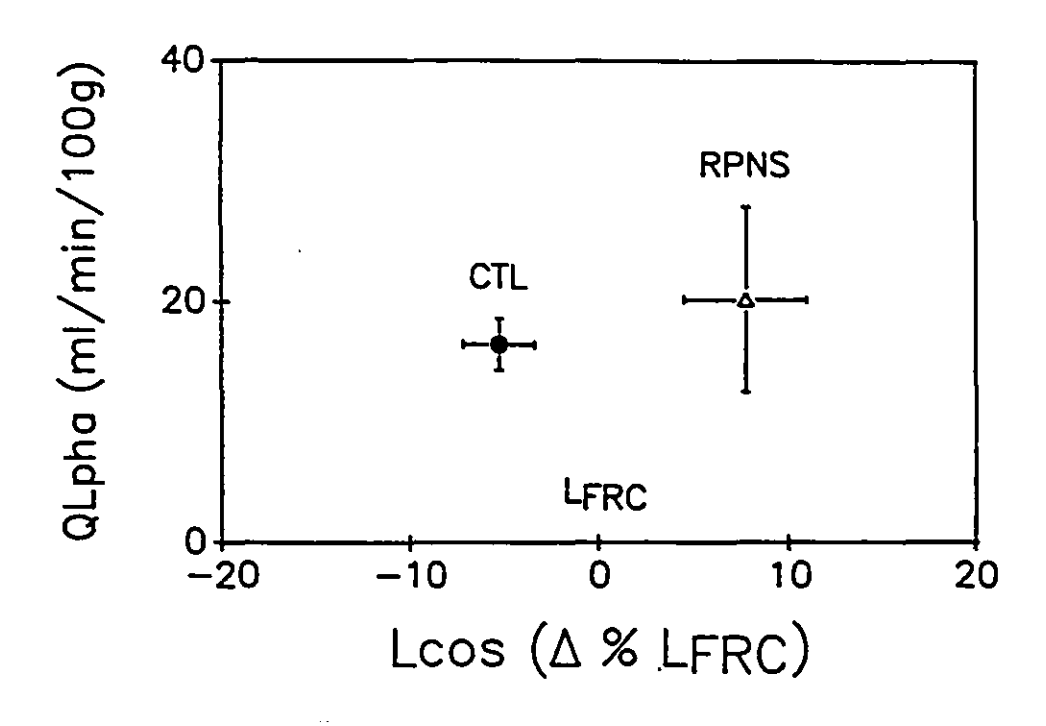


Figure 6. Left phrenic artery blood flow is plotted against passive length changes of the left costal diaphragm during CTL and RPNS. There is a marginal increase (P > 0.05, NS) in resting QLpha when left costal diaphragm is significantly lengthened during RPNS. * P < 0.05, compared with CTL.

We conclude that there is complete independence of right-left hemidiaphragmatic control of circulation during diaphragmatic stimulation. The degree of activity in the individual hemidiaphragm is the main stimulus in regulating blood flow. Passive changes in length or passive changes in Pdi do not seem to affect circulation.

CHAPTER 5 CONTRACTION DEPENDENT MODULATIONS IN REGIONAL DIAPHRAGMATIC BLOOD FLOW

SUMMARY

flow (Q) of the diaphragm Blood asw measured simultaneously with Doppler probes placed on diaphragmatic veins and an artery and by direct volumetric measures obtained from their cannulation. The Doppler converting coefficients obtained were 6.27, 7.25, 4.21 and 41.07 ml/min/Khz for left phrenic artery flow (Qpha), phrenic vein flow (Qphv), internal mammary vein flow (Qimv) and azygos vein flow (Qazv), respectively. The time course of Qpha, Qphv, Qimv and Qazv following imposed patterns diaphragmatic contraction was measured in 9 anesthetized dogs. Each pattern consisted of various combinations of transdiaphragmatic pressure (Pdi), frequency of pacing (f) and duty cycle (DC) obtained by bilateral phrenic nerve stimulation. The dogs had an open chest and a loosely casted abdomen. Qpha, Qphv, Qimv and Qazv at rest (control, passive diaphragm, mechanical ventilation) and at two submaximal levels of stimulation (30 and 60% of Pdi max) were measured. The f of pacing was 10 or 30 cycles/min and DC was 0.25, 0.50 and 0.75. The results show 1) Qpha, Qphy, and Qimv reached stable values (equilibration) after 30 to 36 seconds of pacing; 2) the steady Qpha, Qphv, and Qimv were linearly related to Pdi, and they were related by a parabolic function to DC, whereas Qazv was not significantly affected by Pdi and increased linearly as a function of DC; 3) the diaphragmatic blood drainage was approximately 60% through the intercostal veins leading into azygos trunk, 25% through the phrenic vein, and 15% through the internal mammary vein during pacing of the diaphragm at a duty cycle of 0.50 and 60% of Pdi max; and 4) for a given pacing pattern, Qpha and Qphv increased with f, but Qimv and Qazv did not.

KeyWords: Doppler technique, transdiaphragmatic pressure, duty cycle (Ti/Ttot), diaphragm circulation, diaphragmatic blood flow, dog.

INTRODUCTION

Several techniques have been used to measure blood flow of the diaphragm. The microsphere technique has the advantage of allowing evaluation of blood flow distribution over all regions of the diaphragm. However, it's an evaluation of mean blood flow over a period of a few seconds (16-17, 31, 51, 63, 81-88, 100). On the other side, cannulation of a vein measures regional blood flow directly and allows assessment of the dynamics of perfusion during both the contraction and the relaxation phases over prolonged periods (10, 12, 97).

Regional evaluation of blood flow is possible by use of blood flowmeters based on the Doppler principle. These blood flow meters have a rapid response time and a stable zero base-line value. This technique has been applied to diaphragmatic circulation by Pope et al (80), Comtois et al (19), Hu et al (43), and Nichols et al (76). The data of Nichols and co-workers showed that changes in phrenic artery blood flow correlate with changes in total and regional diaphragmatic blood flow. Using the Doppler method, we measured diaphragmatic blood flow in anesthetized dogs simultaneously from the left phrenic vein (Qphv), left internal mammary vein (Qimv), azygos (Qazv) vein, and left phrenic artery (Qpha) at rest and during two levels of work. The sum of vein flow should account for most of the blood outflow from the diaphragm (20). We hypothesized that each

of the three major vessels draining the diaphragm may show changes in blood flow pattern in accordance to various imposed contractions. The results seem to confirm this hypothesis.

MATERIALS AND METHODS

Animal Preparation

Our model was tested in a group of nine mongrel dogs and is illustrated in Fig 1. Anesthesia was induced and maintained with pentobarbital sodium (25 mg/kg iv). animals were supine and mechanically ventilated through an endotracheal tube via a Harvard respiratory pump. Room air was delivered at a rate of 10 cycles/min with a stroke volume of 19.7 ± 0.5 ml/kg (mean ± SE) so as to maintain PaO2 at/or above 80 mmHg. An intravenous catheter was placed in the anterior forelimb through which a 5% dextrose solution in saline was delivered. A catheter was introduced into the right femoral artery, and the tip was advanced to the level of the abdominal aorta and connected to a waterfilled differential pressure transducer (Sanborn B-670 B) for arterial pressure (Paorta) recording. The distal end of the catheter was used to withdraw arterial blood for blood gaz analysis. The left phrenic veins was exposed through a midline abdominal incision and was dissected free from the surrounding tissues. A 2.5 to 3.0 mm diameter Doppler ultrasonic flow probe (Hard epoxy probes, Series HDP, Crystal Biotech) was placed around the vein and sutured to

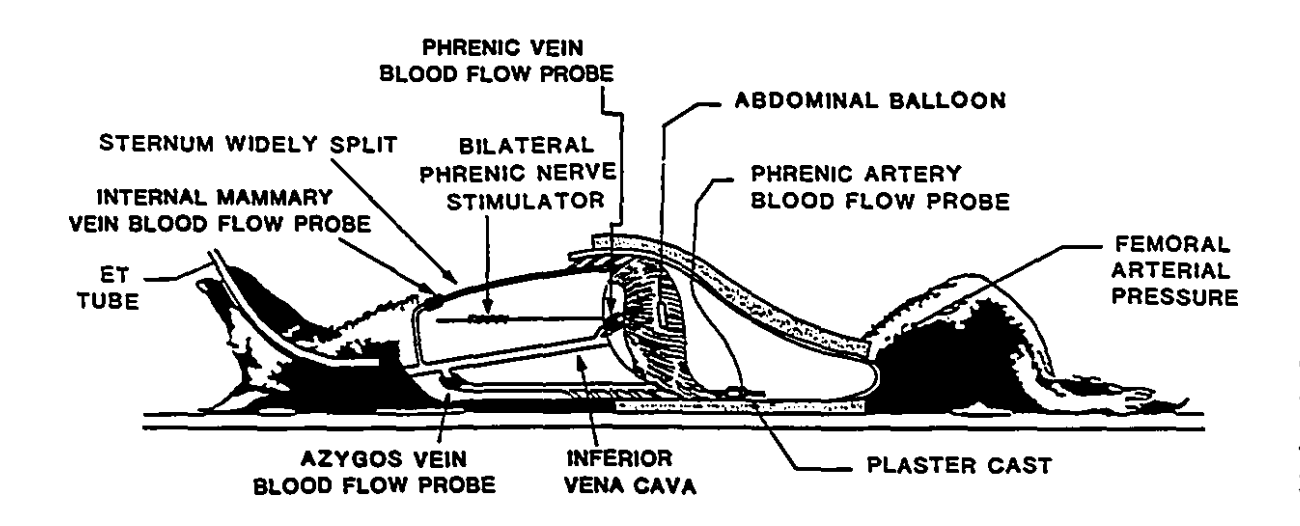


Figure 1. Schematic representation of the animal model. ET, endotracheal tube. For further details see methods.

.

the diaphragm for blood flow (Q) measurements. Similarly the left phrenic artery was exposed, and a flow probe of the same type but with a smaller diameter (1.5-2.0 mm) was placed around the vessel. The retroperitoneum through which the vessel was exposed was closed over the probe. A thin-walled latex balloon (5 cm long) filled with 1.5 ml air was positioned in the peritoneal cavity between liver and the stomach and was connected to a differential pressure transducer (Validyne MP-45.4) for recording of abdominal pressure (Pab) relative to atmospheric pressure. The abdomen was closed in two layers with continuous suture.

A midline sternotomy was performed. The azygos vein was dissected from its surrounding tissues 5 cm above its junction with the superior vena cava. A 5 mm diameter flow probe, of the same type mentioned above, was fixed at this site of azygos vein exposure. The left internal mammary vein was exposed at the level of the 6th intercostal space where a 2.5 mm diameter flow probe of the same type was fixed around the vessel. Two silver wire electrodes (isolated from the surrounding tissues) were wound around each of the phrenic nerves (T2-T3 level) and connected to a Grass S-48 stimulator for stimulation of the diaphragm. The chest was kept open.

A loosely fitting cast was placed around the abdomen from the xiphoid process to the origin of the posterior

limbs. The purpose of the cast was to avoid large diaphragmatic shortenings observed with maximal phrenic nerve stimulation without abdominal wall restriction. The animals rectal temperature was maintained at 37° C.

Calibration of the Doppler Probes

The theory of operation of Doppler probes has been extensively reviewed by Hartley and co-workers (37, 38), while numerous other authors (19, 43, 76, 80) have applied this technique to the study of diaphragmatic circulation. Briefly, the Doppler probe in a pulsed Doppler system (6 channel ultrasonic pulsed blood flowmeter, model VF-1, Crystal Biotech) utilizes a single piezoelectric crystal. The flow probe senses doppler shifts that are linearly related to blood flow within the vessel.

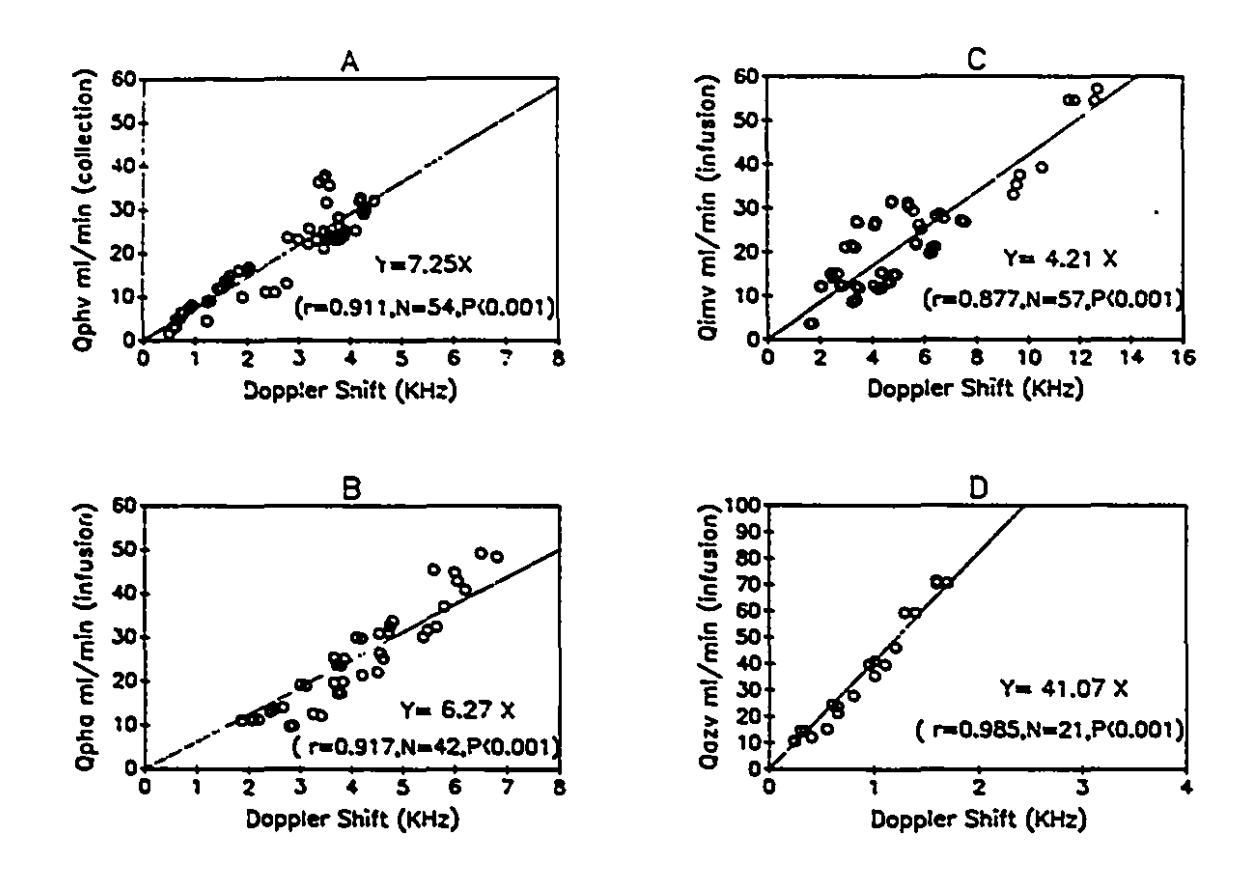
The calibrations were performed on an additional group of eight mongrel dogs. A catheter (2.5 mm ID) was introduced into the left or right femoral vein and the tip was advanced into the left phrenic vein. There the tip of the catheter was sutured so that it would remain within the vessel. The left phrenic vein blood passed through the catheter and was collected into a 50 ml graduated cylinder over known periods of time (timed collection technique). Qphv (ml/min) and Doppler shifts (frequency change in KHz) were measured simultaneously at rest and during various transdiaphragmatic pressure (Pdi) levels obtained by bilateral phrenic nerve stimulation.

Calibration of the other flow probes. Catheters with diameters of 2.0, 2.5, and 4.0 mm were passed into the proximal ends of the left phrenic artery, left internal mammary vein, and azygos vein, respectively. Ten or 20 ml of whole blood were perfused into these vessels, with an infusion pump at 8-10 different flow rates. Doppler recordings were obtained simultaneously from all three vessels.

Figure 2 A-D shows a significant linear relationship (P< 0.001) between Doppler shifts and Qphv measured by direct collection of blood from a cannula, and Qpha, Qimv, Qazv determined by blood perfusion with an infusion pump. The slopes or converting coefficients thus derived were 7.25, 6.27, 4.21 and 41.07 ml/min/KHz, respectively.

Calculation of Blood Flow from Doppler Shifts

In our model (the study group of 9 dogs and all runs), Qpha, Qphv, Qimv, and Qazv were measured cycle by cycle from the Doppler shifts until steady state was reached. Q was normalized for 100g of the left hemidiaphragm, and expressed as ml/100g/min. Because Qazv measures flow from both hemidiaphragms, it was normalized by dividing flow over the weight of both hemidiaphragms. Q during contraction phase (Qc), relaxation phase (QR) and a total pacing cycle (QT) was calculated as follows and reported as blood volume (flow rate time duration of phase) per phase or total cycle:



Relationship between Q measured simultaneously by Doppler technique and by direct volumetric measurement. Qphv: flow of left phrenic vein, Qpha: flow of left phrenic artery, Qimv: flow of left internal mammary vein, Qazv: flow of azygos vein. There is a significant linear relationship (P < 0.001) between A) Qphv (ml/min), B) Qpha (ml/min), C) Qimv (ml/min), D) Qazv (ml/min) and Doppler shifts (KHz). For further details see text.

QC = $\triangle f * b /60 * Ti * f /0.5DW * 100g (ml/100g/min)$

 $QR = \Delta f * b /60 * Te * f /0.5DW * 100g (ml/100g/min)$

QT = QC + QR (ml/100g/min)

where $\triangle f$ is the Doppler shift ($\triangle KHz$), b is the converting coefficient, Ti (s) is contraction time, Te (s) is relaxation time, f is frequency of pacing, and DW is diaphragm weight (g).

Experimental Data Recording

Paorta, Pab, Qpha, Qphv, Qimv, and Qazv were recorded on an eight-channel strip-chart recorder (Hewlett-Packard 7758 A) and an eight-channel tape recorder (Hewlett-Packard 3968 A). Figure 3 shows an example of the simultaneous recording of Qpha, Qphv, Qimv, and Qazv and their time relation to Pdi swings.

Experimental Protocol

At the beginning of each experiment maximal Pab (Pab max) was measured by supramaximal bilateral phrenic nerve stimulation (8 volts, 50 Hz and 0.25 ms pulse duration). After the determination of Pab max, the following protocols were developed.

1), The diaphragm was paced at a frequency of 10 cycles/min, which was maintained until a stable Q was achieved. In each run the duty cycle was either 0.25, 0.50 or 0.75. For each duty cycle the pulse duration was 0.25

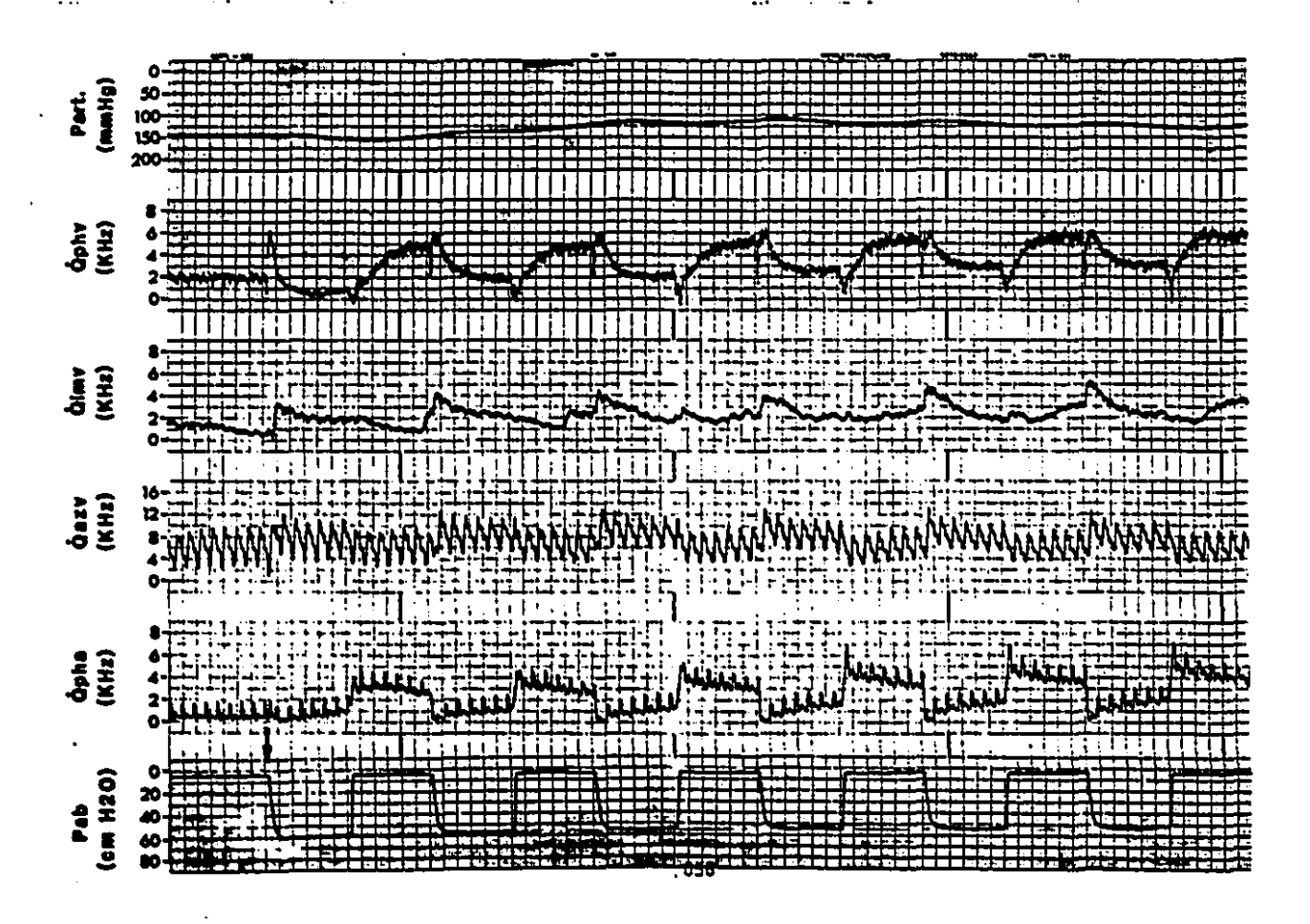


Figure 3. Typical recording showing resting (inactive diaphragm, left of arrow) and 6 successive diaphragmatic contraction cycles obtained by bilateral phrenic nerve stimulation. From top to bottom: mean abdominal aortic blood pressure (Paorta); Doppler shifts of Qphv, Qinv, Qazv, and Qpha; and Pab relative to atmospheric pressure. Arrow beginning of pacing.

=

ms, but both the stimulation voltage (0.5 to 6.0 volts) and stimulation frequency (10-90 Hz) were changed so as to obtain two levels of Pdi (30% and 60% of Pdi max). After each run Q, Pab and Paorta were monitored for at least 5 minutes (Post-pacing hyperemia) or until values returned to control levels. There was an interval of 15 to 20 minutes between runs.

2) In seven of the nine dogs, diaphragmatic pacing was then set at a f of 30 cycles/min and a duty cycle of 0.50. The effect of an increased f on Q was tested until a steady flow was observed.

After the above tests were completed, the animals were killed with an overdose of pentobarbital sodium. The diaphragm was dissected and weighed.

Statistical analysis

All measurements are expressed as mean ± SE. Two-way analysis of variance, linear and nonlinear regression analysis were used.

RESULTS

Time Course of Q during Various Pacing Patterns: Figures 4 to 6 shows the cycle by cycle time course of Qpha, Qphv, Qimv, and Qazv together with the Pab. Each data point represents one cycle and is the average ± SE for all animals. Figures 4 to 6 shows data from three of the eight

TABLE 1

Equilibration Time for Qphat and Qphvt

f = 30 cycles/min					
Duty Cycle					
0.25 0.50 0.75					
32					
36					

Qphar, total flow of phrenic artery; Qphvr, total flow of phrenic vein; Pdi, transdiaphragmatic pressure; f, frequency of pacing. Values expressed in s.

TABLE 2

Pdi/Pdi max, Pdi, and Paorta at rest and during diaphragm											
Pacing											
	30 / min										
Duty Cycle	CTL	0.25		0.50		0.75		CTL 0.50)	
Target Pdi		Lo	Hi	Lo	Hi	Lo	Hi		Lo	Hi	
Pdi/Pdimax	0.09	0.33	0.61	0.34	0.63	0.35	0.58	0.07	0.37	0.59	
± SE	0.01	0.02	0.02	0.01	0.02	0.03	0.04	0.01	0.02	0.03	
Pdi cmH20	8.2	30.6	57.9	31.8	59.5	31.2 :	54.6	6.3	33.7	53.6	
± SE	1.0	2.0	3.2	1.6	2.8	1.7	2.1	0.7	2.5	3.3	
Part mmHg	127	122	124	116	116	111	109	128	117	114	
± SE	2.6	4.3	4.0	4.9	5.4	3.7	7.9	3.0	6.7	8.0	
Values are means ± SE obtained during diaphragm pacing at											
steady state. Pdi, transdiaphragmatic pressure; Pdi max,											

Values are means ± SE obtained during diaphragm pacing at steady state. Pdi, transdiaphragmatic pressure; Pdi max, maximal transdiaphragmatic pressure; Paorta, mean abdominal aortic blood pressure.

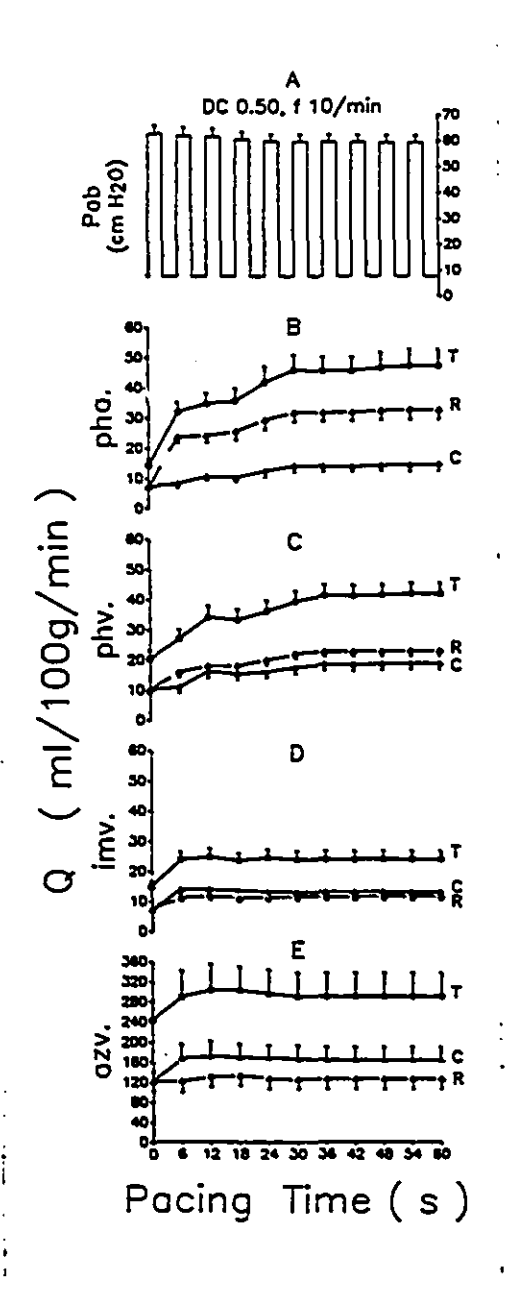


Figure 4. Time course of Qpha, Qphv, Qimv, and Qazv at Pab of about 60 cmH2O, duty cycle (DC) of 0.50 and f of 10 cycles/min. Qdi is shown for each cycle during the contraction (C) and relaxation (R) phases, and the total (T) component. Note that Qphar and Qphvr reaches equilibration after 30 s of pacing. Qimvr and Qazvr reaches equilibration much sooner (after the 2nd cycle). Values are mean ± SE.

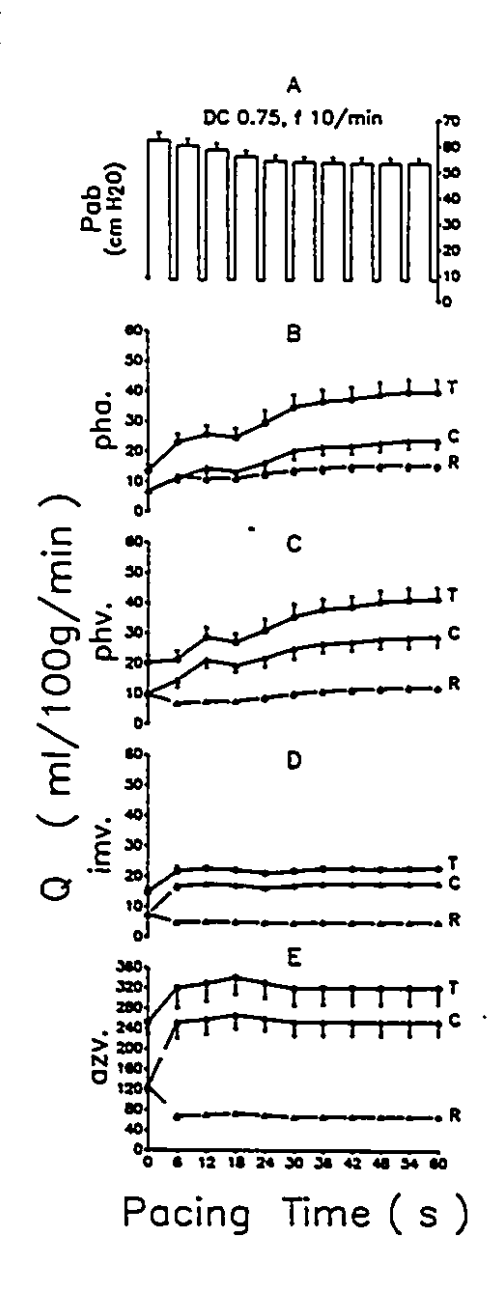


Figure 5. Time course of Qpha, Qphv, Qimv, and Qazv at Pab of about 60 cmH2O, duty cycle (DC) of 0.75 and Qdi is shown for each f of 10 cycles/min. cycle during the contraction (C) and relaxation (R) phases, and during total (T) component. Qphar and Qphvr reaches equilibration after 36 Qimvr and Qazvī pacing. reaches (after equilibration much sooner the A, decreases cycle). In panel Pab progressively from the initial cycle (60 cmH20) to the 10th cycle (53 cmH20), indicating diaphragmatic fatigue. Values are means ± SE.

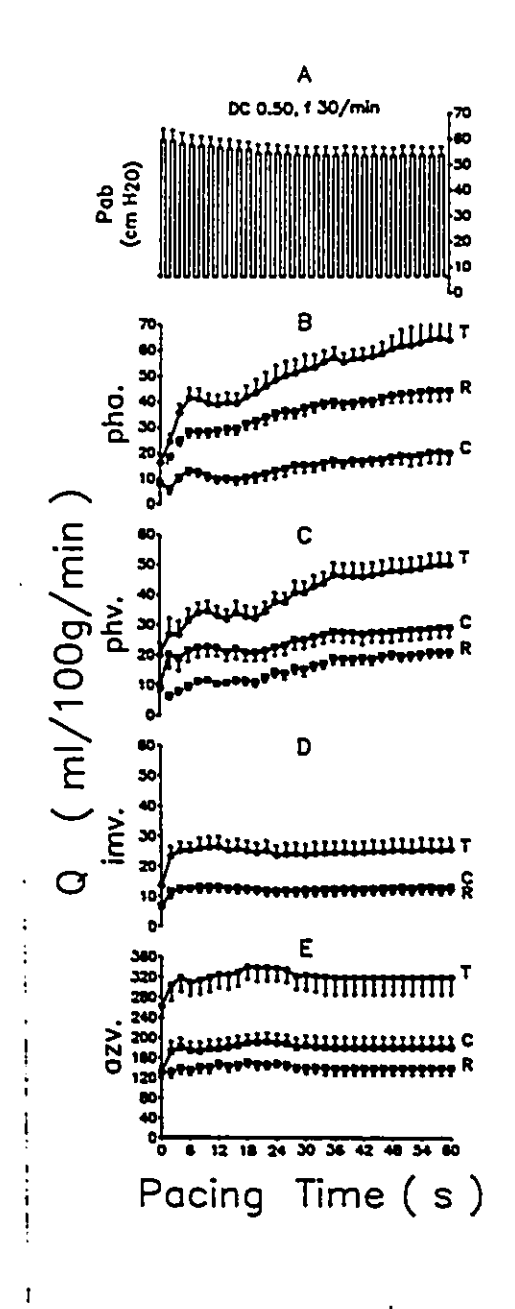


Figure 6. Time course of Qpha, Qphv, Qimv, and Qazv at Pab of about 60 cmH2O, duty cycle (DC) of 0.50 and f of 30 cycles/min. Qdi is expressed cycle by cycle during the contraction (C) and relaxation (R) phases, and during total (T) component. Qphar and Qphvr reaches equilibration after 36 of pacing. Qimvr and Qazvī reaches equilibration much sooner (after the In panel Α, cycle). Pab decreases progressively from the initial cycle (60 cmH20) to the 10th cycle (54 cmH2O), indicating diaphragmatic fatigue. Values are means ± SE.

runs measured. Equilibration time data for all runs is given in Table 1. Equilibration time is the time taken (number of cycles) from onset of a given pacing protocol to plateau in Q. The normalized value of Q at the point of equilibration is given for all runs in Table 2. course is shown only in three runs, because these were the runs with the slowest equilibration time and the most marked differences in Qc and QR. It can be seen that Qphar and QphvT reach equilibration after about 30 s, when duty cycle is 0.25 or 0.50 (Fig. 4), and equilibrate slightly later at a duty cycle of 0.75 (Fig. 5). Qphat and Qphvt at a lower duty cycle (0.25-0.50) are mainly related to QR (Fig. 4, B and C). In contrast, at a higher duty cycle (0.75; Fig. 5, B and C) Qphat and Qphvt are mainly related to Qc. that Qc/QT is greater in phrenic vein than in phrenic artery at iso-duty cycle. It follows that, QR/QT is greater in phrenic artery than in phrenic vein. Qimvt and Qazvt (Figs. 4 and 5, D and E) are similar to QphvT; however, the equilibration time is reached much sooner, often after the first two pacing cycles. Equilibration time at a f of 30 cycles/min is prolonged with respect to that at a f of 10 cycles/min at similar duty cycle and Pdi.

Time Course of Pdi during Bilateral Phrenic Nerve Stimulation: Because the thoracic surface of the diaphragm was exposed to atmospheric pressure, Pab was equal to Pdi. The Pdi max was always obtained at the beginning of each

supramaximal bilateral phrenic bу nerve experiment stimulation. It averaged 93.8 ± 2.7 cmH20 for the nine The resting Pdi was 8.2 ± 1.0 cmH2O. Diaphragmatic stimulation with low voltage and frequency (Pdi of about 0.34 of maximum), at duty cycle of 0.25 and 0.50 and at all f, yielded a constant Pdi through 1 minute, indicating that no fatigue had developed. Stimulation of the diaphragm with high voltage and frequency (Pdi of about 0.60 of maximum) generated a constant Pdi at a duty cycle of 0.25 and f of 10 cycles/min, demonstrating that no diaphragmatic fatigue developed under these conditions. However, during stimulation with high voltage and frequency at a duty cycle of 0.50 and 0.75 and f of 10 cycles/min (Fig. 5A), and at duty cycle of 0.50 and f of 30 cycles/min (Fig. decreased progressively, thus indicating genesis diaphragmatic fatigue (defined as reversible force loss). Diaphragmatic tension was expressed as Pdi/Pdimax, which increased following increments of both stimulation voltage and frequency. For various duty cycles and f the low or high Pdi/Pdimax was approximately equal and averaged 34% and 61% of Pdi max, respectively (see Table 2).

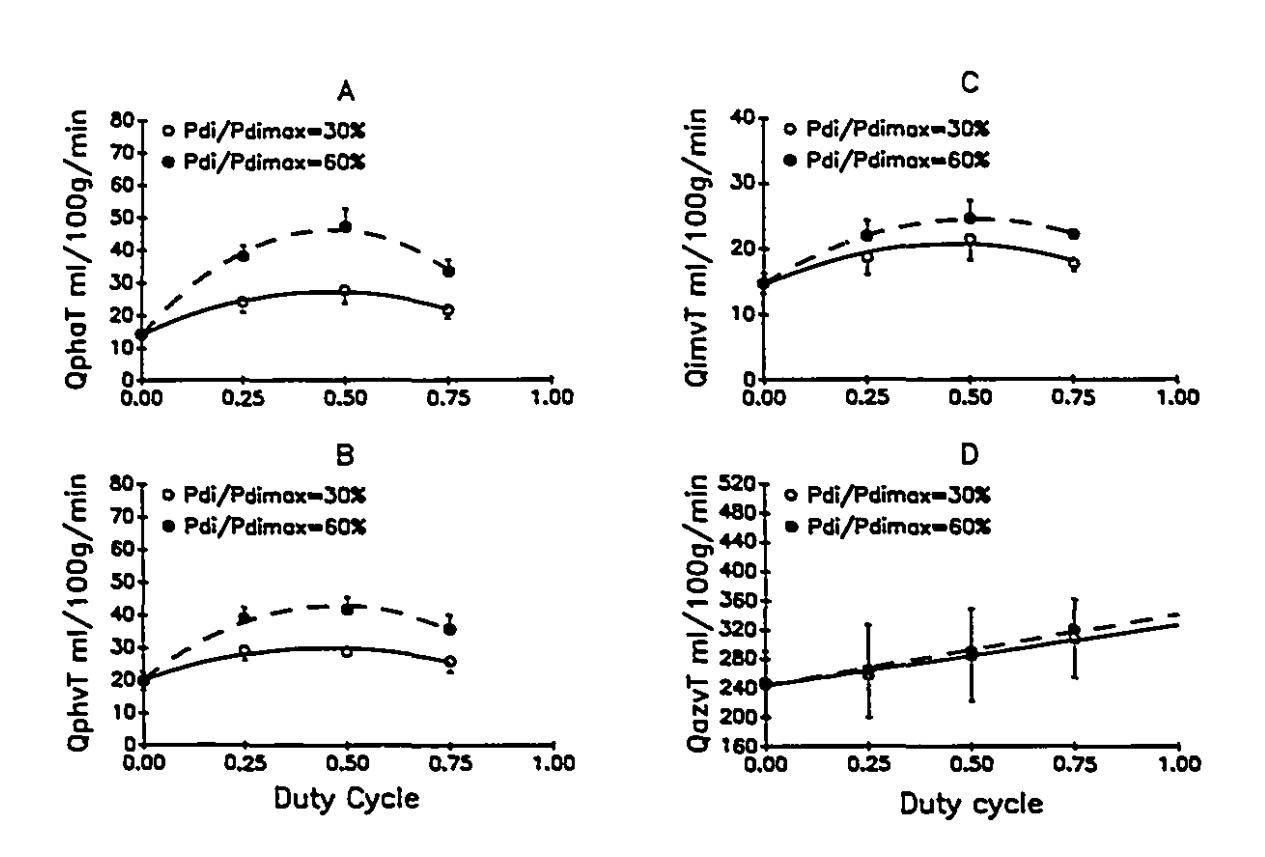
Q as a Function of Pdi: Qphar and Qphvr increased significantly as a direct function of Pdi/Pdimax at all duty cycles and f (Fig. 7, A and B). The increments in Qphar (all duty cycles) and Qphvr (only at a duty cycle of 0.25) were mainly due to increased QR. The increments in Qphvr

TABLE 3

Partition of Qdi into Contraction and Relaxation Phase, and
Total Cycle

Q 	Pdi/Pmax	x CTL	Duty		Cycle	Slope	
Phase			0.25	0.50	0.75	(Q/DC)	r
phaC	0.34 0.61		4.1 4.6	11.0 14.5	15.0 19.3	21.8 29.4	0.988 0.981
phaR	0.34 0.61		19.8 33.3	16.4 32.5	6.5 13.9	-26.6 -38.8	-0.962 -0.884
phaT	0.34 0.61	14.2 14.2	23.9 37.9	27.4 47.0	21.5 33.2		
phvC	0.34 0.61		6.6 10.0	11.7 18.7	18.4 25.2	23.6 30.4	0.997 0.997
phvR	0.34 0.61		22.3 28.8	17.1 22.9	7.3 10.4	-30.0 -36.8	-0.985 -0.979
phvT	0.34 0.61	19.7 19.7	28.9 38.8	28.7 41.6	25.8 35.6		
imvC	0.34 0.61		5.1 6.2	11.1 13.0	13.3 17.1	16.4 21.8	0.966 0.990
imvR	0.34 0.61		13.5 15.6	10.3 11.6	4.4 4.9	-18.2 -21.4	-0.986 -0.990
imvT					17.7 22.0		
azvC						330.6 342.8	
azvR	0.34 0.61		178.9 181.8	123.1 126.4	63.3 65.9	- 231.2 - 231.8	
azvT			258.1 264.3		307.8 319.8		

Steady state blood flow (Q) is expressed in ml/min/100g.



Regional total Qdi (steady state) as a function of duty cycle (DC) at Pdi of 30 and 60% Pdi max. Qphar, Qphvr, and Qimvr are parabolic functions of duty cycle at both low and high Pdi. Note that at a duty cycle of 0.45-0.50 maximal flow is achieved. Qazvr is a linear function of Qazvr of duty cycle. CTL, control.

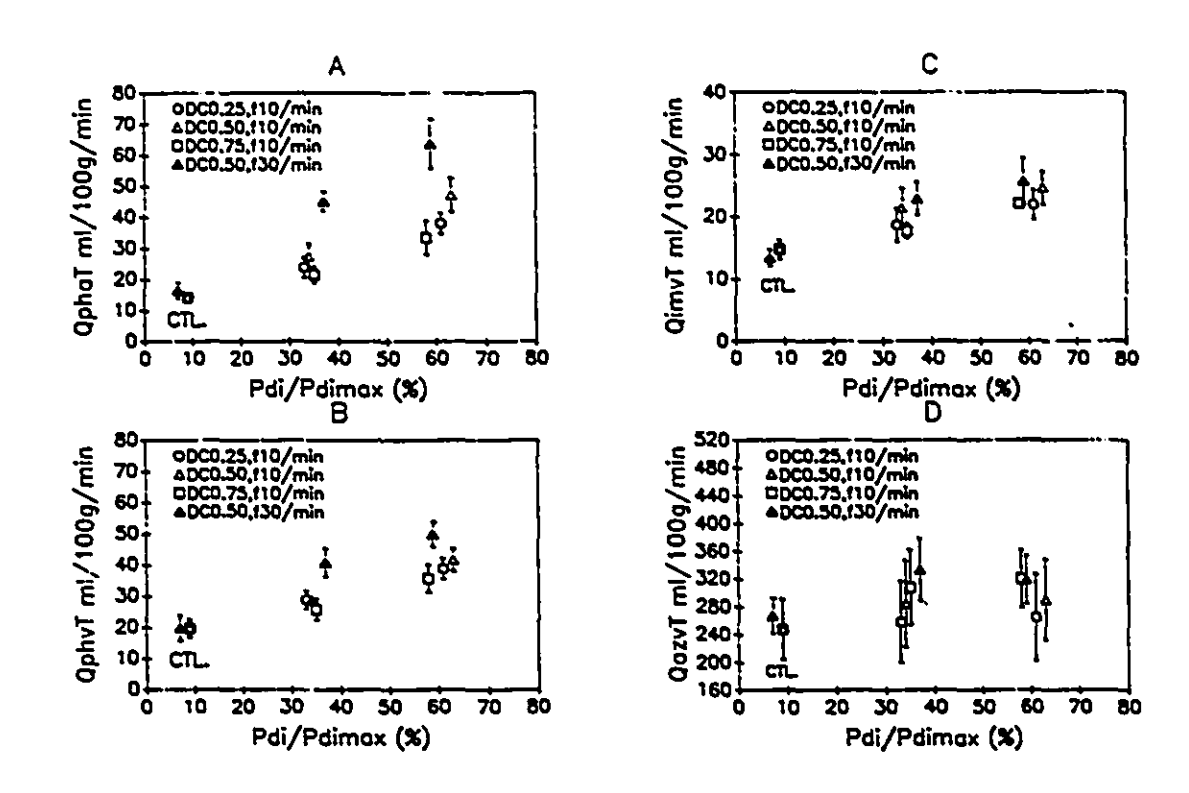


Figure 8. (steady Regional Qdi state) during contraction cycle as a function of Pdi/Pdimar. When Pdi increased from control to 60% of Pdi max, Qphar, Qphvī, and Qimvr increased significantly (P < 0.05). When f increased from 10 to 30 cycles/min, QphaT and increased significantly (P < 0.05). QazvT and QimvT did not change significantly 85 function of f. QazvT did not significantly as a function of Pdi/Pdimax.

(at duty cycles of 0.50 and 0.75) were mainly due to increased Qc (see Table 3). There is only a marginal increment in Qimvī and no change in Qazvī (Fig. 7, C and D; Table 3) as a function of Pdi at iso-duty cycle. During diaphragm pacing at a duty cycle of 0.50 and at 60% Pdi max, the diaphragmatic blood drainage was approximately 60% through the intercostal veins leading into the azygos trunk, 25% through the phrenic vein, and 15% through the internal mammary vein.

Q as a Function of f: Figure 8, A and B shows that when f is 30 cycles/min at duty cycle of 0.50, the Qphar and Qphvr are higher than at a f of 10 cycles/min (P<0.05). The effect of f on Qphar is mainly due to increase in QR (Figs. 4B and 6B). In contrast, the effect of f on Qphvr is mainly due to an increase in Qc (Figs. 4C and 6C). The f does not affect Qimvr or the Qazvr Pdi relationship (Fig. 8, C and D).

Q as a Function of Duty Cycle: As shown in Fig. 7 with a f of 10 cycles/min at both low and high Pdi, Q is a function of the duty cycle. As shown in Table 3, the Q-duty cycle slope indicates a positive relationship during contraction and an inverse relationship during relaxation. However, during steady state conditions, the Qphat, Qphvt and Qimvt are parabolic functions of the duty cycle as shown in Fig. 7, A-C, whereas Qazvt is a linear function of duty cycle (Fig. 7D).

DISCUSSION

Critique of Methods: We compared Q measured via the Doppler technique with Q measured via direct blood volume collection in the same vessels and found that they are significantly correlated. The linear regression coefficient (r) was 0.917 for Qpha, 0.911 for Qphv, 0.877 for Qimv, and 0.985 for Qazv (P<0.001). The calibrations were carried out in a different population of dogs because of the lengthy nature of the procedure and the difficulties involved in calibration. four vessels in each dog made further experimentation in the same animal impractical. The rationale for calibrations in another group of animals is not that different from that for calibration values obtained from individual dogs and eventually reported as group mean values. Our approach is an averaged calibration factor that is used calculate individual flow rates. This approach is analogous to those performed for the calibration of electromagnetic flow Electromagnetic flow probes are calibrated in probes. vitro, and calibration factor is derived. Calibration factors thus obtained have been used previously by Bark and Sharf (9) and Sharf et al (89). We calibrated our Doppler flow probes in vivo and used the same flow probes in all experiments, where Q was evaluated during pacing. Theoretically a decreased in vessel diameter (stenosis produced by a tight fitting probe) could have resulted in an increase in the Doppler shift. Figure 2 shows that the range of blood flow rates for a given Doppler shift is quite small. Under conditions of constant perfusion pressure, while using whole blood (hematocrit of 45%), we observed that the tubing diameter (1-3 mm) only slightly affected the signal for 2-mm-diam flow probes. Similar observations were seen with the other flow probes used on the azygos, internal mammary, and phrenic veins. Thus, in our experiments, the angle of the crystal was the same for every vessel and the only variable remaining was the fit around the vessel, which seemed to have little effect on the Doppler shift. Therefore probe fitting around the vessel was a minor source of error.

Theoretically the sum of the three venous outflows should be representative of total diaphragmatic blood flow (Qdi). In practice, however, it cannot be used as such because extradiaphragmatic blood from other sources contributes an unknown fraction to the Qazv. In effect, the azygos trunk collects venous flow from the intercostal veins, which have considerable anastomosis with the circulation of the costal diaphragm. Although the abdominal azygos was ligated, blood draining from other structures not related to the diaphragm, such as the spinal plexus, can still contribute to Qazv. The trunk of the internal mammary vein has anastomosis with intercostal veins, and in addition, it drains directly from the diaphragm. Hence, the fraction of Qazv that comes from the diaphragm is not

evident. On the other side, the increase in Qazv after stimulation of the diaphragm likely represents the extra drainage from the diaphragm to the intercostal veins into the azygos, because diaphragmatic activity was the only variable introduced. In fact, we have verified inactivity of other respiratory muscles during pacing (which could affect Qazv and Qimv, respectively) by use of the electromyogram (EMG) and by measurement of shortening in the upper and lower intercostal muscles (3rd and intercostal spaces), the paraspinalis muscles (EMG only), and the transversus abdominis muscle (in two dogs). changes in Qazv from control Q values to pacing values (excluding changes in the Qimv) indicate that approximately 60% of the diaphragmatic drainage is through the intercostal veins leading into the azygos trunk. This analysis is similar to measurements of O2 consumption (VO2) of the respiratory muscles, where resting body VO2 is subtracted form the VO2 values observed during stimulated breathing. Using this approach, we found that approximately 25% of Qdi is through the phrenic vein and another 15% is through the internal mammary vein. This is in agreement with the finding of Nichols et al (76), who showed that approximately 20% of diaphragmatic blood flow is accounted for by the phrenic artery. The azygos vein, ligated at the lower thoracic level, would not drain flow from the abdomen. We can see from Table 3 and Fig. 7D that Qazv has a linear increment from diaphragmatic tension-time index (TTdi), behavior quite different from that of Qphv and Qimv, which plateaus and then decreases flow at higher TTdi. The behavior of Qazv is compatible with the diaphragm draining progressively more blood through the intercostal veins at high TTdi, while limitation in phrenic vein and internal mammary vein drainage may be effective because of prolonged periods of high Pab.

Our results of Qpha measured with the diaphragm at rest are comparable with measurements done by Bark and Scharf (9) during similar conditions with similar methods. The Qpha is 11.7 \pm 4.1 ml/min/100g in the study of Bark and Scharf (9) and 14.2 ± 1.9 ml/100g/min in this study. However, when diaphragmatic work is increased, is increased accordingly, and under isowork conditions Qdi values, reported by numerous authors (10, 12, 16-17, 31, 51, 53, 63, 83-88, 97, 100) range from 30 to 210 ml/100g/min. Thus among various techniques (e.g., radioactive microspheres, Kety-Schmidt, vessel cannulation, electromagnetic, and Doppler) there is much variability. Therefore it seems safer at this point to compare changes within a given technique and an experimental setup with reliable calibration than to use interexperiment comparisons. In our work we controlled the calibration; measured and selected studies with constant perfusion pressure; accounted for f, duty cycle, and Pdi; and weighed the diaphragm for normalization. Our Qdi values rest within these ranges, but the point of interest is the fact that the Doppler technique permits instantaneous measure of intracycle Q. Hence, most of the further discussion concentrates on the modification of intercycle Q analysis.

Equilibration Time of Q and Changes in Pacing Patterns: A progression Qphar and Qphvr at duty cycles of 0.25, 0.50, and 0.75 and f of 10 cycles/min and at a duty cycle of 0.50 and f of 30 cycles/min are similar to the results reported by Bellemare et al (12). This progressive response pattern can be attributed to the combination of several events: 1) a slight fall in Paorta and a decrease in cardiac output in the first 30 s of pacing (see Fig. 10), 2) an abrupt dynamic compression of intramuscular blood vessels, and 3) diaphragmatic metabolic demand increasing with time (41, 94).

The proportion of Qc and QR in QT is a function of the duty cycle and is different for phrenic arterial and venous flow. At duty cycles of 0.25 and 0.50, QT is mainly accounted for by QR (>50%). Furthermore, Qc/QT is greater in venous than in arterial circulation. Presumably, in our experiment the intramuscular tension during diaphragmatic contraction compresses the arteries and increases resistance to inflow. However, the increase in tension seems insufficient to collapse the vessels completely. Thus, during the contraction phase, flow does not stop entirely but is nevertheless reduced. In contrast, at the very beginning of the contraction phase, the sudden increase in

intramuscular tension brought on by phrenic nerve stimulation pumps diaphragmatic venous blood out of the muscle in the form of a rapid jet (see Qphv in Fig. 3). In a way, the diaphragm behaves like a pump: it pushes blood out during its contraction and reestablishes this volume during relaxation. An observation compatible with the above concept was made by Anrep and Saalfeld (2) in the gastrochemius muscle of dogs.

Effect of Pdi on the Regulation of Q: These results show a direct relationship between Pdi/Pdi max and Qphat and Qphvt at any duty cycle and f (Fig. 7). The results are consistent with the findings of Reid and Johnson (81), Robertson et al (83-84) and Rochester et al (86-88), which publish the linear relationship between the work of the diaphragm and Qdi. In our experiment, the highest Pdi tested was, on the average, 61% of Pdi max. It is possible that our Pdi is lower than the critical tension required to collapse or nip diaphragmatic blood vessels. In a similar animal model, Bellemare et al (12) also found that Qdi was not abolished at 60% of Pdi max. Our results could be dependent on the fact that Pdi was developed against a casted abdomen and not entirely by the rib cage, which should influence circulation by direct compression of the phrenic vein.

The only data we know that address this question are those of Buchler et al (17). Their data on intermittent

contractions (duty cycle 0.25-0.75) during maximal diaphragmatic stimulation were obtained with casted abdomen and opened chest (as were our data) and with closed chest and opened abdomen. They concluded that there was no significant difference in Qdi between the two conditions. We believe that this maybe so, because, if increased Pab decreases phrenic artery perfusion, it may not impede perfusion from intercostal arteries and internal mammary arteries, which could show a different venous pattern. In fact, 75% of the diaphragmatic perfusion is drained from veins other than the phrenic, and the design of the diaphragmatic circulation seems adequate to cope with this mode of activity.

Effect of f on Q: These results show that, by increasing f from 10 to 30 cycles/min, Qphar and Qphvr increased at both low and high Pdi (Fig. 7). This is consistent with findings from previous studies (16, 83, 84).

It is not clear why f affects QimvT and QazvT less than it affects Qphv. Our f is considerably lower than that used by Buchler et al (16). Therefore, it is possible that the f of 30 cycles/min is not high enough to affect QimvT and QazvT. Note that the resting Qazv is an order of magnitude greater than the resting Qphv, indicating that flow from many areas other than the diaphragm is contributing.

<u>Duty Cycle as a Factor of Q Regulation:</u> Bellemare et al (12), Buchler et al (16-17), Bark et al (9-10), and Hussain

et al (53) have shown that the duty cycle is an important factor in Qdi regulation. Their results have also suggested that Qdi is limited at a high duty cycle. Our results indicate that during both low and high Pdi (30 and 60% of Pdi max, respectively), arterial and venous blood flow are linearly related to the duty cycle during the contraction phase of the breathing cycle (see Table 3). This is so because inspiratory duration (Ti) becomes longer as the duty cycle increases and there is more time for the blood to go through the diaphragm. On the other hand, both arterial and venous blood flow decrease linearly with the duty cycle during relaxation period of the diaphragm (see Table 3). This is because expiratory duration (Te) becomes shorter and there is less time for the blood to pass through. However, the Q-duty cycle slope increases with Pdi. On the other hand, the slopes (absolute value) between Qpha, Qphv, Qimv and duty cycle are greater during diaphragmatic relaxation than during the contraction period, indicating that these Q are more important in the relaxation period. The sum of Qc and QR shows that Qphar, Qphvr and Qimvr are a parabolic function of duty cycle. The optimal Q occurs at a duty cycle of about 0.45-0.50 regardless of Pdi. However, the results from Bellemare et al (12) propose a unique TTdi/Q, including data obtained from contractions in which a Pdi in the range of 50 to 70% of Pdi max was developed (Fig.9). the results of Bellemare cet al, TTdi was calculated by multiplying duty cycle and Pdi (% Pdi max) and the duty

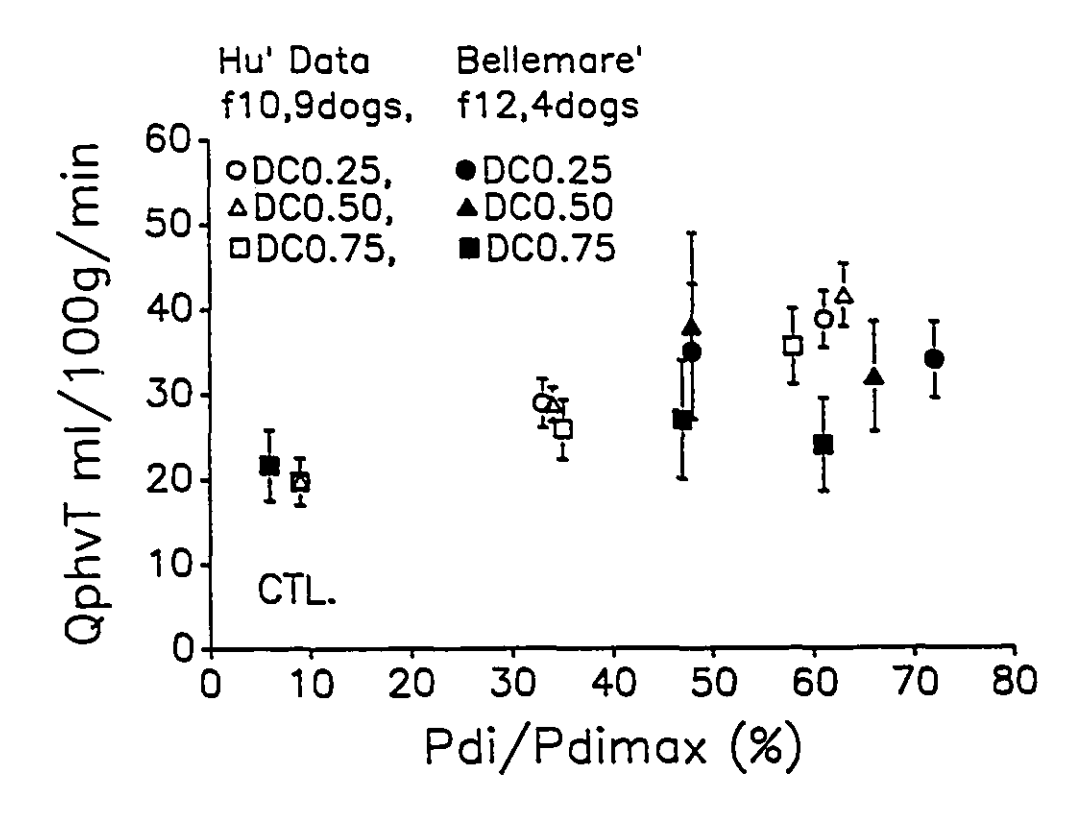
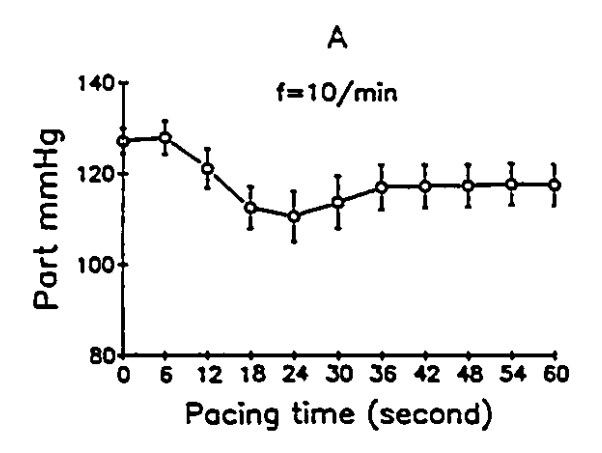


Figure 9. Qphvr as a function of Pdi/Pdimax, including data (mean ± SE) obtained from the study of Bellemare et al (4) with Pdi in the range of 50 to 70% of Pdi max. For further details see text.

cycles explored were 0.25, 0.50, and 0.75. The relationship of Q to TTdi was established by using the best fit line among the data points drawn by hand. It showed an ascending and descending limb with a blunt plateau at a TTdi of 0.15-The present work, while corroborating the data of 0.20. Bellemare et al within the same range of pressure, does not seem to corroborate the concept of a unique TTdi/Q function. In fact, when Pdi was considerably lower (30% Pdi max), the TTdi/Q relationship was different from that at a Pdi of about 60% of Pdi max. This implies that a given TTdi obtained via a different combination of Pdi and duty cycle is not iso-Q. Further analysis of Fig. 8, A and B, shows that both Qphv and Qpha increase by about 50% when Pdi increases from 30 to 60% of Pdi max at all duty cycles explored. On the other side, at either Pdi, changes in the duty cycle induce changes of Q on the order of only 15%. Our data, as shown in Fig. 8, fit a parabolic function with maximal Q at a duty cycle of 0.50 for a Pdi of 30 and 60% of Pdi max. Although we recognize that the numbers of data points are insufficient for definitive conclusions, they seem to indicate that Q (for a given TTdi) is strongly determined by Pdi and modulated by the duty cycle. Furthermore, duty cycles lower and higher than those explored may be more relevant in modulating Q. Hence, Q may have optimal values dependent on the pacing pattern.

Paorta during Phrenic Nerve Stimulation: Figure 10, A and B, shows that Paorta was not significantly modified during the first 6 s of pacing, regardless of Pdi or f. Then Paorta decreases progressively up to 20 s. Thereafter, it increases to reach a stable value at 30-36 s, which was slightly but not significantly lower than the control values (see Table 2). We conclude that Paorta was not a significant factor in affecting the stable Qdi among the different pacing runs we undertook.



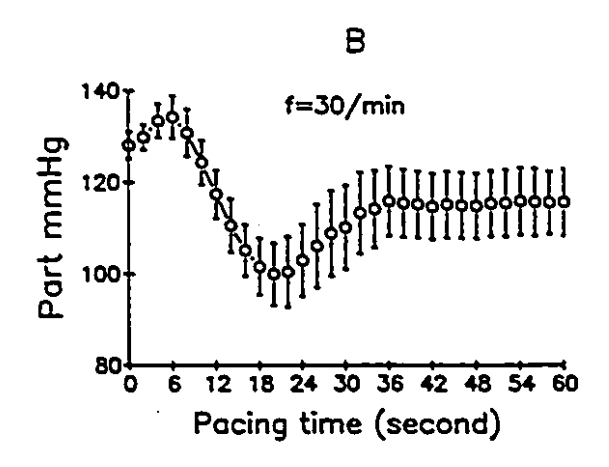


Figure 10. A), Mean abdominal aortic blood pressure (Paorta) in all runs and in all animals at f of 10 cycles/min as a function of time. B), Paorta in all runs and in all animals at f of 30 cycles/min as a function of pacing time. A stable Paorta which is slightly lower than the control value, is reached after 36 s of pacing. There is no significant difference between the stable Paorta (at 30-36 s) and the control value.

Summary: The diaphragm behaves like a pump: it pushes blood out during its contraction and reestablishes its volume during relaxation. Therefore at a given duty cycle, Qphvc/Qphvt > Qphac/Qphat during diaphragmatic contraction, and QphvR/Qphvt < QphaR/Qphat during diaphragmatic relaxation.

Approximately 60% of diaphragmatic drainage is via the intercostal veins into the azygos trunk, 25% is through the phrenic vein into the inferior vena cava, and another 15% is via the internal mammary vein.

Qpha and Qphv are linearly related to the f and to Pdi up to 60% of Pdi max. However, Qimv and Qazv are less affected by Pdi and f.

Qpha, Qphv, and Qimv are related by a parabolic function to the duty cycle. Qazv is linearly related to the duty cycle.

CHAPTER 6

OPTIMAL DIAPHRAGMATIC BLOOD PERFUSION

SUMMARY

The intrabreath time course of phrenic artery blood perfusion (Qpha) was studied in five anesthetized dogs. The diaphragm was paced with submaximal levels of stimulation at various duty cycles (DC) to achieve tension-time index below and above the fatigue threshold (0.03 to 0.60). Left Qpha was measured via Doppler technique during control (inactive diaphragm) and during two submaximal levels of bilateral phrenic nerve stimulation sustained for one minute. Measurements were done when Qpha reached steady state in each run. The frequency of pacing of each run was 10/min and, the DC ranged from 0.1 to 0.9 in 0.1 increments. Shortening of costal and crural segments was measured by It was found that Qpha during the sonomicrometry. diaphragmatic contraction phase (QphaC) was a sigmoidal function of DC and was not affected by the levels of transdiaphragmatic pressure (Pdi) explored (34 to 64% of Qpha during the diaphragmatic relaxation maximal Pdi). phase (QphaR) was a parabolic function of the DC, reaching an optimal value at DC of about 0.3 at any given Pdi. QphaR increased significantly with the preceding level of Pdi. QphaT (the sum of QphaC and QphaR) was a parabolic function of DC, reaching peak values at DC of 0.4 to 0.6 and then decreasing. This function was similar at two levels of Pdi. Post-pacing hyperemia was directly related to tension-time index above 0.20.

Keywords: Diaphragmatic blood flow, diaphragmatic
shortening, transdiaphragmatic pressure (Pdi),
duty cycle (Ti/Ttot), tension-time index (TTdi),
muscle fatigue.

INTRODUCTION

Diaphragmatic blood flow (Qdi) is proportional to transdiaphragmatic pressure (Pdi) during intermittent diaphragmatic contractions (9, 16-17, 31, 47, 52, 57, 63, 75-76, 80-81, 83-88, 96-97, 100). Similarly, coronary circulation in the heart is proportional to the afterload (aortic pressure), and it occurs mainly during diastole (13). As well, when Qdi is expressed as a function of the diaphragmatic tension-time index {TTdi, the product of Pdi and duty cycle [DC, defined as contraction time (T1) over total time (TT) of one breath cycle for the inspiratory muscles]}, a strong relationship exists and it follows a parabolic function (10, 12). Therefore, it seems from the above, that blood flow through an organ tissue is dependent on a vascular waterfall, that is, a pressure gradient between arterial pressure and tissue pressure (13). Thus a close control of DC should be an important factor in providing adequate Qdi. It is of interest that, during increases in ventilation, such as in exercise, the DC remains within a relatively narrow margin (0.4-0.6), a peculiar occurence considering that a wider range of DCs are used during other less taxing activities, such as speech.

The purpose of the present study was to measure phrenic artery perfusion (Qpha) during contraction and relaxation in steady-state contraction patterns, including DCs from 0.1 to 0.9, each held at two levels of Pdi [30 and 60% of maximal

Pdi (Pdimax)]. This provided nonfatiguing and fatiguing contraction patterns. We tested the hypothesis that the DC may have a role in producing an optimal Qdi for any given Pdi, optimal Qdi being defined as the best (highest) flow rate obtained for a given DC under conditions of iso-Pdi and isoperfusion pressure.

MATERIALS AND METHODS

Animal Preparation

Five mongrel dogs, weighing 13-32 kg, were anesthetized with pentobarbital sodium (25mg/kg iv). Maintenance doses were given during the experiment sufficient to keep the corneal reflex abolished. The animals were placed in supine position and were mechanically ventilated through endotracheal tube with a Harvard respiratory pump. intravenous catheter placed in the anterior forelimb delivered a 5% dextrose solution in saline to replace lost fluid. A water-filled catheter was introduced into the right femoral artery to the level of the abdominal aorta and connected to a pressure transducer (Sanborn B-670 B) for recording of arterial pressure (Part). Qpha was measured with the Doppler technique, as described in a preceding paper (47). Briefly, this technique consists of placing a Doppler ultrasonic flow probe around the left inferior phrenic artery (Fig. 1). Diaphragmatic shortening (crural and costal) was measured via

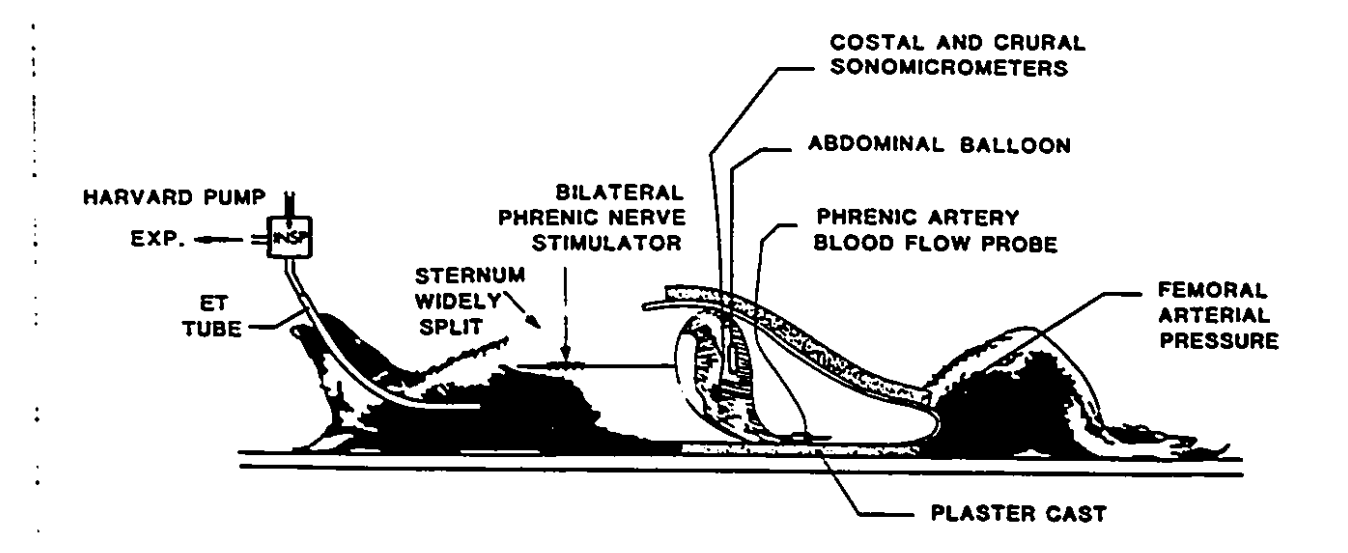


Figure 1. Schematic representation of the experimental model. Consists in open chest dogs with casted abdomen and lower rib cage with electrically stimulated phrenic nerves. Phrenic artery blood flow was measured via Doppler technique. ET, endotracheal tube. For further details see text.

sonomicrometry (5 mHz ultrasound length gauge modules, Valpey-Fisher, Model LG-1) (Fig. 1) by two pairs of piezoelectric transducers mounted 15-20 mm apart along the same muscle fibers. A thin-walled latex balloon (5 cm long) filled with 1.5 ml of air was positioned in the peritoneal cavity between the liver and stomach and was connected to a differential pressure transducer (Validyne MP-45.4) for abdominal pressure (Pab) measurement relative to atmospheric pressure. The abdomen was closed in two layers with suture.

A midline sternotomy was performed. Two silver wire electrodes were wound around each of the two phrenic nerves at T2-T3 level and were isolated from the surrounding tissues. These electrodes were connected to a Grass S-48 stimulator for diaphragmatic pacing.

A loose cast was placed around the abdomen from the xiphoid process to the origin of the posterior limbs. The purpose of the cast was to prevent large diaphragmatic shortening [to levels of 60% of length at functional residual capacity (Lfrc)] observed when maximal stimulation is given without abdominal wall restriction. The animals were kept warm with heating pads and surgical lamps. The core temperature was recorded by an electronic rectal thermometer and was maintained at 37° C.

Experimental Data Recording

Part, Pab, crural and costal diaphragm length (Lcos and Lcru) and Qpha were recorded on an eight-channel strip-chart recorder (Hewlett-Packard 7758 A). Figure 2 shows an example of simultaneous recording of Qpha and its relation to Pab and Part.

Experimental Protocol

At the beginning of each experiment, we determined maximal Pab by stimulating bilaterally the phrenic nerve with 8 volts at a frequency of 80 Hz with a pulse duration of 2.5 ms. After an adequate rest period, the following protocol was developed.

Qpha was measured at rest (the initial 3 sec shown in Fig. 2) while the animal was mechanically ventilated. Next, the effect on Qpha of steady intermittent diaphragmatic contractions at DCs of 0.1 to 0.9, in 0.1 increments, was investigated. The DCs were selected in a random manner. At each DC, the diaphragm was stimulated for 1 minute with a pacing rate of 10/min. The intensity of stimulation was 1-6 volts, delivered at a frequency of 10-40 Hz. The pulse duration was 0.1-0.3 ms. Intensity and frequency was changed as to obtain two levels of Pab (about 30 and 60% of maximal Pab), which resulted in two levels of diaphragmatic shortening, 21 and 37% of LFRC, respectively. experiments we were careful to produce similar Pdi values (external work) in every run for every animal

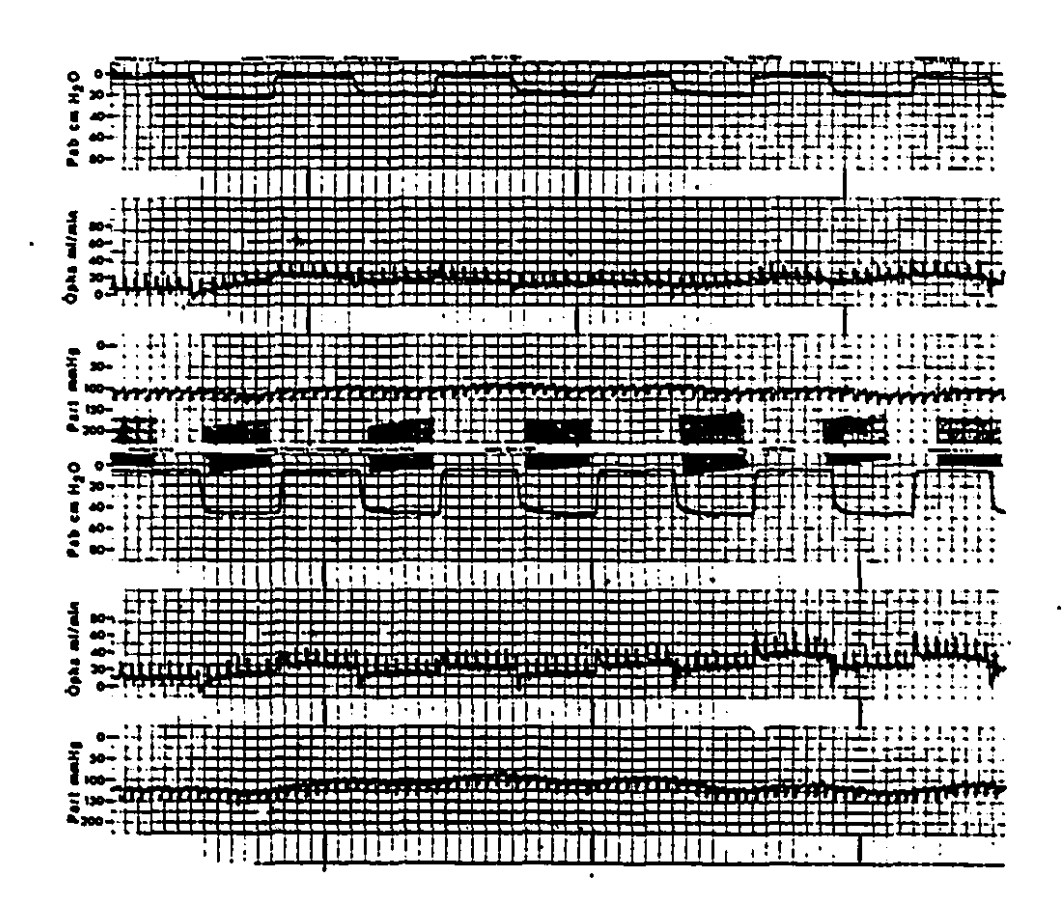


Figure 2. Stripchart recording obtained in one animal before and during submaximal stimulation with a duty cycle of 0.5 and a pacing frequency of 10/min. Top 3 channels are from a run stimulated with 0.1 ms duration, 15 Hz and 1 v. Bottom 3 channels are from another run stimulated with 0.1 ms, 25 Hz and 2 V. Pab, abdominal pressure; Qpha, phrenic artery blood flow; Part, mean abdominal aorta blood pressure.

studied. As well, we examined Qpha values under iso-Pdi conditions produced by high voltage (4-6 volts) or low frequency of stimulation (10-20 Hz) or low voltage (1-3 volts) and high frequency of stimulation (30-40 Hz). We found that Qpha values were similar in both circumstances for iso-Pdi conditions. After each run, all parameters were monitored for at least 5 minutes (post pacing activity) until they returned to control levels. There was at least a 20 min interval between runs. This protocol allowed us to explore the Qdi through TTdi values ranging from 0.03 to 0.60, i.e., from nonfatigue to fatiguing contraction patterns.

When the above tests were completed, the animals were killed with an overdose of anesthetic, and then the diaphragm was dissected and weighed.

Calculation of Qdi

In these experiments the contraction and relaxation phases were determined by the onset of mechanical parameters. The type of diaphragmatic pacing used for these experiments produced square wave Pab swings, as demonstrated in Fig. 2. The contraction phase was defined as the period from onset of rise in Pab until peak pressure was reached at the end of the contraction. The relaxation phase was the period ranging from the peak pressure at the end of the contraction phase to the initial moments of the next Pab swing. Under those circumstances, values for Qpha during

the contraction phase (Qphac), the relaxation phase (Qphar), and the total contraction cycle (Qphar) were calculated and normalized to milliliters per 100 g of diaphragm per minute, as described in a previous paper (47). The values obtained for Qphac, Qphar, and Qphar are reported as blood volume (flow rate * time duration of phase) and are expressed as ml/100g/min.

Statistical analysis

All measurements were expressed as mean \pm SE. Two-way analysis of variance, and linear and nonlinear regression analyses were used.

RESULTS

Arterial Blood Pressure during Diaphragmatic Pacing: Figure 3 and Table 1 show that the perfusion pressure was kept constant throughout the experiments and pacing did not significantly change Part values with respect to the resting non contracting diaphragm (DC of 0).

Transdiaphragmatic pressure (Pdi): Because the thoracic surface of the diaphragm was exposed to the atmospheric pressure, Pab was equal to Pdi. The resting swing in Pdi, generated by the respirator, was 7.3 ± 1.1 cmH2O. The Pdimax was always obtained at the beginning of each experiment via supramaximal bilateral electrical stimulation of the phrenic nerves (8V, 80Hz). It averaged 88.1 ± 3.1 cmH2O. Diaphragmatic tension was expressed as Pdi/Pdimax.

TABLE 1

Part, Pdi, Pdi/Pdimax and Diaphragmatic Shortening at

Various Duty Cycles during Low (L) and High (H) Submaximal

Levels of Bilateral Phrenic Nerve Stimulation.

Н
0.0
34.3
35.6
37.7
38.2
38.4
39.0
38.7
37.7
36.1
37.3
0.5

DC - duty cycle; CTL - control; \triangle L - amount of diaphragmatic shortening expressed as % of Lfrc; L is equal to a mean Pdi value of 29.7 cmH2O; H is equal to a mean Pdi of 56.0 cmH2O.

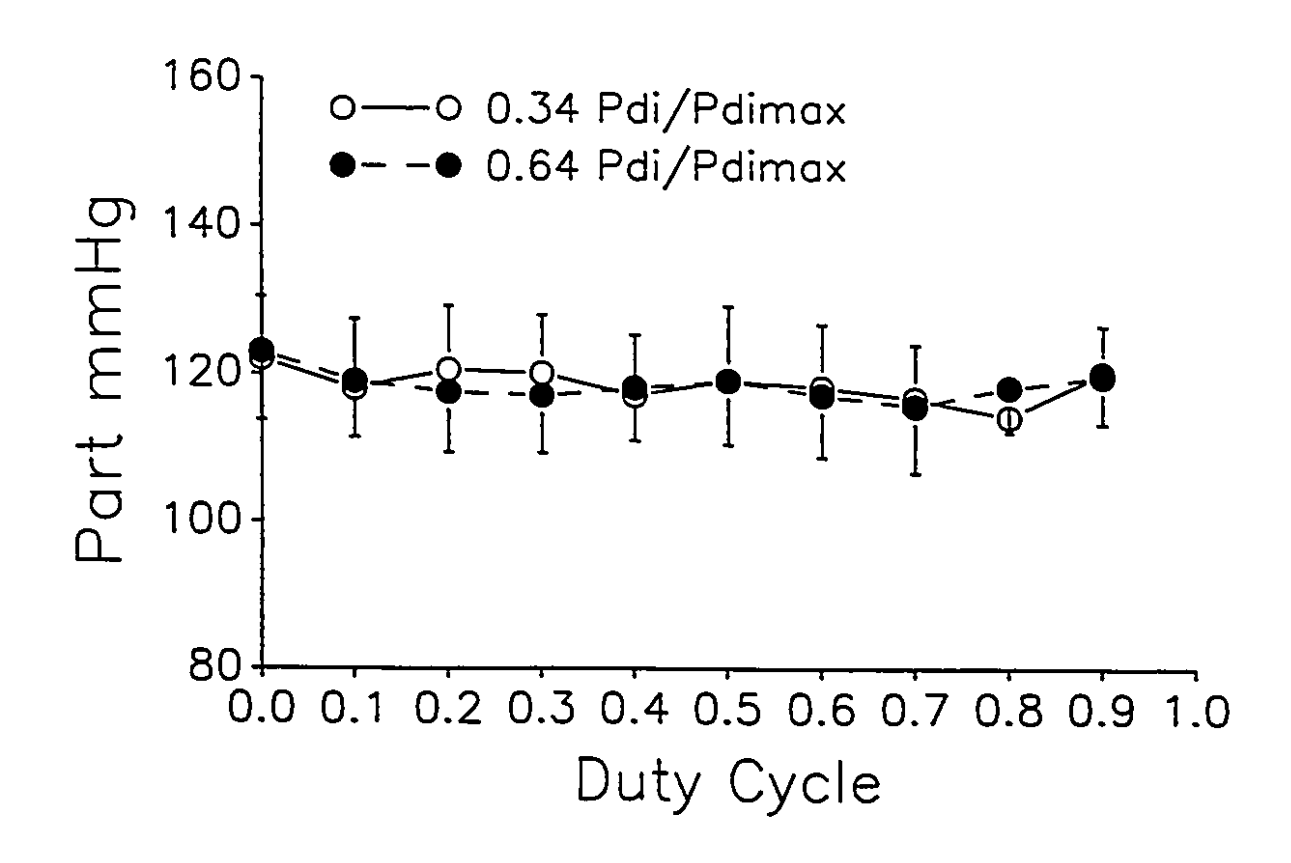


Figure 3. Mean abdominal aorta blood pressure (Part) vs duty cycle. There is no significant difference between any duty cycle and control (non stimulated diaphragm). Data is average ± SE.

Pdi was increased in the experimental runs by increments of both stimulation voltage and frequency. The two levels of Pdi/Pdimax obtained at each DC are shown in table 1. The values of low or high Pdi were similar at all DC and averaged 34 and 64% of Pdimax. These values were significantly different from control, and from one another (P < 0.01).

Shortening of the diaphragm during stimulation: The shortening of the costal and crural segments of diaphragm induced by bilateral submaximal pacing of the phrenic nerves was expressed as a percentage of the length at FRC (4% LfRc). Shortening increased after increments of both the stimulation frequency and voltage. In general. shortening was slightly higher in the crural segment than in the costal segment. We used the average of costal and crural shortening as an expression of diaphragmatic shortening (A% LfRc in Table 1). The two levels of shortenings in all dogs and DCs averaged 20.9 ± 1.2 and 37.3 ± 1.6 % of LFRC for a Pdi of 34 and 64% of Pdimax. respectively. There was a significant difference (P < 0.01) between shortenings obtained during stimulation with respect to that of the passive resting diaphragm (control) at all There was also a significant difference in shortening between both levels of stimulation (P < 0.01). Figure 4 shows that there is a linear relationship between Pdi and % LFRC when all experimental results are considered.

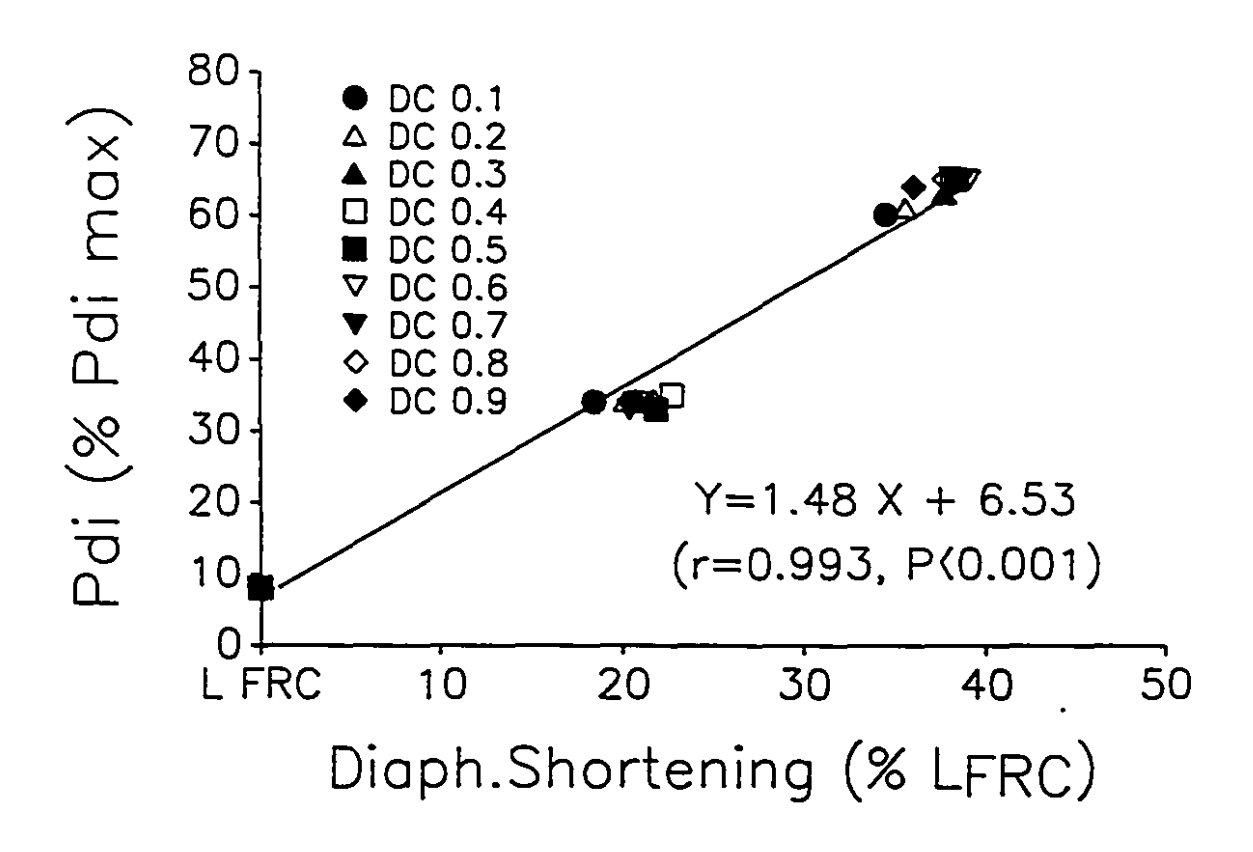


Figure 4. Transdiaphragmatic pressure (% Pdi max) vs diaphragmatic shortening (% Lfrc). There is a significant linear relationship (P<0.001) between Pdi and diaphragmatic shortening. Data is from all runs, all animals.

Opha as a function of the contraction and relaxation time:

Figure 5A shows that QphaC is a sigmoidal function of the DC at both 34 and 64% of Pdimax. The slope (AQphaC/ADC) is not affected by Pdi. QphaC seems to be linearly related to the duration of contraction through DCs ranging from 0.1 to 0.8.

Figure 5B shows that QphaR is a parabolic function of the DC, reaching an optimal value at a DC of about 0.3. But QphaR is greater at 64% than at 34% Pdimax. Notice that QphaR is greatest at low DCs (0.1-0.3), and is largely reduced at high DCs (0.7-0.9), thereby showing the volume-limiting effect of a shorter relaxation time. Notice also, that the increase in Pdi is more important in increasing blood perfusion than the modulation of the DC. In fact, at 34% Pdimax, the blood perfusion remains constant in the DC range of 0.1 to 0.6. Differences in blood perfusion as a function of DC are larger at 64% Pdimax.

Figure 5C shows that QphaT is a parabolic function of the DC. The maximal value of QphaT occurs at a DC of 0.4 to 0.6 regardless of Pdi/Pdimax.

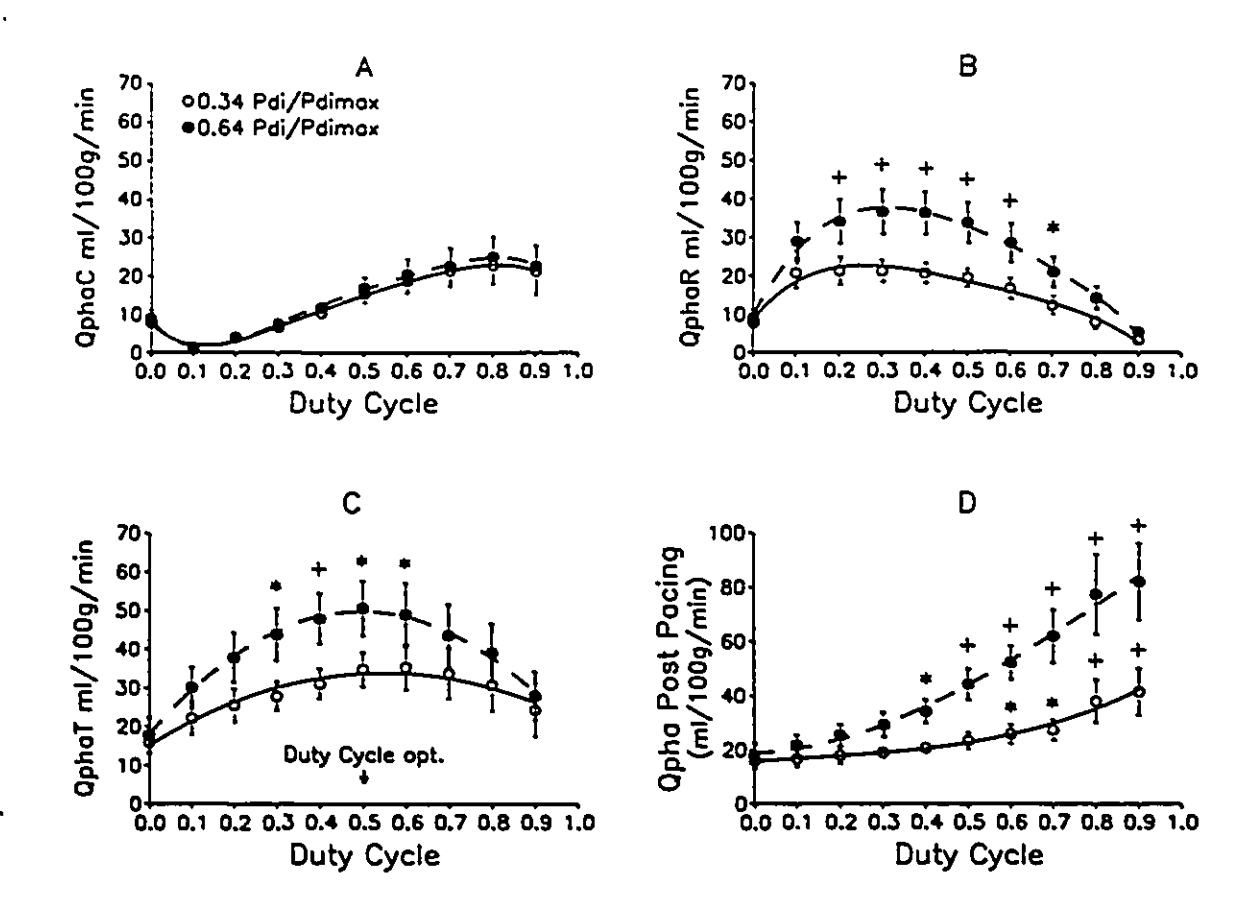


Figure 5. Panel A, phrenic artery blood perfusion (Qpha) during diaphragmatic contraction phase plotted as a function of duty cycle held at Pdi= 0.34 or 0.64 of Pdi max . The slope (AQphaC/Aduty cycle) is not affected by Pdi. Panel B, Qpha during diaphragmatic relaxation phase (R) as a function of duty cycle. A highest value of Q occurs at a duty cycle of 64% of Pdi max has higher QphaR. * about 0.3. P<0.05, + P<0.01 when compared between 64% and 34 % of Pdimax at iso-duty cycle. Panel C, Qpha during the total cycle (T) as a function of duty cycle. An optimal value occurs at duty cycles of 0.4 to 0.6 regardless of Pdi. Pdi max has higher QphaT. * and + as in Panel Panel D, Post-pacing hyperemia function of duty cycle and Pdi. There is a significant difference (P<0.01) between 64% and 34 % of Pdi max at iso-duty cycles of 0.5-0.9. differences Significant between control diaphragm, cycle = (resting duty 0) stimulation are (*) P < 0.05 and (+) P < 0.01. Data is average ± SE.

Figure 5D indicates that phrenic artery post-pacing hyperemia is a function of both the preceding DC and tension developed by the diaphragm. The slope (post-pacing hyperemia/DC) is significantly steeper at a Pdi of 64% Pdimax than at 34% Pdimax (P < 0.001). The hyperemia became significant at a DC of 0.6 (TTdi 0.20) during the runs at 34% of Pdimax, whereas at 64% Pdimax it was already significant at a DC of 0.4 (TTdi 0.25); i.e., the hyperemia became evident at a TTdi above 0.20. The hyperemia probably reflected the oxygen debt incurred during the runs.

Opha as a function of Pdi: Table 2 shows the overall values of QphaT for all the DCs studied in all of the animals. It shows that on the average, QphaT was higher at 64% of Pdimax than at 34% Pdimax. It was noticeable as well that the highest QphaT values were obtained at DCs ranging from 0.4 to 0.6 at either Pdi, whereas the lowest QphaT values occured at DCs of 0.1 and 0.9. It is of interest that, if a Pdi of 64% Pdimax, is produced at DC of 0.1 or 0.9, it will result in a lower QphaT than at a Pdi of 34% Pdimax sustained with a DC of 0.5. The pattern with a Pdi of 64% of Pdimax and a DC of 0.1 will not have incurred an oxygen debt, whereas that of a Pdi at 64% Pdimax and DC of 0.9 will have a tremendous oxygen debt (Fig. 5D).

TABLE 2

Phrenic Artery Blood Perfusion Per Contraction Cycle (QphaT ml/min/100g) at Various DCs during Two Levels (0.34 and

0.64) of Pdi/Pdimax

DC	0 (CTL)	0.1	0.2	0.3	0.4	0.5	0.6	0.7	0.8	0.9
0.34	15.9	22.1	25.5	27.8	31.1	34.8	35.4	33.8	30.8	24.4
± SE	3.0	4.3	4.3	3.8	4.0	4.5	6.0	6.6	6.8	7.0
0.64	17.8	30.1	38.0	44.0	47.9	50.6	49.0	43.6	39.2	28.0
± SE	4.6	5.3	6.5	6.9	6.6	7.2	8.2	8.1	7.5	6.3

DC - duty cycle, CTL - control.

Opha as a function of TTdi: The TTdi was calculated as the product of Pdi/Pdi_{max} and the DC. The average maximal TTdi obtained in these experiments was 0.58 ± 0.03 . Because there was no active diaphragmatic contraction during control (the dogs were slightly hyperventilated), the TTdi was equal to zero.

The effects of various TTdi on Qpha and its post-pacing hyperemia are shown in Fig. 6, A-D, which was derived from the data shown in Fig. 5. In these plots each data point represents mean ± SE for each of the runs in the 5 dogs. Best-fitted lines were drawn through the data points of Pdi 34 and 64 % of Pdimax.

Figure 6A shows that QphaC is a sigmoidal function of TTdi if resting blood flow values are included. Otherwise, if calculations are done from a DC of 0.1, a parabolic function is the best fit. It is of interest that QphaC increases as a direct function of the time of contraction (DC) and blood perfusion is almost independent of Pdi (horizontal line at an iso-DC of 0.5, Fig. 6A).

Figure 6B shows that QphaR is a parabolic function of TTdi. It becomes evident that the relaxation phase is responsible for accommodating most of the changes in blood perfusion brought about by increased diaphragmatic work. The slope of the

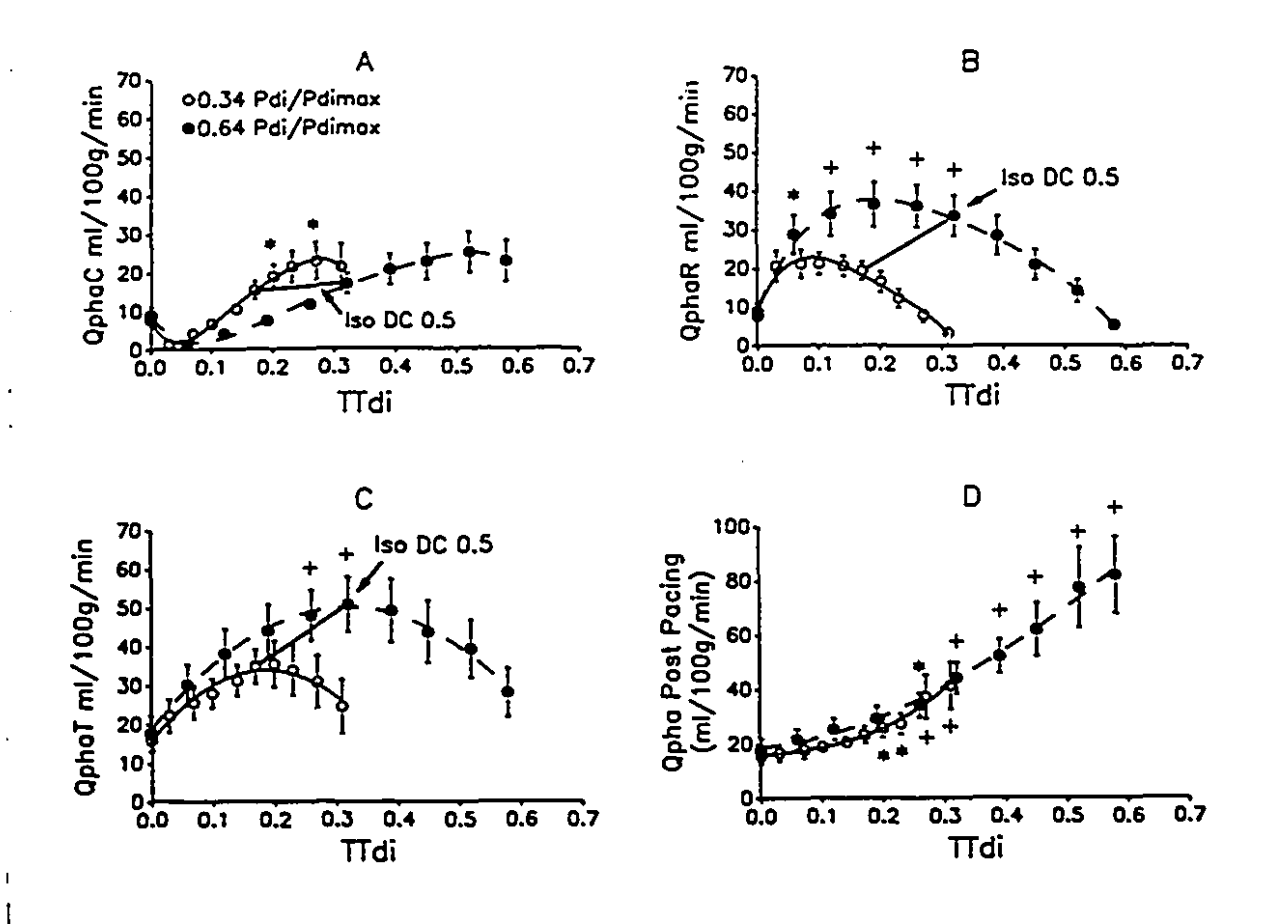


Figure 6.

Panel A, phrenic artery blood perfusion (Qpha) during diaphragmatic contraction phase (C) plotted as a function of TTdi (a product of duty cycle and Pdi/Pdimax). The (AQphaC/Aduty cycle) is greater at 34% Pdimax than at 64% pdimax. (*) P<0.05 between 34 and Pdimax at iso-TTdi. Panel B, Qpha 64% of during diaphragmatic relaxation phase (R) as a function of TTdi. QphaR is greater at 64% than 34% Pdi max. (*) P < 0.05 and (+) P < 0.01. Panel C, Qpha during the total cycle (T) as a function of TTdi. QphaT is uniquely related to TTdi up to 0.20. Beyond TTdi 0.20, there is direct relationship between QphaT and Pdi at Panel D, Post-pacing of TTdi. There are no iso-TTdi (+) P<0.01. hyperemia as a function of TTdi. significant increases in Q up to TTdi of 0.20 with Pdi. either Hyperemia significantly related to TTdi at values above 0.20 for both 34 and 64% of Pdimax runs. differences Significant between control (resting diaphragm, duty cycle = 0) stimulation are (*) P < 0.05 and (+) P < 0.01. Data is average ± SE.

solid line at an iso-DC of 0.50 shows that the increased blood perfusion brought about by changes in Pdi is fully accommodated during the relaxation phase, showing the great relevance of the relaxation time on the magnitude of the Qdi.

Figure 6C shows the relation of QphaT, i.e., the integral of Fig. 6, A and B. Here we can observe that patterns with a DC of about 0.50 can accommodate greater blood perfusion demands brought about by higher Pdi. It seems that the DC at which either of the two Pdi tested reaches its maximal blood perfusion is in the range of 0.4 to 0.6. Beyond that level blood perfusion is limited. It shows as well that there is not a unique relationship between blood perfusion and TTdi at a Pdi of 34 and 64% of Pdimax.

Figure 6D shows that the post-pacing hyperemia is directly related to TTdi. The slope has a flat initial portion up to a TTdi of about 0.20, after which it becomes linearly related to TTdi. This is a strong indication that at low TTdi levels there is no oxygen debt. However, at TTdi values greater than 0.20 to 0.25, hyperemia is an indication of insufficient blood flow and could be related to the development of fatigue.

DISCUSSION

Myocardial and skeletal muscle blood flow are affected by several factors, among them perfusion pressure, extravascular compression, and the autoregulatory vascular tone. In these experiments we have mainly explored the effects of varying the contraction pattern (TI/TT) on Qdi at two different levels of Pdi or extravascular compression. The major finding was that Qdi was a parabolic function of the DC and that blood flow was optimal (highest) at a TI/TT of 0.5 regardless of the Pdi.

Perfusion pressure and autoregulatory tone: Early studies (13) on coronary circulation have shown that perfusion pressure (aortic pressure minus intraventricular pressure) was the main determinant of coronary blood flow (CBF). Later, several studies (13) showed that a relative constancy of flow was present despite rapidly elicited transients in perfusion pressure; this indicated that autoregulation of CBF was present. Similar responses have been shown in skeletal muscle perfusion (48), and Hussain et al. (52-53) have demonstrated that autoregulation was present in the diaphragm. These investigators demonstrated that vascular autoregulatory mechanisms in the diaphragm were functional between perfusion pressures of 75 and 120 mmHg. below 75 mmHg, Qdi became a function of the perfusion In our experiments we had a perfusion pressure that was kept constant at 120 mmHg, within the range of

autoregulation for the diaphragm. Thus the blood flow changes observed during our experiments were independent of perfusion pressure.

Extravascular compression: Decramer and co-workers (26) have shown that intramuscular pressure (extravascular compression) of the diaphragm was linearly related to Pdi. In the diaphragm, during intermittent contraction patterns, Qdi becomes affected by the intramuscular pressure (12, 47). In the heart it is known as extravascular compression (13). Increases in extravascular compression affect the vascular transmural pressure, which can lead to a limitation in organ blood flow (Starling resistor model: waterfall effect) (13). When the extravascular compression surrounding the vasculature is equal to or higher than the intravascular blood pressure, blood flow can become extremely limited or even stopped (9, 12, 16, 48, 53). The autoregulation of the diaphragmatic vascular bed is affected by such a mechanical event, as is well documented in coronary circulation during systole. In fact, extravascular compression in the left ventricle during systole is so great that CBF is stopped and in some instances even reversed. In the diaphragm, at the levels (60 cmH20) of Pdi (intramuscular pressure) that we have studied, we were never able to produce cessation of Even at Pdimax, some Qpha was still present Qpha. (unpublished observations). However, it has been shown previously that venous blood flow stops at a Pdi of 70% of Pdimax (12). The presence of arterial flow is likely due to the presence of head to head anastomosis in the costophrenic arcades of the arterial system (20), and may not represent capillary flow.

Dynamics of Qpha during the diaphragmatic contraction phase: It is interesting to notice that volume of blood perfusion per breath is a function of TT, as shown in Fig. 5A, from a DC of 0.2 (Tr 1.2 sec.) to a DC of 0.8 (Tr 4.8 sec). contrast, the Pdi (30 to 60% of Pdimax) seems to have a minimal effect. This finding seems to contrast with previous observations by Bellemare et al. (12) and Bark et al. (10) who showed that continuous contractions at low Pdi resulted in an increase of flow, whereas contractions at/or above 70% of Pdimax almost stopped the blood flow. conclusions, however, were drawn from sustained contractions lasting 30 seconds. A closer analysis of the data of Bellemare et al. (12) shows that flow rates over the first 4 to 5 seconds at Pdi of 15 and 70% Pdimax are the same and that most changes thereafter develop exponentially as a function of time. Bark's data do not provide information on the instantaneous flow over the first 10 seconds. important point worth mentioning is that the above authors 12) were measuring blood flow on the venous circulation, which is the most compliant and collapsible compartment of the diaphragmatic vascular bed. In our study, blood perfusion was measured on the arterial side.

The progressive increase in flow in long-lasting continuous contractions (>10s) can be related, as well, to a hypoxic acidosis buildup, which could eventually lead to muscle ischemia, fatigue, and a decay in Pdi (9). Thus the loss in diaphragmatic muscular force releases the compression on the vascular bed (reduces the extravascular compression) and thereby causes Qpha to increase. Because the breathing patterns studied during our experiments have contraction times in the 1 to 4 second range, the above effect is not expected.

Another concept to analyze is that Qdi can change as a function of muscle length during intermittent contractions, as shown by Supinski et al. (97). Our study strongly indicates that the contraction is not isometric (Fig. 4); in fact, shortening was 21 or 37% of LFRC, and the . diaphragm shortened as a direct function of Pdi. conceivable that in our study there was a "force effect" during shortening (contraction phase), decreasing Qpha, which was also affected by a simultaneous "muscle shortening effect" facilitating flow, but the length effect certainly does not sway QphaR, when length always returned to control (Lfrc) values. However, in Supinski's experiments, during intermittent isometric contractions, it is conceivable that the length effect did influence the QphaR. Data from Hussain et al. (53), on QphaC in intermittent contraction, agrees with our data.

Dynamics of Qpha during the relaxation phase: Steady state QphaR is a parabolic function of DC, with the optimal perfusion being at a DC of about 0.3. Beyond this point perfusion decreases as a function of the DC. This is true for Pdi values of both 34 and 64 % of Pdimax. The low blood flow at low DC results from the small TTdi. The optimal perfusion being at a DC of 0.3 is likely originated by the metabolic demands of the muscle and local vasodilation. Beyond the optimal point, QphaR is limited by the reduction in relaxation time. The instantaneous flow, however, is not affected.

In the study by Hussain et al (53), values of instantaneous QphaR seemed to be at variance with the concept that there was an optimal DC. In fact, the pertinent portion of Hussain co-worker's data (Fig. 5 in ref. 53) is plotted in Fig. 8 (filled circles) together with our data from Fig. 6 (filled squares), which are recalculated as instantaneous flow, as Hussain et al (53). Neither study, analyzed in this fashion, shows an optimal The open squares in Fig. 8 shows the same data as in DC. the filled squares, but calculated as volume, and show an There are several reasons from this apparent optimal DC. discrepancy. Fig. 7 shows that Qpha at 62% Pdimar and DC of 0.5 (TTdi 0.31) is similar to the one at a DC of 0.7 (TTdi 0.43). This agrees with the data of Hussain et al. (53) in showing little effect of DC on Qpha. However, when blood volume per cycle is calculated (area under flow tracing), it becomes evident that DC of 0.5 has considerable more perfusion than DC of 0.7, explaining our finding shown in Fig. 8 (open squares). If our data from Fig. 6B are recalculated in terms of instantaneous flow (see Fig. 8, filled squares), it can be seen that there is good qualitative agreement with Hussain et al. (53). The most important fact is that Hussain et al. (53) measured mean flow over the relaxation period, whereas we reported volume. Volume can be affected by a shorter relaxation period (high DC) whereas Qpha is not necessarily limited. From Fig. we expect QphaR to be related to Pdi at iso-TTdi. rather lower values of blood perfusion from Hussain et al. (53) may be largely due to the lower Pdi (50% of Pdimax) with respect to our experiments (group average: Pdimax).

We believe that blood volume perfused per unit of time is the relevant parameter to measure, because it is linked to oxygen supply and clearance, whereas instantaneous flow alone is not, relating mainly to the hemodynamics of the vascular system of the diaphragm. Hence, an optimal DC for perfusion during the relaxation phase was found to be 0.3 to 0.4 at both 34 and 64% Pdimax.

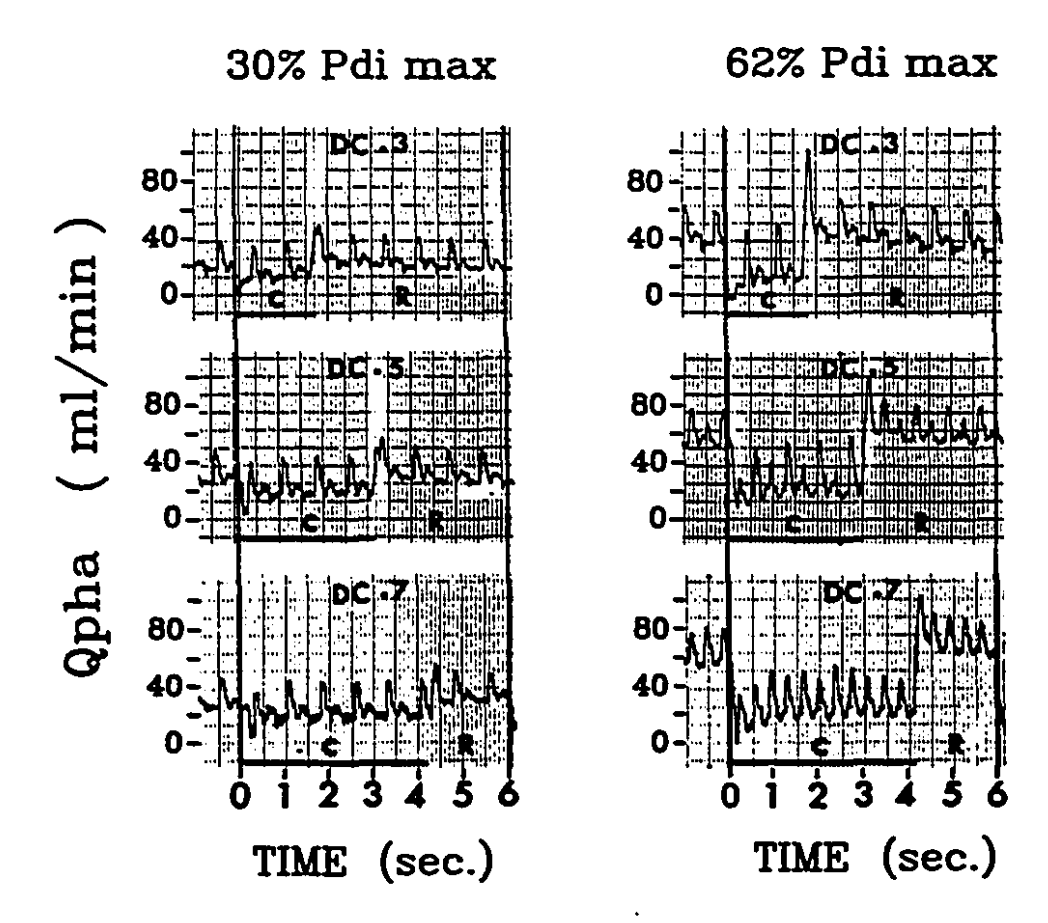


Figure 7. Time course of intrabreath phrenic artery blood flow obtained in one animal at 30 and 62% of Pdimax each held at duty cycle of 0.3, 0.5 and 0.7. C, contraction phase; R, relaxation phase. Blood perfusion (Q) is the integral of Q over the duration of C and R. Notice that Q at 62% of Pdimax is similar at duty cycle of 0.5 and 0.7. The integral of Q is considerably higher at duty cycle of 0.5.

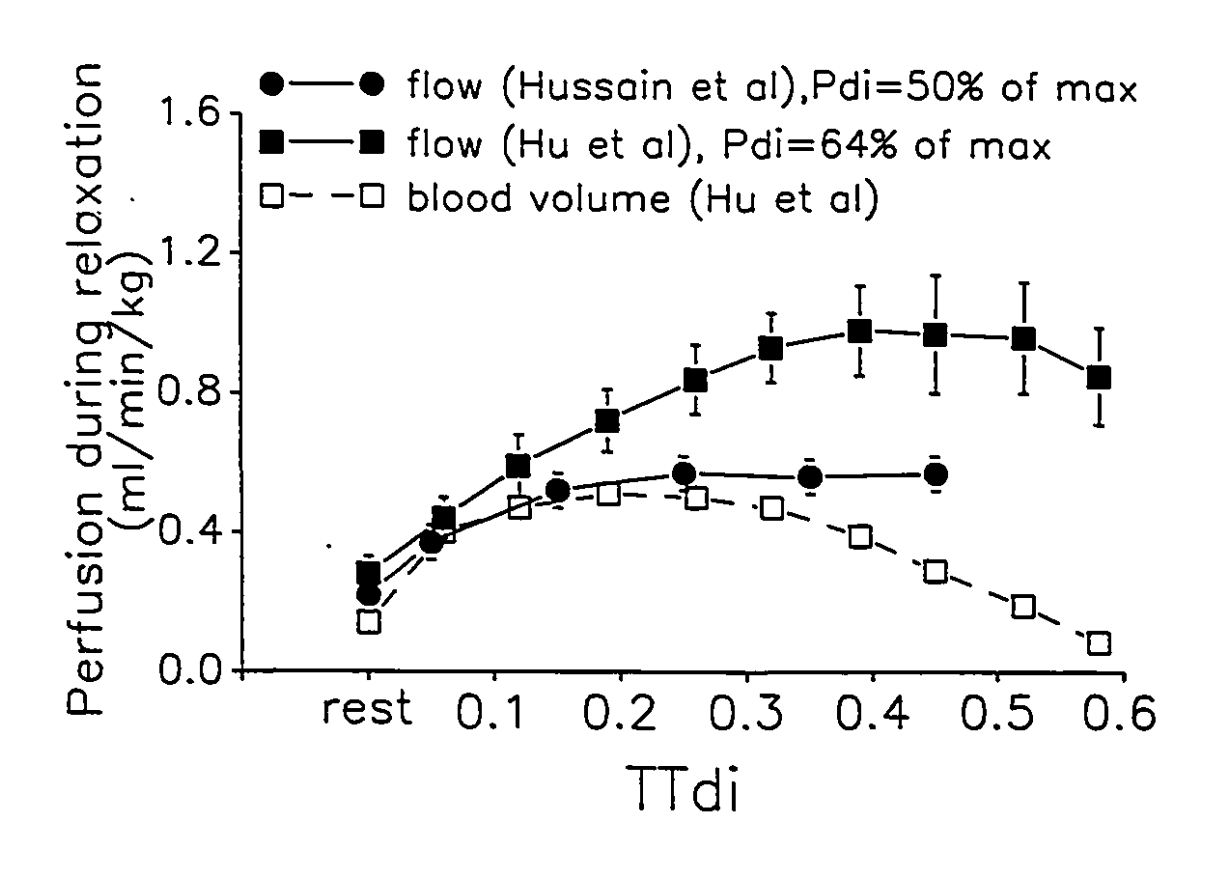


Figure 8. Plotting the pertinent portion of Hussain et al's data (53, Fig. 5) together with our data from Fig. 6B recalculated as instantaneous flow and volume in the same unit (ml/min/kg). Notice blood volume decreases as a function of duty cycle (), while instantaneous flow does not (). The rather lower value of Q from Hussain et al. at iso-TTdi may be due to the lower Pdi (50% of Pdimax) in their experiments with respect to our experiments (64% of Pdimax).

Dynamics of Qpha during the total contraction cycle: QphaT becomes a parabolic function of DC, as shown in Fig. The maximal QphaT is reached at a DC of 0.4 to 0.6, regardless of the level of Pdi. This is similar to the finding in Bellemare et al. (12) that the Qdi was highest at a DC of 0.5. Similarly, in the heart, total CBF is affected by the duration of the relaxation time between systole. With tachycardia, systole / cycle increases because of a relative shortening in diastole time (57). Fitt and Gregg (79) have shown that CBF progressively increases along with heart rate and that, even at a heart rate of 250 beats/min, CBF continues to increase. It is interesting to notice, however, that at 250 beats/min, systole / cycle was 0.5, a value similar to the one found in this study for the diaphragm. However, when one looks at the data of Bark et al. (10) the optimal Qdi is observed at a DC of 0.3. their study blood perfusion was observed during intermittent isometric contractions at optimal length. In contrast, our study was performed during intermittent nonisometric contractions from supine LfRc with a casted abdomen. suspect that the change in vascular architecture produced with shortening could account for the discrepancies observed between Bark's study and other studies (12, 79), including our's.

Opha as a function of TTdi: Plotting TTdi against diaphragmatic arterial volume per minute allowed to see a

functional correlation between blood perfusion and fatigue development. Bellemare et al. (12) showed that Qdi increases with TTdi up to 0.20. At such a level, postpacing blood flow increased, indicating an accumulated oxygen This level of TTdi coincides with the fatigue deficit. threshold, and the association of both factors is evidence of the important role that perfusion has on muscle endurance. While supporting the results of Bellemare et al. (12), this protocol included more data points over a wider range of Pdi and DC, allowing new information to expand the previous concept. Our data (Fig. 6C) suggests that, first, at both levels of Pdi studied, there is a unique DC (about 0.5) where blood perfusion is optimal, and second, the optimal blood perfusion increases with the level of Pdi. QphaT is uniquely related to TTdi up to values of 0.15 to Within this range any combination of DC and Pdi 0.20. leading to a given TTdi results in the same QphaT. Beyond a TTdi of 0.20, blood flow is no longer a unique function of TTdi. Fig. 6C shows that a TTdi reached with a higher Pdi and lower DC will result in a higher blood flow than the opposite, emphasizing the importance of the duration of the relaxation phase of the DC to restore muscle function during fatiguing contractions.

Most physiological activities requiring an increase in ventilation, including submaximal exercise, can be sustained with a TTdi smaller than 0.15 - 0.20 (29, 77). During

maximal exercise maximal voluntary or ventilation. particularly in obese patients, TTdi can exceed the fatigue threshold (11). It is remarkable that, in circumstances in which work of breathing increases, the DC remains in the 0.4 to 0.6 range, which would maximize diaphragmatic perfusion. The general consensus is that diaphragmatic response to increase work of breathing is mediated by feedback mechanisms through the vagus nerves. Recent evidence. however, has demonstrated that phrenic afferents (group III and IV fibers) could play a role in modulating diaphragmatic activity (32). The response produced by electrical stimulation of the central cut end of the phrenic nerve inhibits phrenic efferent activity; this response has been termed the phrenic-to-phrenic inhibitory reflex (32).Potassium release in contracting skeletal muscle has been shown to stimulate group III and IV affarent fibers of skeletal muscle motoneurons (32). As well, extracellular potassium concentrations ([K]o) increase proportionally to skeletal muscle activity. Phrenic affarents stimulated by changes in [K]o and this could influence the modulation of diaphragmatic activity. Affarent phrenic nerve signals may help maintain a DC of 0.5, which produces optimal perfusion thus enabling efficient catabolite washout and bringing the system toward an equilibrium of [K]o that maintains a TI/TT in the range of 0.4 to 0.6.

In summary: 1), Optimal (highest) QphaT per breathing cycle is achieved at DC of 0.4 to 0.6, regardless of Pdi.

2), The hyperemia becomes evident when the TTdi is above 0.20. 3) In nonfatiguing contractions (up to TTdi 0.15 - 0.20), there is a unique relationship between TTdi and Qphat, regardless of the combination of Pdi and DC. At patterns with a TTdi above 0.20, Pdi becomes the predominant factor in regulating Qphat. However, our findings could be condition specific. Our model offers many possibilities for further studies. We looked for force-timing effects within this model. Different diaphragmatic lengths (Lfrc) and force (Pdi) outside the range we explored could yield another family of Qdi values.

CHAPTER 7

CONCLUSION

CONCLUSION

The present work examined the blood circulation of the respiratory muscles and most particularly the circulation of the diaphragm. Five aspects of diaphragmatic circulation were investigated: 1) the macroscopic anatomy of diaphragmatic circulation; 2) the functionality and physiological relevance of the proposed anatomical model; 3) left and right hemidiaphragmatic arterial communications (shunts); 4) the relative contribution of the venous vessels to diaphragmatic drainage; and 5) the effects of various contraction patterns in optimizing diaphragmatic blood flow rate. These experiments constitute an original contribution to the understanding of diaphragmatic circulation in the face of various breathing patterns.

Early work on respiratory muscle blood flow measured diaphragmatic circulation with methods allowing total organ blood flow measurements. This permitted to conclude that the main determinant of respiratory muscle blood flow was their level of activity, and that diaphragmatic circulation had a tremendous, even limitless capacity to increase its blood flow. Subsequent studies, using similar methods of blood flow measurements, reported that blood flow to the diaphragm was limited when the tension developed by the diaphragm was 85% of the maximal tension (28). The initial studies on diaphragmatic circulation increased diaphragmatic activity by loaded breathing and stimulated breathing (CO2).

The latter study employed electrophrenic nerve stimulation which resulted in larger tensions developed by the diaphragm than those observed during spontaneous loaded breathing. It was also demonstrated, in additional studies by various groups of investigators, that other factors could affect respiratory muscle blood flow. These were found to be the cardiac output and arterial pressure, both of which could be influenced by cardiogenic, septic and hemorrhagic shock, the contraction (intramuscular force of pressure), the contraction pattern (duty cycle), the breathing frequency, the pleural pressure and the abdominal pressure, and humoral However, the majority of these factors such as hypoxia. studies assumed that diaphragmatic circulation maintained entirely by inferior phrenic artery blood flow and/or drained entirely by the inferior phrenic veins. A working model that consisted of an organ supplied by a single arterial source and drained by a single venous On the basis of this model some studies have effluent. utilized instantaneous methods of blood flow measurements. It was shown that diaphragmatic circulation was related to the level of tension (1). A conclusion that was consistent with observations made in other skeletal muscles that blood flow became limited when muscle tension was increased. Recent studies using similar methods of instantaneous blood flow measurements have shown that diaphragmatic circulation was uniquely related to the product of transdiaphragmatic pressure and the duty cycle, i.e. the TTdi (12).

studies reported that blood flow to the diaphragm was inadequate to meet metabolic demands when the TTdi became greater than 0.20. An observation consistent with those reported in limb skeletal muscles.

Our model of diaphragmatic circulation gives further support to the concept of blood flow limitation when the TTdi becomes greater than 0.20. However, in our model the major determinant modulating blood flow through the diaphragm, on a breath by breath basis, is the duty cycle. Our model shows that blood circulation is linearly related to the tension (Pdi) and that the blood flow, regardless of the Pdi generated, is a parabolic function of the duty cycle with an optimal blood flow rate at a duty cycle of 0.5. The model of diaphragmatic circulation that we propose is a pool of blood for both hemidiaphragms supplied by a complex multiple artery system which is drained by a similar pattern of multiple venous vessels. This model is supported by the following original observations:

1. The diaphragm in dogs is supplied by a multiple arterial system composed of end to end anastomosis of the ipsilateral inferior phrenic arteries and the internal mammary arteries that form an interior arterial circle along the musculous tendinous junction of the central tendon. The interior arterial circle anastomoses end to end with the

intercostal arteries of the 8th to 13th intercostal spaces to form costo-phrenic arcades within the muscular leaflet of the costal and crural diaphragm. This pattern of arterial system was also observed in the human diaphragm.

- 2. Simultaneous occlusion of the inferior phrenic arteries and of the internal mammary arteries (diaphragmatic perfusion maintained by the intercostal arteries only) does not affect diaphragmatic contractility at a TTdi of 0.20.
- 3. Both hemidiaphragms behave as two distinct muscles according to their arterial circulation and oxygen consumption. An observation consistent with the proposed model (two muscle concept) based on mechanical observations.
- 4. The venous effluent is produced by three groups of vessels (inferior phrenic veins, internal mammary veins and intercostal veins) in a pattern similar to the arterial system.
- 5. The venous effluent is produced mostly by the intercostal veins (60% of total venous outflow) which drain into the azygos trunk.

- 6. Diaphragmatic circulation reaches an optimal blood flow rate when the duty cycle reaches 0.5 regardless of the tension (Pdi) being developed.
- 7. Diaphragmatic circulation was related to the duty cycle by a parabolic function and linearly related to the tension (Pdi).
- 8. Diaphragmatic circulation was linearly related to the TTdi up to 0.20 but departed from this relationship above this value.
- 9. The post contraction hyperemia was linearly related to the TTdi with an increase in slope above 0.20. Suggesting that blood flow was limited beyond this point.

These observations summarize the fact that the diaphragmatic circulation is a complex system that is perfused by distinct arterial sources subjected to a rigorous control tending to optimize arterial perfusion as described in chapter 6. The relevance of chapter 6 is the concept that the duty cycle is the main determinant in optimizing the blood volume going through the diaphragm.

LIST OF REFERENCES

- Anrep, G.V., S. Cerqua, and A. Samaan. The effect of muscular contraction upon the blood flow in the skeletal muscle, in the diaphragm and in the small intestine. <u>Proc. R. Soc. Lond. (Biol.)</u> 114: 245-357, 1933.
- Anrep, G.V., and E.V. Saalfeld. The blood flow through the skeletal muscle in relation to its contraction. J. Physiol. London. 85: 375-399, 1935.
- 3. Barclay, J.K., and W.N. Stainsby. The role of blood flow in limiting maximal metabolic rate in muscle.

 Med. Sci. Sports Exerc. 7: 116-119, 1976.
- 4. Barclay, J.K. A delivery-independent blood flow effect on skeletal muscle fatigue. J. Appl. Physiol. 61: 1084-1090, 1986.
- 5. Barcroft, H., and J.L.E. Millen. The blood flow through muscle during sustained contraction. J. Physiol. 97: 17-31, 1939.
- 6. Barcroft, H., and A.C. Dornhorst. The blood flow through the human calf during rhythmic exercise. J. Physiol. 109: 402-411, 1949.
- 7. Barcroft, H. Circulation in skeletal muscle. Handb.

 Physiol. (Sec. 2. Circulation): 1353-1385, 1963.

- 8. Bark, H., G.S. Supinski, R.J. Bundy, and S.G. Kelsen.

 Effect of acute hypoxia on diaphragmatic muscle
 contractile function, blood flow, and metabolism. Am.

 Rev. Resp. Dis. 133: A249, 1986.
- 9. Bark, H., and S.M. Scharf. Diaphragmatic blood flow in the dog. J. Appl. Physiol. 60: 554-561, 1986.
- 10. Bark, H., G.S. Supinski, J.C. Lamanna, and S.G. Kelsen.

 Relationship of changes in diaphragmatic muscle blood

 flow to muscle contractile activity. J. Appl. Physiol.

 62: 291-299, 1987.
- 11. Bellemare, F., and A. Grassino. Effect of pressure and timing of contraction on human diaphragm fatigue. J. Appl. Physiol. 53: 1190-1195, 1982.
- 12. Bellemare, F., D. Wight, C.M. Lavigne, and A. Grassino. Effect of tension and timing of contraction on the blood flow of the diaphragm. <u>J. Appl. Physiol.</u> 54: 1597-1606, 1983.
- 13. Berne, R. M., and R. Rubio. Coronary circulation. In:

 The Cardiovascular System. Edited by R. M. Berne, N.

 Sperelakis, and S. R. Geiger. Handbook of Physiology.

 Vol. 1, Section 2: 873-952, 1979.
- 14. Biscoe, T.J., and A. Bucknell. The arterial supply of the cat diaphragm with a note on the venous drainage.

 Quart. J. Exp. Physiol. 48: 27-33, 1963.

- 15. Bonde-Petersen, F., A.L. Mork, and E. Nielsen. Local muscle blood flow and sustained contractions of human arm and back muscles. <u>Europ. J. Appl. Physiol.</u> 34: 43-50, 1975.
- 16. Buchler, B., S. Magder, and C.Roussos. Effect of contraction frequency and duty cycle on diaphragmatic blood flow. J. Appl. Physiol. 58: 265-273, 1985.
- 17. Buchler, B., S. Magder, H. Katsardis, Y. Jammes, and C. Roussos. Effects of pleural pressure and abdominal pressure on diaphragmatic blood flow. J. Appl. Physiol. 58: 691-697, 1985.
- 18. Ceretelli, P., D. Pendergast, C. Marconi, and J. Piiper. Blood flow in exercising muscles. Int. J. Sports Med. 7: 29-33, 1986.
- 19. Comtois, A., F. Hu, and A. Grassino. Diaphragmatic contractility and tension as a function of selective diaphragmatic arterial occlusions. <u>Fed. Proc.</u> 46(4): 1105, 1987.
- 20. Comtois, A., W. Gorczyca, and A. Grassino. Anatomy of diaphragmatic circulation. <u>J. Appl. Physiol.</u> 62: 238-244, 1987.
- 21. Comtois, A., F. Hu, and A. Grassino. Anatomy of human diaphragmatic circulation. Am. Rev. Resp. Dis. 137: 384, 1988.

- 22. Comtois, A., F. Hu, and A. Grassino. The effect of diaphragmatic fatigue on phrenic artery blood volume (Qpha). FASEB Journal. 2(5): A1498, 1988.
- 23. Comtois, A., F. Hu, and A. Grassino. Diaphragmatic blood flow during spontaneous breathing (SB) and pacing (PAC). FASEB Journal. Vol. 3, 1989.
- 24. Dawson, M.J., D.G. Guardian, and D.R. Wilkie. Muscular fatigue invvestigated by phosphorous nuclear magnetic resonance. Nature. 274: 861-866, 1978.
- 25. Decramer, M., A. DeTroyer, S. Kelly, and P.T. Macklem. Mechanical arrangement of costal and crural diaphragms in dogs. J. Appl. Physiol. 56: 1484-1490, 1984.
- 26. Decramer, M., T. Jiang, and M.B. Reid. Respiratory changes in diaphragmatic intramuscular pressure. J. Appl. Physiol. 68: 35-43, 1990.
- 27. Detroyer, A., V. Ninane, and J.J. Gilmartin.

 Triangularis sterni muscle use in supine humans. J.

 Appl. Physiol. 62: 919-927, 1987.
- 28. Donovan, E., T. Trippenbach, A. Grassino, P.T. Macklem, and C. Roussos. Effect of isometric diaphragmatic contraction in cardiac output and muscle blood flow.
 Fed. Proc. (Abstract). 38: 1382, 1979.

- 29. EL-Manshawi, A., K.J. Killian, and E. Summers et al. Breathlessness during exercise with and without resistive loading. J. Appl. Physiol. 61: 896-905, 1986.
- 30. Evans, H.E., and G.C. Christensen. Miller's anatomy of the dog. (2ndEd.). Saunders, Philadelphia. p. 22-323, 1979.
- 31. Fixler, D.E., J.M. Atkins, J.H. Michell, and L.D. Horwitz. Blood flow to respiratory, cardiac, and limb muscles in dogs during graded exercise. Am. J. Physiol. 231: 1515-1519, 1976.
- 32. Frazier, D. T., and R. Revelette. Role of phrenic afferents in the control of breathing. J. Appl.

 Physiol. 70: 491-496, 1991.
- 33. Gray, H. Anatomy, descriptive and surgical. Running Press. Philadelphia, 1980.
- 34. Greig, H.W., B.J. Anson, and S.S. Coleman. Inferior phrenic artery; Types of origin in 850 body-halves and diaphragmatic relationship. Quart. Bull. Northwestern Univ. M. School. 25: 345-350, 1951.
- 35. Hammersen, F. The terminal vascular bed in skeletal muscle with special regard to the problems of shunts.

 In "Capillary permeability", ed. C. Crone, N. Lassen, Munksgaard, Copenhagen, p. 351, 1970.

- 36. Harris, K., P.M. Walker, D.A.G. Mickle, R. Harding, R. Gatley, G.J. Wilson, B. Kuzon, N. Mckee, and A.D. Romaschin. Metabolic response of skeletal muscle to ischemia. Am. J. Physiol. 250: H213-H220, 1986.
- 37. Hartley, C.J., and J.S. Cole. An ultrasonic pulsed Doppler system for measuring blood flow in small vessels. J. Appl. Physiol. 37: 626-629, 1974.
- 38. Hartley, C.J., H.G. Hanley, R.M. Lewis, and J.S. Cole.

 Synchronized pulsed Doppler flow and ultrasonic dimension measurement in conscious dogs. Ultrasound

 Med. Biol. 4: 99-110, 1978.
- 39. Heyndrickx, G.R., H. Baig, P. Nellens, I. Leusen, M.C. Fishbein, and S.F. Vatner. Depression of regional blood flow and wall thickening after brief coronary occlusions. Am. J. Physiol. 234: H653-H659, 1978.
- 40. Heyndrickx, G.R., R.W. Millard, R.J. McRitchie, P.R. Maroko, and S.F. Vatner. Regional myocardial functional and electrophysiological alterations after brief coronary artery occlusion in conscious dogs. <u>J. Clin. Invest.</u> 56: 978-985, 1975.
- 41. Hirche, H.J., W.K. Raff, and D. Grun. The resistance to blood flow in the gastrocnemius of the dog during sustained and rhythmical isometric and isotonic contraction. Pflugers Arch. 314: 97-112, 1970.

- 42. Hobbs, S.F., and D.I. McCloskey. Effects of blood pressure on force production in cat and human muscle.

 J. Appl. Physiol. 63: 834-839, 1987.
- 43. Hu, F., A. Comtois, and A. Grassino. Diaphragm venous flow as a function of length and frequency of pacing.

 Fed. Proc. 46: 1105, 1987.
- 44. Hu, F., A. Comtois, and A. Grassino. Effect of hypoxia on diaphragmatic blood flow. Am. Rev. Resp. Dis. 137: 321, 1988.
- 45. Hu, F., A. Comtois, and A. Grassino. Optimization of phrenic artery blood volume (Qpha). FASEB Journal. 2(5): A1498, 1988.
- 46. Hu, F., A. Comtois, and A. Grassino. Effect of separate hemidiaphragmatic contractions on left phrenic artery flow (LQpha) and oxygen consumption (LVO₂).

 FASKB Journal. Vol. 3, 1989.
- 47. Hu.F., A.Comtois, and A. Grassino. Contraction dependent modulation in regional diaphragmatic blood flow. J. Appl. Physiol. 68: 2019-2028, 1990.
- 48. Hudlicka, O. <u>Muscle blood flow</u>. <u>Its relation to muscle metabolism and function</u>. Swets and Zeitlenger.

 B. V. Amsterdam. 1973.

- 49. Humphreys, P.W., and A.R. Lind. The blood flow through active and inactive muscles of the forearm during sustained hand-grip contractions. J. Physiol. 166: 123-135, 1963.
- 50. Hussain, S.N.A., G. Simkus, and C. Roussos.

 Respiratory muscle fatigue: A cause of ventilatory
 failure in septic shock. J. Appl. Physiol. 58: 20332040, 1985.
- 51. Hussain, S.N.A., and C. Roussos. Distribution of respiratory muscle and organ blood flow during endotoxic shock in dogs. J. Appl. Physiol. 59: 1802-1808, 1985.
- 52. Hussain, S.N.A., C. Roussos, and S. Magder.

 Autoregulation of diaphragmatic blood flow in dogs. J.

 Appl. Physiol. 64: 329-336, 1989.
- 53. Hussain, S.N.A., C. Roussos, and S. Magder. Effect of tension, duty cycle, and arterial pressure on diaphragmatic blood flow. J. Appl. Physiol. 66: 968-976, 1989.
- 54. Kanan, C.V. The arterial blood supply to the diaphragm of the camel. Acta Morphol. Neerl. Scand. 8: 333-341, 1971.

- 55. Kety, S.S., and C.F. Schmidt. The determination of cerebral blood flow in man by the use of nitrous oxide in low concentrations. Am. J. Physiol. 143: 53-66, 1945.
- 56. Laporta, D., and A. Grassino. Assessment of transdiaphragmatic pressure in humans. <u>J. Appl. Physiol.</u> 58: 1469-1476, 1985.
- 57. Levy, M. N., and P. J. Martin. Neural control of the heart. Handb. Physiol. (Sec. 2. The Cardiovascular System): 581-620, 1979.
- 58. Lind, A.R., and G.W. McNichol. Local and central circulatory responses to sustained contractions and the effect of free or restricted arterial inflow on post-exercise hyperaemia. <u>J. Physiol.</u> 192: 575-593, 1967.
- 59. Lockhat, D., C. Roussos, and C.D. Iannuzzo. Metabolite changes in the loaded hypoperfused and failing diaphragm. J. Appl. Physiol. 65: 1563-1571, 1988.
- 60. Lockhat, D., S. Magder, and C. Roussos. Collateral sources of costal and crural diaphragtmatic blood flow.

 J. Appl. Physiol. 59: 1164-1170, 1985.

- 61. Mainwood, G.W., and D. Cechetto. The effect of bicarbonate concentration on fatigue and recovery in isolated rat diaphragm muscle. Can. J. Physiol. Pharmacol. 58: 624-632, 1980.
- 62. Magder, S. Pressure-flow relations of diaphragm and vital organs with nitroprusside-induced vasodilation. J. Appl. Physiol. 61: 409-416, 1986.
- 63. Magder, S., D. Lockhat, B.J. Luo, and C. Roussos.

 Respiratory muscle and organ blood flow with inspiratory elastic loading and shock.

 Physiol. 58: 1148-1156, 1985.
- 64. Magnoni, P., F. Saibene, G. Sant'Ambrogio, and E. Camporesi. Perfusion of inspiratory muscles at different levels of ventilation in rabbits. <u>Resp. Physiol.</u> 20: 171-179, 1974.
- 65. Manohar, M., C.M. Parks, M.A. Busch, W.J. Tranquilli, G.E. Bisgard, T.A. McPherron, and M.C. Theodorakis. Regional myocardial blood flow and coronary vascular reserve in unasthesized young calves exposed to a simulated altitude of 3500 m for 8-10 weeks.

 Circulation Research. 50: 714-726, 1982.
- 66. Manohar, M. Vasodilator reserve in respiratory muscles during maximal exertion in ponies. <u>J. Appl. Physiol.</u> 60: 1571-1577, 1986.

- 67. Manohar, M., T.E. Goetz, L.C. Holtse, and D. Nganwa.

 Diaphragmatic O2 and lactate extraction during submaximal and maximal exertion in ponies. J. Appl.

 Physiol. 64: 1203-1209, 1988.
- 68. Manohar, M., T.E. Goetz, and D. Nganwa. Costal diaphragmatic O2 and lactate extraction in laryngeal hemiplegic ponies during exercise. J. Appl. Physiol. 65: 1723-1728, 1988.
- 69. Martin, E.C., A.R. Bazzy, M.R. Gandhi, and G.G. Haddad.

 An investigation into the venous drainage of the diaphragm of the sheep. <u>Invest. Radiol.</u> 18: 272-274, 1983.
- 70. McMinn, R.M.H. <u>Color atlas of human anatomy.</u> Year Book Medical Publisher, Inc. Chicago, Illinois, 1982.
- 71. Morgan, C.D. and R.L. Johnson, Jr. Alteration of diaphragmatic perfusion and work of breathing by ligation of the inferior phrenic artery (Abstract).

 Clin. Res. 28: 530A, 1980.
- 72. Mountcastle, V.B. <u>Medical physiology.</u> (14th Ed.).

 C.V. Mosby Company, St-Louis. p. 951-1125, 1980.

- 73. Newman, S., J.Road, F. Bellemare, J.P. Clozel, C.M. Lavigne, and A. Grassino. Respiratory muscle length measured by sonomicrometry. <u>J. Appl. Physiol.</u> 56: 753-764, 1984.
- 74. NHLBI Workshop Summary. Respiratory Muscle Fatigue.

 Report of the respiratory Muscle Fatigue Workshop

 Group. Am. Rev. Respir. Dis. 142: 474-480, 1990.
- 75. Nichols, D.G., S. Howell, J. Massik, R.C. Koehler, C.A. Gleason, J.R. Buck, R.S. Fitzgerald, R.J.Traystman, and J.L. Robotham. Relationship of diaphragmatic contractility to diaphragmatic blood flow in newborn lambs. J. Appl. Physiol. 66: 120-127, 1989.
- 76. Nichols, D.G., S.M. Scharf, R.J. Traystman, and J.L. Robotham. Correlation of left phrenic arterial flow with regional diaphragmatic blood flow. J. Appl. Physiol. 64: 2230-2235, 1989.
- 77. Pardy, R.L., and C.Roussos. Endurance of hyperventilation in COPD. Chest 83: 744-750, 1983.
- 78. Parry, G.H. and D.J. Linn. Transient focal conduction block following experimental occlusion of the vasa nervorum. Muscle Nerve. 9: 345-348, 1986.

- 79. Pitt, B., and D. E. Gregg. Coronary hemodynamic effects of increasing ventricular rate in the unanesthetized dog. <u>Circulation Res.</u> 22: 753-761, 1968.
- 80. Pope, A., S.M. Scharf, and R. Brown. Diaphragm metabolism during supramaximal phrenic nerve stimulation. J. Appl. Physiol. 66: 567-572, 1989.
- 81. Reid, M.B., and R.L.Johnson, Jr. Efficiency, maximal blood flow, and aerobic work capacity of canine diaphragm. J. Appl. Physiol. 54: 763-772, 1983.
- 82. Roberts, JP., M.O. Perry, R.J. Hariri, and G.T. Shires. Incomplete recovery of muscle cell function following partial but not complete ischemia. Circ. Schock. 17: 253-258, 1985.
- 83. Robertson, C.H., Jr., G.H. Forster, and R.L. Johnson, Jr. The relationship of respiratory failure to the oxygen consumption of, lactate production by, and distribution of blood flow among respiratory muscles during increasing inspiratory resistance. J. Clin. Invest. 59: 31-42, 1977.

- 84. Robertson, C.H., Jr., M.A. Pagel, and R.L. Johnson, Jr.

 The distribution of blood flow, oxygen consumption, and
 work output among respiratory muscles during
 unobstructed hyperventilation. J. Clin. Invest. 59:
 43-50, 1977.
- 85. Robertson, C.H., Jr., W.L. Eschenbacher, and R.L. Johnson, Jr. Respiratory muscle blood flow distribution during expiratory resistance. <u>J. Clin. Invest.</u> 60: 473-480, 1977.
- 86. Rochester, D.F. Measurement of diaphragmatic blood flow and oxygen consumption in the dog by Kety-Schmidt technique. J. Clin. Invest. 53: 1216-1225, 1974.
- 87. Rochester, D.F., and G. Bettini. Diaphragmatic blood flow and energy expenditure in the dog. Effect of inspiratory air flow resistance and hypercapnia. J. Clin. Invest. 57: 661-672, 1976.
- 88. Rochester, D.F., and M. Pradel-Guena. Measurement of diaphragmatic blood flow in dogs from xenon 133 clearance. J. Appl. Physiol. 34: 68-74, 1973.
- 89. Scharf, S.M., H. Bark, S. Einhorn, and A. Tarasiuk.

 Blood flow to the canine diaphragm during hemorrhagic schock. Am. Rev. Respir. Dis. 133: 205-211, 1986.

- 90. Schraufnagel, D.E., C. Roussos, P.T. Macklem, and N.S. Wang. The geometry of the microvascular bed of the diaphragm: Comparison to intercostals and triceps.

 Microvasc. Res. 26: 291-306, 1983.
- 91. Simionuscu, N., M. Simionuscu, and G.E. Palade.

 Structural basis of permeability in sequential segments

 of the microvasculature of the diaphragm. Microvasc.

 Res. 15: 1-16, 1978.
- 92. Sjogaard, G. Muscle fatigue. <u>Medicine Sport Sci.</u> 26: 98-109, 1987.
- 93. Sjogaard, G. Water and electrolyte fluxes during exercise and their relation to muscle fatigue. Acta Physiol. Scand. 128(Suppl. 556): 129-136, 1986.
- 94. Stainsby, W.N. Autoregulation of blood flow in skeletal muscle during increased metabolic activity.

 Am. J. Physiol. 202: 273-276, 1962.
- 95. Stainsby, W.N., and E.M. Renkin. Autoregulation of blood flow in resting skeletal muscle. Am. J. Physiol. 201: 117-122, 1961.

- 96. Supinski, G.S., A. Dimarco, L. Ketai, and M. Altose. Reversibility of diaphragm fatigue by mechanical hyperperfusion. Am. Rev. Respir. Dis. 138: 604-609, 1988.
- 97. Supinski, G.S., H. Bark, A. Guanciale, and S.G. Kelsen. Effect of alterations in muscle fibre length on diaphragm blood flow. J. Appl. Physiol. 60: 1789-1796, 1986.
- 98. Testut, L. <u>Traité d'anatomie humaine.</u> (7eme Ed.). Librairie Octave Doin, p. 202-204, 1921.
- 99. Vatner, S.F., D. Franklin, and R.L. VanCitters.

 Simultaneous comparison and calibration of the doppler and electromagnetic flowmeters. J. Appl. Physiol. 29: 907-910, 1970.
- 100. Viires, N., G. Sillye, M. Aubier, A. Rassidakis, and C. Roussos. Regional blood flow distribution in dog during induced hypotension and low cardiac output. J. Clin. Invest. 72: 935-947, 1983.
- 101. Wiedeman, M.P., <u>Patterns of the arteriovenous pathways</u>.

 Handbook of physiology, Section 2, Circulation, Vol.

 II, p. 891, 1963.